NRC RAI Letter No. PTN-RAI-LTR-041

SRP Section: 02.05.01 - Basic Geologic and Seismic Information

QUESTIONS from Geosciences and Geotechnical Engineering Branch 2 (RGS2)

NRC RAI Number: 02.05.01-7 (eRAI 6024)

FSAR Section 2.5.1.1.1.2.1.1, "Holocene Stratigraphy of the Florida Peninsula" states that hurricanes complicate the preservation of Pleistocene and Holocene deposits on the east and west coasts of the Florida Peninsula by eroding these deposits and depositing them elsewhere. In order for the staff to evaluate the Holocene geologic record at the site and in support of 10 CFR 100.23 please address the following:

a) Within the context of the Holocene sedimentary record at the site discuss the nature and extent of paleostorm deposits.

b) Provide a discussion that compares and contrasts deposits of Hurricane Andrew or other historical hurricanes, and any paleostorm deposits preserved in the Holocene stratigraphy, with potential tsunami deposits at the site.

c) Provide a figure or a map that illustrates these deposits.

FPL RESPONSE:

Part a) of the response addresses the nature and extent of the Holocene stratigraphic units at the Turkey Point Units 6 & 7 site based on the borings obtained during the subsurface investigations (FSAR 2.5.1 References 708, 995, and 996). Part a) of the response also discusses evidence, or lack thereof, of paleostorm deposits at the site. Part b) of the response compares and contrasts deposits of Hurricane Andrew and other historical hurricanes, and any paleostorm deposits preserved in the Holocene stratigraphy, with any potential tsunami deposits at the site. Lastly, part c) of the response illustrates the locations of the storm deposits.

a) Within the context of the Holocene sedimentary record at the site discuss the nature and extent of paleostorm deposits.

The Holocene section at the Turkey Point Units 6 & 7 site is classified as marl and wetland soils belonging to the saprist (muck) group, and peat. Surficial deposits in the relatively flat areas outside the vegetated depressions at the Turkey Point site were variably characterized as either marls (clay and elastic silt), organic-rich elastic silt, or peat sediments (FSAR 2.5.1 Reference 996). The surficial layers within the vegetated surface depressions at the Turkey Point site were characterized as peat (FSAR 2.5.1 Reference 996). Laminated surficial deposits found mostly outside vegetated depressions are interpreted to have likely resulted from cyclical changes in oxidation-reduction conditions and/or chemical equilibria, in which dark colored, organic-rich sediments were likely deposited under flooded, low-oxygen (reducing) conditions, and light colored, carbonate-rich (HCl reactive) laminae were likely deposited under open marsh, shallow water (and thereby less anaerobic) conditions (FSAR 2.5.1Reference 996). In coastal Florida wetlands, marl deposition is typically associated with freshwater conditions. Within the Turkey Point site cores, evidence for historic freshwater conditions is provided by the presence of intact specimens of *Planorbella* spp., a freshwater gastropod (FSAR 2.5.1 Reference 996).

Saprist soils are generally defined as those in which two-thirds or more of the material is decomposed, and less than one-third of plant fibers are identifiable (FSAR 2.5.1 Reference 276). Eighty-eight borings were drilled and sampled (standard penetration test [SPT] samples in soil, continuous coring in rock) as part of the Turkey Point Units 6 & 7 initial subsurface investigation (FSAR 2.5.1 Reference 708). During the supplementary investigation, a total of nine borings were drilled (FSAR 2.5.1 Reference 995), with three of the borings inclined towards surface depressions. In addition, surficial "muck" deposits (soft, surficial soil, and sediment layers) samples were collected at nine locations (FSAR 2.5.1 Reference 996). Drilling and sampling locations are shown on Figure 2.5.1-378. The description of the Holocene section (i.e., "muck" deposits [soft, surficial soil, and sediment layers]) in the soil borings across the Units 6 & 7 site (FSAR 2.5.1 References 708, 995, and 996), includes the thickness, color, hardness, and the presence of organics, silt, roots, and shell fragment contents. The surficial deposits were sampled at the site every 2.5 feet (0.8 meters) using the SPT geotechnical sampling method during the initial site investigation (FSAR 2.5.1 Reference 708) and sampled continuously in 2013 using a McCauley Sampler (FSAR 2.5.1 Reference 996). The muck soils are classified under the Unified Soil Classification System in accordance with ASTM D2488-06. Modifiers such as trace (< 5 percent), few (5 to 10 percent), little (15 to 25 percent), some (30 to 45 percent) and mostly (50 to 100 percent) were used to provide an estimate of the percentage of gravel, sand and fines (silt or clay size particles), or other materials such as organics (muck) or shells. In general, the thickness of the surficial deposits ranges from 2 to approximately 11 feet (0.6 to 3.4 meters). Muck is observed in the geotechnical borings and the MASW (multi-channel analysis of surface waves) survey data across the site. The surficial deposits are thicker in the areas of the surficial dissolution features (vegetated depressions), filled entirely with peat (Figures 2.5.4-229 and 2.5.4-230). The color of the peat ranges from black to light gray, dark grayish brown to light brownish gray, and dark olive brown to light olive brown. Mottled coloration is also noted in the muck. The consistency of the muck is very soft-to-soft. Peat, with fibrous internal structure is identified within organic soils in thirteen of the site borings: B-614, B-625, B-626, B-702, B-715, B-725, B-727, B-729, B-729, R-6-1a, R-6-1a-A, R-6-1b, R-6-2, and R-7-4 as well as in all borings sampled continuously using the McCauley Sampler (FSAR 2.5.1 Reference 996). The organic content of the muck (elastic silt and organic-rich silt) was estimated to vary from some 2.9 to 30.3 percent, with an average of 10.6 percent (FSAR 2.5.1 Reference 996). The Holocene surficial deposits have been disturbed intermittently since the 1960s by construction activities (FSAR Figure 2.5.1-337).

Only one sample from boring B-601 (DH) contains "mostly silt." Trace to some sand is noted in three borings: B-617, B-623, and B-723. Neither the sand nor the silt can be correlated across the site as continuous stratigraphic units. However, fine-grained calcareous material, marl, appears to overlie the muck in borings: B-736, B-738, B-802, B-810, B-812, B-813, M-6-1b, M-6-2a, M-7-1a, and M-7-2c. This marl-like material is described as a fat clay to sandy fat clay and elastic silt that is light/dark gray to greenish gray, very soft, moist to wet, with some fine grained sand and strong hydrochloric reaction (FSAR 2.5.1 References 708 and 996). Where present, the marl/elastic silts represent the uppermost surficial sediments. This type of marl forms when the ground surface is flooded for several months each year in the summer followed by a number of dry months during the winter (hydroperiod). During the hydroperiod, the microalgae (periphyton) grow on the water surface. The precipitation of the microalgae from the calcium bicarbonate saturated water creates marl (Reference 1).

Examples of storm deposits discussed in the response to part (b) are not observed in samples obtained from the Turkey Point Units 6 & 7 site subsurface investigation borings.

The conclusion that there are no paleostorm (or paleotsunami) deposits at the site is based on the interpretation of the soil boring data (FSAR 2.5.1 References 708, 995 and 996). Analysis of the samples collected did not show evidence of discrete sedimentary structures (anomalous sand sheets or layers) at the PTN site that could be interpreted as evidence for a high-energy depositional event. Hydrometer analyses on samples from borings M-6-1a, M-6-2a, M-7-1a, M-7-2c, and M-7-3b (FSAR 2.5.1 Reference 996) suggest that, on average, silt and clay sized particles (fines) constitute approximately 85 percent (by weight) of the soft, surficial sediment deposits at the site. Significant sand content was identified by laboratory testing in only one sample, from location M-7-1a, extracted from near-basal sediments equated with the Miami Limestone. Surface sediment particle size determinations by hydrometer analysis are also largely consistent with sieve analysis results. The sediment record described in samples from the site provided no direct evidence for material and sedimentary structures that could be interpreted as evidence for high-energy depositional events (e.g., hurricane or tsunami landfalls). That is, no storm bed, tsunamigenic deposits (upward fining clastic sequences), peaks in sand content (sand sheets), nor erosive surfaces, were identified in any borings at the site.

It is important to note that the surficial deposits described at the Turkey Point site generally correspond to the surficial sediment sequences described within other coastal wetland systems adjacent to Biscayne Bay (FSAR 2.5.1 References 397, 997, and 998). Moreover, the thickness of the surficial sediments at the Turkey Point site is similar to those reported for other coastal wetland locations in southern Florida and the greater circum-Caribbean, including the Bahamas and Bermuda (FSAR 2.5.1 Reference 996).

b) Provide a discussion that compares and contrasts deposits of Hurricane Andrew or other historical hurricanes, and any paleostorm deposits preserved in the Holocene stratigraphy, with potential tsunami deposits at the site.

Although preserved storm deposits have not been observed at the Turkey Point Units 6 & 7 site, storm deposits have been observed elsewhere in southern Florida. Storm deposits have been preserved at scattered locations on the east coast of Florida at Biscayne Bay and Soldier Key to Elliot Key. Similar deposits are documented on the west coast at Northwest Cape and Cape Sable in the Gulf Coastal Highlands of the Reticulated Coastal Swamps Physiographic Subprovince. This physiographic subprovince is shown on FSAR Figure 2.5.1-217 and the locations of preserved storm deposits are shown on Figure 1.

The Reticulated Coastal Swamps Physiographic Subprovince has been modified by numerous hurricanes in the past. Hurricanes have modified the environment in this physiographic subprovince as follows:

- Decimation of mangrove forests.
- Removal of sufficient beach sand near the Middle Cape Canal.
- Erosion (steps) in the west-and south-facing coastlines of Cape Sable.
- Alteration of the interior marshes.

- Decimation of marginal wetlands and uplands.
- Intrusion of saltwater into an isolated fresh to brackish lake (Lake Ingraham) within the coastal system (Reference 3).

An example of a historical storm deposit is illustrated in a split core taken from a flood tidal delta in the northwest part of Lake Ingraham (Figure 1) (Figure 79, core 24 of Reference 3). The layered delta sequence has accumulated over the past 70 years (as of 2004), following the opening of the Middle Cape Canal by the 1935 Labor Day Hurricane. From a depth of 0 to 70 centimeters, the split core material, a post-1935 flood tidal delta sequence, is composed of layered carbonate fine sand, mud, and organic detritus. The dark organic detritus is fibrous and likely derived from the tidal input during winter storms from eroding mangrove substrates from the north. The light layers are carbonate sands washed in by tropical storm and hurricane events. The darker layers are organic rich carbonate fine sand and mud swept into Lake Ingraham by prevailing tides and winter storms. From a depth of 70 to 100 centimeters, the underlying split core material is composed of bioturbated light grey-tan carbonate mud with black roots and minor shell fragments (Reference 3).

An example of recent sediments deposited by Hurricane Charley (2004) is located between East Cape and Middle Cape (Figure 1) (Reference 3, Figure 117). The top photograph from Figure 117 of Reference 3 illustrates large weed and shell overwash deposits. The two lower photographs from Figure 117 of Reference 3 illustrate a sharp beach escarpment with a 15-centimeter thick coarse shell layer on top (Reference 3).

During the 20th century, several powerful hurricanes (intensity greater than Category 3 on the Saffir-Simpson Scale) affected Miami-Dade county: Key West Hurricane (1919), The Hurricane of 1926/Fort Lauderdale and Miami Areas (1926), Palm Beach Hurricane (1928), Labor Day Hurricane (1935), Hurricane Donna (1960), Hurricane Cleo (1964), Hurricane Betsy (1965), Hurricane Andrew (1992), Hurricane Opal (1995), and Hurricane Charley (2004). Due to the resulting destruction and loss of life, Hurricane Andrew is well documented in the scientific literature. Swiadek (Reference 4) discusses the damages from Hurricane Andrew to coastal mangroves in Southern Florida. High wind velocities and storm surges are associated with Hurricane Andrew. The high winds and storm surges caused shoreline erosion, which in turn affected the mangroves. Three factors minimized the impacts of the storm surge: 1) the keys in Biscayne National Park acted as an offshore breakwater, 2) the Bahamas Islands and offshore carbonate shoals limited the fetch of hurricane-force winds, and 3) the continental shelf in southeastern Florida is very narrow (Reference 4).

From late August through mid-September 1992, Swiadek (Reference 4) evaluated sedimentary sequences deposited by Hurricane Andrew in southern Florida. These deposits appear to have originated from shoreline erosion elsewhere in southern Florida. On the west coast of Florida, a widespread layer of mud and muddy sand, up to 50 centimeters thick, was deposited in subtidal banks. Also on the west coast, a grayish mud layer 20 to 50 centimeters thick was deposited underwater in protected off-shore depressions and interior bays. On the east coast, a tan to brownish sedimentary layer, up to 50 centimeters thick, was deposited in the depressions along the western margin of Biscayne Bay. Lastly, on the east coast, a grayish mud layer, up to 50 centimeters thick, was deposited on the east side of Biscayne Bay (Figure 1) (Reference 4).

An example of a sequence of sand overwash deposits is illustrated in Figure 27 in Reference 3. It depicts beach (sand) overwash stratigraphy on a beach north of Northwest Cape (Figure 1) (Figures 28A and 28 in Reference 3). The lower sand in the scarp is a washover deposit from the Labor Day Hurricane (1935), overlain by soil, deposited by a Hurricane Donna (1960) washover layer, in turn overlain by soil and capped by a Hurricane Andrew (1992) sand layer.

According to Swiadek (Reference 4), the waters receding from mangrove swamps on the west coast formed ebb deltas along tidal channels and on Cape Sable. On the east coast, from Soldier Key to Elliot Key, vegetation was removed; however, the limestone surface was not affected (Figure 1) (Reference 4).

Generally, the physical attributes of sedimentary deposits that appear to reflect a modern or paleostorm origin are:

- A moderately thick (average > 30 centimeters) sand bed composed of numerous subhorizontal planar lamination organized into multiple lamina sets.
- Maximum bed thickness is near the shore.
- Landward thinning of the deposit is usually abrupt.
- Abundant shell fragments organized in laminations.
- Storm deposit fill in topographic lows with an upper surface along the shore that is relatively uniform in elevation (FSAR 2.5.1 Reference 890).

As discussed in FSAR 2.5.1.1.5, Tsunami Geologic Hazard Assessment:

Tuttle et al. (FSAR 2.5.1 Reference 889) distinguish tsunami from storm surge deposits, based on a comparison of deposits from the 1929 Grand Banks tsunami and the 1991 Halloween storm. As noted by Tuttle et al. (FSAR 2.5.1 Reference 889), the challenge of discriminating between the two types of deposits was that both tsunami and storm surge processes result in the onshore transport and re-deposition of sediments. Tuttle et al. (FSAR 2.5.1 Reference 889) conclude that four discriminators (included verbatim below) could be used to distinguish between tsunami and storm deposits:

- Tsunami deposits exhibit sedimentary characteristics consistent with landward transport and deposition of sediment by only a few energetic surges, under turbulent and/or laminar flow conditions, over a period of minutes to hours; whereas characteristics of storm deposits are consistent with landward transport and deposition of sediment by many more, less energetic surges, under primarily laminar flow conditions, during a period of hours to days.
- Both tsunami and storm deposits contain mixtures of diatoms indicative of an offshore or bay ward source, but tsunami deposits are more likely to contain broken valves and benthic marine diatoms.
- Biostratigraphic assemblages of sections in which tsunami deposits occur are likely to indicate abrupt and long-lasting changes to the ecosystem coincident with tsunami inundations.

- Tsunami deposits occur in landscape positions, including landward of tidal ponds, that are not expected for storm deposits.

Similarly, Morton et al. (FSAR 2.5.1 Reference 890) characterize the distinction between tsunami and storm deposits as being related to differences in the hydrodynamics and sediment-sorting processes during transport. Tsunami deposition results from a few high-velocity, long-period waves that entrain sediment from the shoreface, beach, and landward erosion zone. Tsunamis can have flow depths greater than 10 meters (33 feet), transport sediment primarily in suspension, and distribute the load over a broad region where sediment falls out of suspension when flow decelerates. In contrast, storm inundation generally is gradual and prolonged, consisting of many waves that erode beaches and dunes with no significant overland return flow until after the main flooding. Storm flow depths are commonly < 3 meters (9.8 feet), sediment is transported primarily as bed load by traction, and the load is deposited within a zone relatively close to the beach (FSAR 2.5.1 Reference 890). A schematic of typical tsunami and storm deposits is shown in FSAR Figure 2.5.1-348. As noted by Dawson and Stewart (FSAR 2.5.1 Reference 891), hurricane deposits are quite different from tsunami deposits. For example, Scoffin and Hendry (FSAR 2.5.1 Reference 892) use coral rubble stratigraphy on Jamaican reefs to identify past hurricane activity, while Perry (FSAR 2.5.1 Reference 893) use storm-induced coral rubble in reef facies from Barbados to identify episodes of past hurricane activity.

However, based on Shanmugam's (Reference 5) review, the problem of differentiating paleotsunami from paleostorm deposits is not straightforward. The sedimentary records of both types of deposits can exhibit the following sedimentary features: basal erosional surfaces, anomalously coarse sand layers, exotic boulders, imbricated boulders and gravel clusters with imbrications, chaotic bedding, rip-up mud clasts, normal grading, inverse grading, multiple upward-fining units, landward-fining trend, horizontal planar laminae, cross-stratification, richness of marine fossils, changes in chemical elements, and lastly, sand injection and soft-sediment deformation. There are no reliable sedimentological criteria for distinguishing paleotsunami and paleostorm deposits in various environments. Both paleotsunamis (tsunamis) and paleostorms (storms) can generate identical depositional processes and related sedimentary features (Reference 5).

The boring logs from the subsurface investigations of the Units 6 & 7 site are described in detail in Subsection 2.5.1.2. The logs indicate that geologic conditions are uniform across the site (Figures 2.5.1-231 and 2.5.1-232) and show no evidence of interruption by a tsunami-like event. The vegetated depressions and surficial drainage channel areas were targeted with inclined borings and surficial soils sediment ("muck") sampling during the supplemental field investigation (FSAR 2.5.1 References 995 and 996). This supplemental program was an effort to further examine the characteristics of these surficial deposits. The sediment record described in surficial samples from the site provided no direct evidence for deposits or sedimentary structures that could be interpreted as evidence for high-energy depositional events (e.g., hurricane or tsunami landfalls). That is, no storm beds, tsunamigenic deposits (upward fining clastic sequences), peaks in sand content (sand sheets), nor erosive surfaces, were identified in any borings at the site.

c) Provide a figure or a map that illustrates these deposits.

Since there are no paleostorm or paleotsunami deposits preserved or observed in the borings at the Turkey Point Units 6 & 7 site, there are no data from which a map can be generated. FSAR Figure 2.5.1-337, Surficial Deposits Map, shows the soils to be disturbed at the footprint of the proposed Turkey Point Units 6 & 7 and the existing cooling canals. As discussed in the response to part (b), storm deposits are only intermittently preserved in southern Florida. Storm deposits are preserved at scattered locations in southwest Florida (Reference 3) and on the shorelines of Biscayne Bay (Reference 4). The examples of storm deposits documented by Wanless and Vlaswinkel (Reference 3) and Swiadek (Reference 4) are discussed in part b) of this response and the locations are shown in Figure 1.

Figure 1 Locations of Storm Deposits in Southern Florida

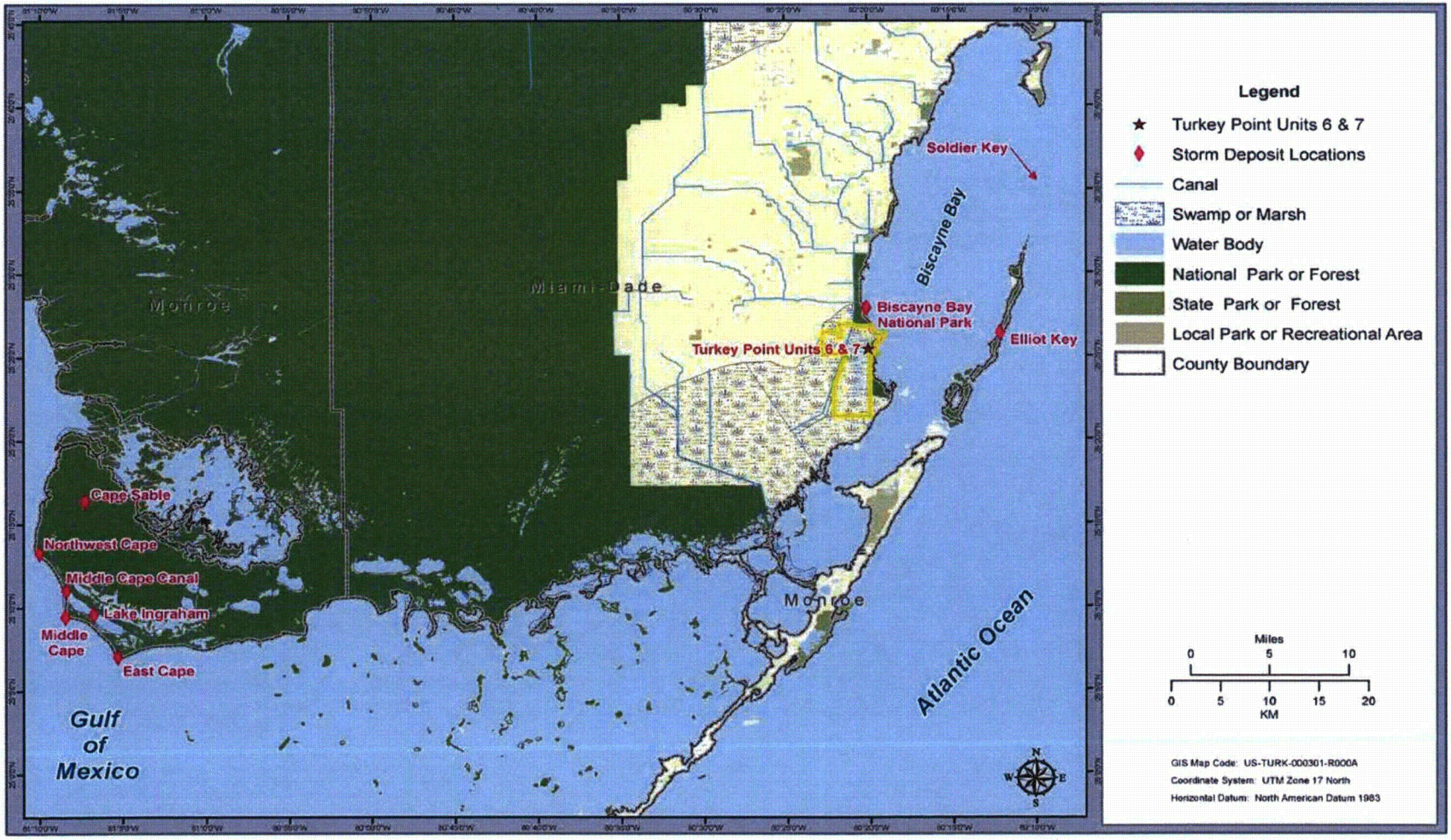

This response is PLANT SPECIFIC.

References:

1. Li, Y. *Calcareous Soils in Miami-Dade County*, Fact Sheet SL 183, Soil and Water Science Department, Florida Cooperative Extension Service, Institute of Food and Agricultural Sciences, University of Florida, 2001.
2. Abtew, W., Pathak, C., Huebner, R.S., and Ciuca, V., "Hydrology of the South Florida Environment," *2010 South Florida Environmental Report,* Vol. I, Chapter 2, p. 73, 2010. Available at http://www.sfwmd.gov/portal/page/portal/pg_grp_sfwmd_sfer/portlet_sfer/tab2236037/2010%20report/v1/chapters/v1_ch2.pdf, accessed August 21, 2012.
3. Wanless., H. R., and Vlaswinkel., B. M., *Coastal Landscape and Channel Evolution Affecting Critical Habitats at Cape Sable, Everglades National Park, Florida,* Final Report to Everglades National Park Service United States Department of Interior, p. 196, 2005.
4. Swiadek, J. W., "The Impacts of Hurricane Andrew on Mangrove Coasts in Southern Florida: A Review," *Journal of Coastal Research*, Vol. 13, No. 1, pp. 242–245, 1997.
5. Shanmugam, G., "Process-sedimentological challenges in distinguishing paleo-tsunami deposits," *Natural Hazards*, Vol. 63, pp. 5–30, 2011.

ASSOCIATED COLA REVISIONS:

The fifth paragraph in FSAR Subsection 2.5.1.2.2 will be replaced with the following paragraphs in a future revision of the FSAR:

The Holocene section at the Turkey Point Units 6 & 7 site is classified as marl, wetland soils belonging to the saprist (muck) group, and peat. Surficial deposits in the relatively flat areas outside the vegetated depressions at the Turkey Point site were variably characterized as either marls (clay and elastic silt), organic-rich elastic silt, or peat sediments (Reference 996). The surficial layers within the vegetated surface depressions at the Turkey Point site were characterized as peat (Reference 996). Laminated surficial deposits found mostly outside vegetated depressions are interpreted to have likely resulted from cyclical changes in oxidation-reduction conditions and/or chemical equilibria, in which dark colored, organic-rich sediments were likely deposited under flooded, low-oxygen (reducing) conditions, and light colored, carbonate-rich (HCl reactive) laminae were likely deposited under open marsh, shallow water (and thereby less anaerobic) conditions (Reference 996). In coastal Florida wetlands, marl deposition is typically associated with freshwater conditions. Within the Turkey Point site cores, evidence for historic freshwater conditions is provided by the presence of intact specimens of Planorbella spp., a freshwater gastropod (Reference 996).

Saprist soils are generally defined as those in which two-thirds or more of the material is decomposed, and less than one-third of plant fibers are identifiable (Reference 276). Eighty-eight borings were drilled and sampled (standard penetration test [SPT]

samples in soil, continuous coring in rock) as part of the Turkey Point Units 6 & 7 initial subsurface investigation (Reference 708). During the supplementary investigation, a total of nine borings are drilled (Reference 995), with three of the borings inclined towards surface depressions. In addition, surficial "muck" deposits (soft, surficial soil, and sediment layers) samples are collected at nine locations (Reference 996). Drilling and sampling locations are shown on Figure 2.5.1-378. The description of the Holocene section (i.e., "muck" deposits [soft, surficial soil, and sediment layers]) in the soil borings across the Units 6 & 7 site (References 708, 995, and 996), includes the thickness, color, hardness, and the presence of organics, silt, roots, and shell fragment contents. The surficial deposits were sampled at the site every 2.5 feet (0.8 meters) using the SPT geotechnical sampling method during the initial site investigation (Reference 708) and sampled continuously in 2013 using a McCauley Sampler (Reference 996). The muck soils are classified under the Unified Soil Classification System in accordance with ASTM D2488-06. Modifiers such as trace (<5 percent), few (5 to 10 percent), little (15 to 25 percent), some (30 to 45 percent) and mostly (50 to 100 percent) were used to provide an estimate of the percentage of gravel, sand and fines (silt or clay size particles), or other materials such as organics (muck) or shells. In general, the thickness of the surficial deposits ranges from 2 to approximately 11 feet (0.6 to 3.4 meters). Muck is observed in the geotechnical borings and the multichannel analysis of surface waves (MASW) survey data across the site. The surficial deposits are thicker in the areas of the surficial dissolution features (vegetated depressions), filled entirely with peat (Figures 2.5.4-229 and 2.5.4-230). Color ranges from black to light gray, dark grayish brown to light brownish gray, and dark olive brown to light olive brown. Mottled coloration is also noted in the muck. The consistency of the muck is very soft-to-soft. Peat with fibrous internal structure, is identified within organic soils in 13 of the site borings (B-614, B-625, B-626, B-702, B-715, B-725, B-727, B-729 R-6-1a, R-6-1a-A, R-6-1b, R-6-2 and R-7-4) as well as in all borings sampled continuously using the McCauley Sampler (FSAR 2.5.1 Reference 996). The organic content of the muck (elastic silt and organic-rich silt) was estimated to vary from some 2.9 to 30.3 percent, with an average of 10.6 percent (Reference 996)

Only one sample from boring B-601 (DH) contains "mostly silt." Trace to some sand is noted in three borings: B-617, B-623, and B-723. Neither the sand nor the silt can be correlated across the site as continuous stratigraphic units. However, fine-grained calcareous material, marl, appears to overlie the muck in 10 borings: B-736, B-738, B-802, B-810, B-812, B-813, M-6-1b, M-6-2a, M-7-1a, and M-7-2c. This marl-like material is described as a fat clay to sandy fat clay and elastic silt that is light/dark gray to greenish gray, very soft, moist to wet, with some fine grained sand and strong hydrochloric reaction (References 708 and 996). Where present, the marl/elastic silts represent the uppermost surficial sediments. This type of marl deposit forms when the ground surface is flooded for several months each year in the summer followed by a number of dry months during the winter (hydroperiod). During the hydroperiod, the microalgae (periphyton) grow on the surface water. The precipitation of the microalgae from the calcium bicarbonate saturated water creates marl (Reference 909).

It is important to note that the surficial deposits described at the Turkey Point site generally correspond to the surficial sediment sequences described within other

coastal wetland systems adjacent to Biscayne Bay (References 397, 997, and 998). Moreover, the thickness of the surficial sediments at the Turkey Point site is similar to those reported for other coastal wetland locations in southern Florida and the greater circum-Caribbean, including the Bahamas and Bermuda (Reference 996).

~~The surface of the site consists of approximately 2 to 6 feet (0.6 to 1.8 meters) of organic soils called muck. The muck comprises recent light gray calcareous silts with varying amounts of organic content. The surface elevations for the top of the organic soil ranged from +0.2 to 1.8 feet (0.06 to 0.55 meters) MSL (Figures 2.5.1-334 and 2.5.1-337).~~

The following reference will be added to FSAR Subsection 2.5.1.3 in a future revision of the FSAR.

909. Li, Y. *Calcareous Soils in Miami-Dade County*, Fact Sheet SL 183, Soil and Water Science Department, Florida Cooperative Extension Service, Institute of Food and Agricultural Sciences, University of Florida, 2001.

ASSOCIATED ENCLOSURES:

None

NRC RAI Letter No. PTN-RAI-LTR-041

SRP Section: 02.05.01 - Basic Geologic and Seismic Information

QUESTIONS from Geosciences and Geotechnical Engineering Branch 2 (RGS2)

NRC RAI Number: 02.05.01-8 (eRAI 6024)

FSAR Section 2.5.1.1.5, "Tsunami Geologic Hazard Assessment," Section 2.5.1.2.1, "Site Physiography and Geomorphology," and Section 2.5.1.2.4, "Site Geologic Hazards," state that an extensive review of scientific literature resulted in no evidence of Quaternary seismically induced or landslide-generated tsunami deposits within the 200-mile radius of the Units 6 & 7 site region. The FSAR adds that sampling performed as part of the subsurface investigations at the Turkey Point site encountered about 1 meter (3 feet) of organic muck overlying Pleistocene and older carbonate strata and that the muck is the dominant surficial sediment type varying in thickness across the site from 2 to 6 feet (0.6 to 1.8 meters). FSAR Figure 2.5.1-332 shows the organic muck section as Holocene. Finally, the FSAR states that examination of Units 6 & 7 has provided no evidence of known tsunami deposits. In light of the foregoing conclusion, the staff notes that the FSAR does not provide an analysis of the Holocene section (muck layers) in the site vicinity with respect to paleo-tsunami or paleo-storm surge events and core data regarding the muck layers is absent from the FSAR.

In order for the staff to understand the Holocene geologic setting of the TPNPP and in support of 10 CFR 100.23 please address the following questions:

a) Provide justification for your conclusion that there are no tsunami deposits at the site with a detailed presentation of the Holocene section, including how it varies across the site in terms of thickness and internal structure.

b) Discuss the organic sediment ("muck") and included silt layers within an appropriate framework for the description of biogenic deposits, such as the Troels-Smith sediment classification system. Provide sufficient detail to illustrate how you evaluated silt layers as either potential storm or tsunami-derived sources.

FPL RESPONSE:

The information requested in part a) and the second sentence of part b) of this RAI is addressed in the responses to RAI 02.05.01-6 and 02.05.01-7. The response to part b) of this RAI addresses the use of the Troels-Smith sediment classification system and an example of how the organic sediment ("muck") and included silt layers are described within this sediment classification system.

The muck soils at the Turkey Point Units 6 & 7 site are classified under the Unified Soil Classification System (USCS) in accordance with ASTM D2488-06 and D2487 instead of the Troels-Smith sediment classification system. The USCS was used because the geotechnical engineering subsurface investigation was conducted for the purpose of foundation design. The USCS provides nomenclature to describe soil in terms of gradation, plasticity, and organic content as determined visually or based on laboratory testing. This widely used classification system is applicable to a wide variety of geotechnical engineering projects. The major soil divisions of the USCS are coarse grained (gravel and sand), fine

grained (silts and clays or clays and silts that are either organic or inorganic), organic soils (organic matter with gravel, sand, silt or clay), and peat.

The Troels-Smith classification system is not applicable for standard geotechnical practice for field subsurface investigations because the focus of the Troels-Smith classification system is to reconstruct paleodepositional environments and climate. The Troels-Smith sediment classification system is a comprehensive classification system that is used by palynologists, paleoclimatologists, paleoecologists, and limnologists to describe organic-rich sediments deposited in northern temperate lakes, and wetlands. The classification was originally designed primarily as a field-based system but could be expanded to include laboratory analysis (i.e. determining peat humification, quantifying peat bulk density, organic matter, and carbon content). It has been widely applied by European paleoecologists because the more specialized terms are applicable to northwestern Europe (i.e. Finland, Sweden, Norway, northern Russia, Great Britain, and Ireland), the region for which they were originally devised (Reference 1).

The Troels-Smith classification system describes deposits based on physical properties, humicity (the degree of decomposition of organic substances), and composition. Physical properties are further characterized in terms of the degree of darkness (Nigror), the degree of stratification (Stratifacto), the degree of elasticity (Elasticitas), and the degree of dryness (Siccitas). Composition comprises six classes to describe the properties of sediments. The classes are Substantua humosa, Turfa, Detritus, Limus, Argilla and Grana. For all composition classes, a scale of 0-4 is used for characterization. Zero describes the absence of the element concerned and 4 the maximum presence (References 1 and 2). If FPL had used the Troels-Smith classification system at the Turkey Point Units 6 & 7 site, a hypothetical example of sample descriptions of the deposits of marl and muck with silt layers would be as follows:

Class: Limus calcareus

Symbol: Lc

Description: Marl

Degree of Darkness: clear

Degree of Stratification: 0

Degree of Elasticity: 0

Degree of Dryness: 2

Color: very dark gray

Structure: homogenous

Sharpness of Boundary: diffuse

Humicity: no record

Class: Argilla granosa

Symbol: Ag

Description: Silt

Degree of Darkness: 0

Degree of Stratification: 3, 4

Degree of Elasticity: 1

Degree of Dryness: 2

Color: white

Structure: homogenous mixed with marl and or muck

Sharpness of Boundary: gradual and sharp

Humicity: no record

Class: Turfa

Symbol: Th

Description: Herbaceous Peat

Degree of Darkness: 3

Degree of Stratification: 0

Degree of Elasticity: 3

Degree of Dryness: 2

Color: very dark brown to black

Structure: fibrous, muck

Sharpness of Boundary: sharp

Humicity: no record

Furthermore, using the Troels-Smith sediment classification system would not have been compatible with the USCS and additional geotechnical laboratory analyses and calculations. This classification system is normally not used in the United States, with the exception of possible studies in limnology, paleoclimatology, paleoecology, and palynology.

This response is PLANT SPECIFIC.

References:

1. Schnurrenberger, D., Russell, J., and Kelts, K, 2003. Classification of lacustrine sediments based on sedimentary components, Journal of Paleolimnology, Vol 29, pp. 141-154.
2. Kershaw, A. P., 1997. A modification of the Troels-Smith system of sediment description and portrayal, Quaternary Australasia, Vol 15, no. 2, pp. 63-68.

ASSOCIATED COLA REVISIONS:

COLA revisions associated with this revised RAI response are presented in the revised response to RAI 2.5.1-7.

ASSOCIATED ENCLOSURES:

None

NRC RAI Letter No. PTN-RAI-LTR-041

SRP Section: 02.05.01 - Basic Geologic and Seismic Information

QUESTIONS from Geosciences and Geotechnical Engineering Branch 2 (RGS2)

NRC RAI Number: 02.05.01-9 (eRAI 6024)

FSAR Figures 2.5.1-243 and -262 illustrate seismic reflectors of the Florida and Bahamas Platform, and a large slump offshore from the site area is labeled "HOLO.-UP. OLIG." on Figure 2.5.1-243. This feature is located at kilometer 50 on Line 71 and 73 on Figure 2.5.1-262. However the staff notes that there is no discussion in the FSAR regarding this feature.

In order for the staff to fully understand site-specific geology and in support of 10 CFR 100.23, please clarify if this feature is a slump and if it bears upon the tsunami hazard of the site area.

FPL RESPONSE:

FSAR Figures 2.5.1-243 and -262 illustrate seismic reflectors in the northern Straits of Florida. The feature at the top of the upper Oligocene-Holocene ("HOLO.-UP. OLIG.") seismic stratigraphic section is a sigmoid clinoform rather than a large offshore slump. This same feature is also seen in FSAR Figure 2.5.1-262, located approximately at kilometer 50 on Lines 71 and 73.

A clinoform is a sloping dipping surface that is commonly associated with strata prograding into deep water (Reference 6). Sigmoid clinoforms (s-shaped reflection patterns) are interpreted as strata with thin, gently dipping upper and lower segments, and thicker, more steeply dipping middle segments. In general, sigmoid clinoforms tend to have low depositional dips or angles for the upper segments, typically less than 1 degree, and are parallel with the upper surface of the facies unit with no strata termination with the bounding surfaces (Reference 5). The sigmoid clinoforms that formed
in the northern Straits of Florida nearly match the third order sea level fluctuations on the global cycle chart (Reference 3). A third order sea level fluctuation or sequence is a depositional sequence that has a duration in the order of 1 million to 10 million years with a relative sea level amplitude of 50 to 100 meters and a relative sea level rise/fall rate of 1 to 10 centimeters per 1,000 years (Reference 4).

The progradation of sediments that form the clinoforms in the Straits of Florida was caused by a sea level drop. The drop in sea level occurred approximately during the middle Miocene. Steep prograding drift clinoforms within the Straits of Florida indicate that a western boundary paleo-Florida Current had developed and the Straits of Florida had become the major pathway for the Florida-Gulf Stream surface current system by the middle Miocene (Reference 1 and Reference 2).

FSAR Figure 2.5.1-243

Multichannel seismic line MC92 was run across the northern Straits of Florida to tie to the Key Largo well, KL, and the Great Isaac Island well, GI-1. The seismic-stratigraphic evidence seen in line MC92 indicates that the Straits of Florida first began to develop as a

deep-water area during the Cenomanian (lower Upper Cretaceous). Prior to this, Albian (upper Lower Cretaceous) and older sedimentary units were deposited on a shallow-water bank, which was continuous from southern Florida to the Great Bahama Bank (FSAR 2.5.1 References 307 and 424).

The upper Oligocene-Holocene seismic unit, "HOLO.-UP. OLIG," indicates progradation toward the west (i.e. sigmoidal clinoform beds), resulting in an asymmetric ridge. This asymmetric ridge, as seen in single-channel seismic reflection profiles, is an elongate north-south ridge building towards the southwest as a tongue of sediments. Sheridan et al., (FSAR 2.5.1 References 307 and 424) interpreted a near-bottom countercurrent as the depositional mechanism for this ridge.

FSAR Figure 2.5.1-262

FSAR Figure 2.5.1-262 consists of continuous seismic profiles across the Straits of Florida. The profiles have a vertical exaggeration of 10 X. The profiles were drawn from the original recordings obtained in the field.

On Profiles 71 and 73, the slope flanking the Miami Terrace on the east is covered by a thin veneer of sediments and is separated from a broad sedimentary ridge to the east by a narrow depression, labeled "E." This ridge extends to latitude 26 degrees N where it grades into the western side of the slope of the Straits of Florida. Reference 7 suggests that the ridge formed by sediment progradation in a southward direction with some outbuilding to the east and west.

Conclusion

Since the apparent slump is interpreted as a progradational depositional feature, it does not bear upon the tsunami hazard in the site region.

This response is PLANT SPECIFIC.

References:

1. Anselmetti, F., Eberli, G., and Ding, Z., "From the Great Bahama Bank into the Straits of Florida: A Margin Architecture Controlled by Sea-Level Fluctuations and Ocean Currents," *GSA Bulletin*, v. 112, no. 6, pp. 829-844, Geological Society of America, 2000.
2. Bergman, K.L., *Seismic Analysis of Paleocurrent Features in the Florida Straits: Insights into the Paleo-Florida Current, Upstream Tectonics, and the Atlantic-Caribbean Connection*, University of Miami, Coral Gables, Florida, p. 238, 2005.
3. Eberli, G., Kendall, C., Moore, P., Whittle, G., and Cannon, R., Testing a Seismic Interpretation of Great Bahama Bank with a Computer Simulation., AAPG Bulletin, v. 78, pp. 981-1004, 1994.

4. SEPM, Third-order Sequence, http://sepmstrata.org/terminology/third-order-cyc.html, accessed on 10/12/2011.
5. SEPM, Sigmoid configuration, http://sepmstrata.org/terminology/sigmoid.html, accessed on 10/12/2011.
6. Miall, A., Principles of Sedimentary Basin Analysis, Springer, 3rd Edition, Berlin, 1999.
7. Uchupi, E., Shallow Structure of the Straits of Florida, Science, v. 153, no. 3735, pp. 529-531, 1966.

ASSOCIATED COLA REVISIONS:

None

Enclosures:

None

NRC RAI Letter No. PTN-RAI-LTR-041

SRP Section: 02.05.01 - Basic Geologic and Seismic Information

QUESTIONS from Geosciences and Geotechnical Engineering Branch 2 (RGS2)

NRC RAI Number: 02.05.01-10 (eRAI 6024)

FSAR Section 2.5.1.1, Regional Geology, describes Large Igneous Province (LIP) magmatic events and the East Coast Margin Igneous Province (ECMIP) which includes the eastern edge of the Blake Plateau and Bahamas Platform. The FSAR states that the LIPs are massive crustal emplacements of mafic rock that include oceanic plateaus. Conceivably this would be an area of thickened oceanic crust. FSAR Figure 2.5.1-224 illustrates a schematic cross section of the crust and overlying carbonate bank system that changes from extended, transitional continental ultimately to normal oceanic crust (presumably), but also illustrates a zone of apparently thin oceanic crust with a thick, overlying carbonate bank system. In order for the staff to understand the variability in the nature and thickness of the underlying crust of the TPNPP region and in support of 10 CFR 100.23, please provide information for the following:

a) Discuss the location of the ECMIP with respect to transitional continental, thickened and normal oceanic crust; the location of the carbonate bank system and; the current platform bathymetry.

c) Discuss the impact of crustal thickness variations on the ground motion models and subsequent impacts on the seismic hazard curves of the Caribbean sources.

d) Discuss the possibility that the magnetic highs located along the eastern Bahamas Platform and Little Bahamas Bank reflects the location of a southern extension of the ECMIP and thickened oceanic crust.

FPL RESPONSE:

This response addresses the following: (a) the location of the east coast margin igneous province (ECMIP) (east coast magnetic anomaly, ECMA) and its associated transitional continental, thickened, and normal oceanic crust, and the location of the Florida-Bahama carbonate bank system with respect to the ECMIP (Blake Spur Magnetic Anomaly, BSMA); and the current platform bathymetry, (c) the impact of crustal thickness variations on the ground motion models and subsequent impacts on the seismic hazard curves of the Caribbean sources and (d) the potential that the magnetic highs that are located along the eastern portion of the Bahama Platform are related to the ECMIP (BSMA).

(a) Large igneous provinces (LIPs) consisting of tholeiitic basalt lava flows, sills and dikes have formed throughout the geologic history of the Earth. In general, the LIPs are major bodies of extrusive igneous rock underlain by intrusive rock with crustal thickness ranging from 20 to 40 km. The crustal structure of LIPs are comprised of an extrusive upper crust and a lower crust characterized by high seismic velocities (7.0-7.6 kms/s) and are different from "normal" oceanic or continental crust. The possible compositions of lower crustal bodies on volcanic margins are gabbroic, strongly mafic, and ultramafic rocks. Some lower crustal bodies have been explained as magmatic underplating by accumulating mantle-derived material below the original crust (FSAR Reference 237). During the initial breakup

of Pangea in the Late Triassic-early Jurassic, many LIPs formed as the result of rifting, basalt extrusion, and mafic intrusions. The most notable LIPs are the Central Atlantic Magnetic Province (CAMP) and the east coast margin igneous province (ECMIP). The total volume of lava for both the ECMIP, which is the source of the east coast magnetic anomaly (ECMA), and CAMP had exceeded 2.3 million km^3 (FSAR Reference 239).

The CAMP is among the largest of the continental igneous provinces on Earth, emplaced synchronously with, or just prior to, the Triassic-Jurassic boundary ca. 200 Ma. Magmatism associated with the CAMP occurred from 202 to 190 Ma. Intrusive CAMP magmatism commenced as early as 202 Ma. Extrusive activity initiated abruptly ~200 Ma, reaching peak volume, and intensity around 199 Ma on the African margin. There were at least two phases over ~ 1.5 Ma, with magmatism commencing along the Africa-North American margins and slightly later along the South American margin (Nomade et al. 2007). The extent of CAMP during the Mesozoic as described by McHone (FSAR Reference 239) was from "within Pangea from modern central Brazil northeastward about 5000 km across western Africa, Iberia, and northwestern France, and from Africa westward for 2500 km through eastern and southern North America as far as Texas and the Gulf of Mexico".

The precursor to the formation of the Central Atlantic Ocean (CAO) crust and the opening of the CAO was widespread groups of dike-fed fissure eruptions and flood basalts, which started during the Early to Middle Jurassic along sections of the central Atlantic rift (Janney and Castillo, 2001, and FSAR 2.5.1 References 239 and 241). The occurrence of CAMP magmatism and the volcanic rift margin adjacent to the newly forming oceanic crust along the eastern margin of North America is interpreted as subaerial volcanic flows or basalt wedges (also indicated by seaward-dipping seismic reflectors [SDRs], FSAR Figure 2.5.1-284) (FSAR Reference 239).

Within the South Georgia rift basin, in the southeastern United States, the continental flood basalts overlap the SDRs. The SDRs are ~ 25 km thick basalt and plutonic wedges that is about 55 km wide along roughly 2000 km of the eastern North American margin. These SDRs comprise the East Coast Magnetic Anomaly (ECMA), which has been referred to by Holbrook and Kelemen (1993) as the east coast margin igneous province or ECMIP (McHone, 2000 and FSAR Reference 239).

The ECMA marks the boundary between continental and ocean crust (FSAR Figure 2.5.1-266). It forms the seaward edge of the deep, sediment-filled basins and the landward edge of normal oceanic crust (Behrendt and Klitgord, 1980). The location of the ECMA segmented magnetic high (200-300nT, positive magnetic anomaly) as seen in the total field magnetic anomaly, bathymetry, free-air gravity, isostatic anomaly and R-T-P anomaly maps parallels the East Coast margin from the Blake Spur fracture zone (BSFZ) to Nova Scotia (Figures 1 and 2) (Keen, 1969; Emery et al., 1970, Behn and Lin, 2000 and Wyer and Watts, 2006). Holbrook and Kelemen (1993) were able to create a velocity model that showed lateral changes in deep crustal structure across the ECMA margin. Lower crust velocities average 6.8 km/s at what were believed to be rifted crust areas, whereas the velocity (*Vp*) of units below the outer continental shelf were recorded as 7.5 km/s, decreasing to 7 km/s with lateral shift to the oceanic crust. Holbrook and Kelemen (1993) were able to determine that the high velocity (*Vp*) lower crust and SDRs comprise a 100 km

wide, 25 km thick oceanic-continental transition zone that they interpreted to be almost entirely mafic igneous material. This created an abrupt boundary between rifted continental crust and thick igneous crust, comprising only 20 km of the margin. Holbrook and Kelemen (1993) found that the Appalachian intracrustal reflectivity largely disappears across the boundary as velocity (*Vp*) increases from 5.9 km/s to greater than 7 km/s, implying that the reflectivity is disrupted by massive intrusion and that very little (if any) continental crust can be found east of the SDRs.

The Blake Spur Magnetic Anomaly (BSMA) is a linear anomaly located near the Blake Escarpment, east of the southern portion of the ECMA (ECMA and the BSMA are conjugate anomalies and they both coincide with the ocean-continent boundary) and north of the Little Bahama Bank (FSAR Figure 2.5.1-266) (FSAR Reference 466). The BSMA represents points of initiation of sea floor spreading between North America and northwest Africa (FSAR Reference 692) and is interpreted as a continental margin modified by a jump in the spreading center (FSAR Reference 424) during the early Callovian (middle Jurassic). Ridge jumps are possibly caused by the reheating of the lithosphere as magma penetrates it to feed near-axis volcanism (Mittelstaedt et al. 2008) and can be related to plate interactions as North America separated from Gondwana (FSAR Reference 466). It has been suggested that the BSMA is the result of an eastward jump of the spreading center away from the ECMA prior to 170 Ma (FSAR Reference 466).

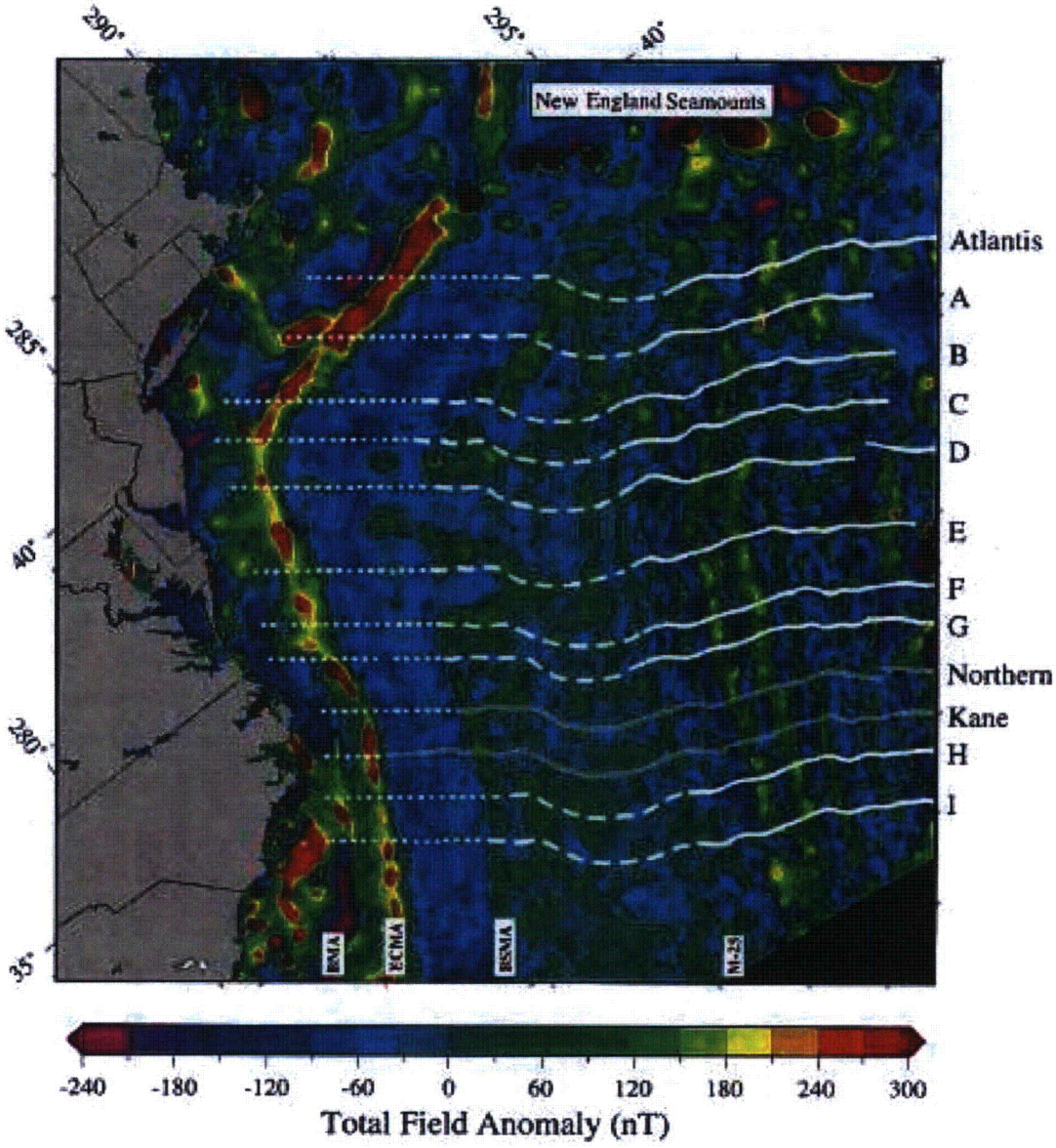

Figure 1. Total field magnetic anomaly from the Geological Survey of Canada modified in Behn and Lin, 2000. Areas without adequate data control are masked in black. The segmented magnetic high running parallel to the margin is the ECMA. Solid gray lines show the location of the Kane and Northern fracture zones, white lines show the location of the offset zone traces identified in Behn and Lin (2000), solid lines represent areas where the offset zone traces are constrained by offsets in magnetic lineations; dashed lines are used where the traces are primarily constrained and the dotted lines are used to represent the high uncertainty in the location of the offset zone traces between the BSMA and the East Coast margin. The right hand margin labels are major offset zones (Atlantis, Kane, Northern, and A-I).

Source: Behn and Lin, 2000

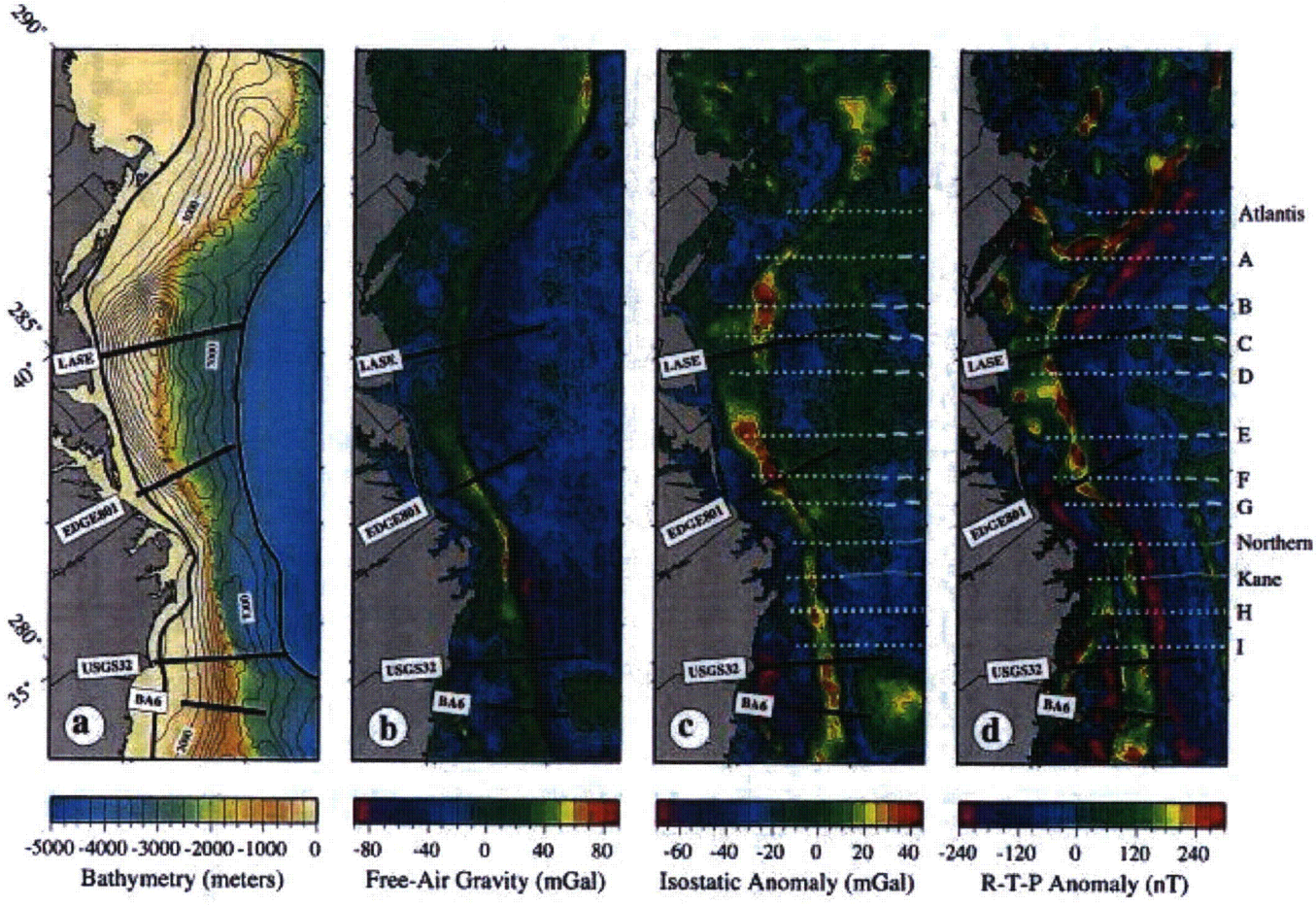

Figure 2. (a) Shaded bathymetry of the U.S. East Coast, combining National Geophysical Data Center (NGDC) ship track data and ETOPO5 (Earth Topography 5-minute) digital bathymetry data.Light black contour lines show sediment thickness from USGS seismic reflection grids and thick black lines show the extent of the USGS data coverage. (b) Free-air gravity satellite gravity map. (c) Isostatic gravity anomaly map. (d) Reduced-to-the-pole (R-T-P) magnetic anomaly along the East Coast margin. LASE (Large Aperture Seismic Experiment), EDGE-801, USGS32 and BA-6 are seismic transect lines.

Source: Behn and Lin, 2000

(c) The development of the Caribbean ground motion prediction equations (GMPEs) was based on the regional attenuation parameters (e.g., anelastic Q attenuation model and geometrical spreading model) from the Motazedian and Atkinson (2008) study (FSAR Reference 287). In their study, regional attenuation parameters were estimated from the empirical ground motion dataset of earthquake recordings located within 500 km of the island of Puerto Rico. These empirically estimated regional attenuation parameters are correlated with the regional crustal structure in the region around the island of Puerto Rico. For the development of the Caribbean GMPEs, the anelastic Q attenuation model, which is frequency-dependent, was varied to account for any possible variation of ground motion amplitudes related to any crustal differences between the regions around the island of Puerto Rico and the regions closer to the Turkey Point site.

In addition, a sensitivity study was conducted in which the Q model from a more typical Gulf Coast crustal structure was used rather than a region-specific crustal structure. The conclusion of this sensitivity study was that the use of the Gulf Coast Q model led to lower ground motions and as such was not included in the final GMPEs for the Caribbean seismic sources. To be consistent with the GMPEs used for the EPRI-SOG seismic sources, the Caribbean GMPEs were developed for a hard rock site condition with a minimum shear-wave velocity (Vs) = 9200 feet per second (fps), which at the site is located at about 10,000 feet (3050 meters) below the ground surface (FSAR Subsection 2.5.2.5).

Based on the large azimuthal range in relative crustal ray paths from all seismic sources (i.e., both Caribbean and EPRI-SOG seismic sources) to the Turkey Point site, both the Caribbean and EPRI GMPEs are intended to represent the average regional ground motion amplitudes, not the specific ground motion amplitudes that one might expect for a specific seismic ray path and associated crustal structure. The potential variation in ground motion amplitudes caused by specific ray paths through different crustal structures is expected to be accounted for through the range of GMPEs used in the analysis.

(d) Magnetic highs located near the eastern portion of the Bahamas Platform (including the Little Bahamas Bank) represent both positive and negative magnetic anomalies related to structural controls from post Lower Cretaceous folding or faulting in the basement rocks of the Bahama Platform (see FSAR Subsection 2.5.1.1.1.3.2.2.). The density contrasts below the sea floor as seen from the Bouguer gravity anomaly maps (FSAR Figures 2.5.1-254 and 256) in this area show that the intraplatform straits (and channels) and basins correlate with the present day platform topography (FSAR Figure 2.5.1-254). In general, the straits and basins are areas of negative anomaly while the platforms are generally areas of positive anomaly. The negative anomalies occupied areas of structural lows, probably downfaulted, and that their negative signature stemmed from a combination of downfaulting of relatively light material and infilling of the resulting lows with light sediments (Ball, 1967).

The Blake-Bahamas Platform is related to and limited by, a regional structural feature, the crustal transition zone, in which Jurassic volcaniclastics are tilted in fault blocks (Ball, 1967, and FSAR 2.5.1 References 307 and 424). The transitional crust has a smooth, circular magnetic anomaly pattern (FSAR Figures 2.5.1-254 and 256). This zone is known as the ECMA and includes the BSMA (FSAR Figure 2.5.1-266) (Dietz, 1973 and FSAR Reference 466). The presence of thick volcanics on the oceanic basement of the Blake Plateau infers

that the Bahamas Platform and Little Bahamas Bank overlie seamounts that were produced by CAMP magmatism. This also infers that volcanic activities continued as seafloor was accreted in the CAO (Dietz, 1973 and FSAR Reference 466). A basement map of the Florida-northern Bahamas region using seismic data complied by Sheridan et al. (FSAR Reference 307) (Figure 3) shows the continental, transitional, and oceanic basement rocks along with their approximate ages. Sheridan et al. (FSAR Reference 307) concluded that the "transitional crust underlies the northwestern Bahamas to the projected BSMA, and that oceanic crust underlies the Bahamas farther southeast".

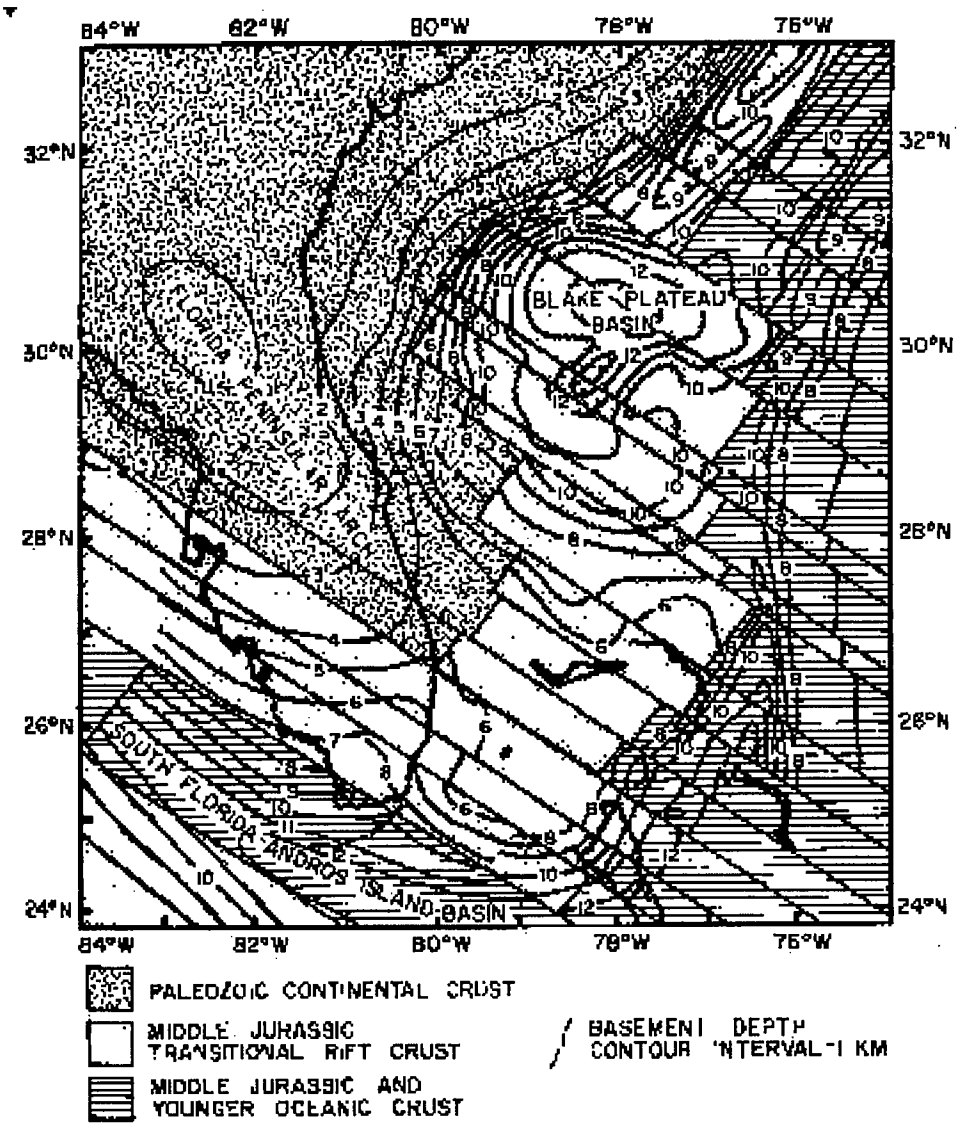

Figure 3. Basement map of the Florida-northern Bahamas region showing depth in kilometers and basement type (continental, transitional or oceanic with approximate age ranges).

Source: modified from FSAR Reference 307

Conclusion

In general, the LIPs are large bodies of extrusive igneous rock underlain by intrusive rock with crustal thickness ranging from 20 to 40 km. The crustal structure of LIPs are comprised of an extrusive upper crust and a lower crust characterized by high seismic velocities (*Vp* 7.0-7.6 km/s) and are different from "normal" oceanic or continental crust. The possible compositions of lower crustal bodies on volcanic margins are gabbroic, strongly mafic, and hot ultramafic rocks. Some lower crustal bodies have been explained as magmatic underplating by accumulating mantle-derived material below the original crust (FSAR Reference 237).

Examples of LIPs on the eastern seaboard of the United States are the ECMA and the BSMA both of which are part of the CAMP magmatic event (approximately 202-190 Ma). The ECMA is a segmented linear magnetic anomaly from Nova Scotia to the Blake Spur Fracture Zone that has a high amplitude, 200-300nT. The BSMA is a linear anomaly just east of the southern portion of the ECMA and north of the Little Bahama Bank.

Kelemen and Holbrook (FSAR Reference 240) report that seismic reflection profiles on the eastern seaboard of the United States show a zone between rifted continental crust and normal oceanic crust that consists of thick (up to 25 kilometers), high velocity (*Vp* of 7.2 to 7.3 kilometers/second) crust interpreted as mafic igneous rocks emplaced during Triassic-Jurassic rifting of Pangea. This zone is part of the CAMP and is known as the ECMA with its conjugate of the BSMA. The BSMA underlies the Bahamas. The presence of thick volcanics on the oceanic basement of the Blake Plateau infers that the Bahamas overlie seamounts that were produced by CAMP magmatism this also infers that volcanic activities continued as seafloor was accreted in the CAO (Dietz, 1973, McHone, 2000 and FSAR Reference 466).

The development of the Caribbean GMPEs was based on the regional attenuation parameters estimated from an empirical dataset of earthquakes recorded in and around the island of Puerto Rico (FSAR Reference 287). To account for any possible variation in ground motions due to the variation in crustal structure between the area around Puerto Rico and the area around the Turkey Point site, the final Caribbean GMPEs included a variation of the anelastic Q model. This variation and resulting variation in the suite of recommended Caribbean GMPEs was intended to capture the range in ground motions from the noted variation in the crust in the region and is consistent with the GMPEs used for the EPRI-SOG seismic sources.

This response is PLANT SPECIFIC.

References:

Ball, M., Tectonic Control of the Configuration of the Bahama Banks, GCAGS Transactions, V. 17, p. 265-267, 1967.

Behn, M.D., and Lin, J., Segmentation in gravity and magnetic anomalies along the U.S. East Coast passive margin: Implications for incipient structure of the oceanic lithosphere, Journal of Geophysical Research, v. 105, p. 25,769-25,790, 2000.

Behrendt, J.C., and Klitgord, K.D., High-sensitivity aeromagnetic survey of the U.S. Atlantic continental margin: Geophysics, v. 45, no. 12, p. 1813-1846, 1980.

Dietz, R. S., Morphologic fits of North America/Africa and Gondwana: A review, in Tarling, D. H., and Runcorn, S.K., (eds.) Implications of continental drift to the earth sciences, vol. 2, London, Academic Press, p. 865-872, 1973.

Emery, K.O., Uchupi, E., Phillips, J.D., Brown, C.O., Bunce, E.T., and Knott, S.T., Continental rise off eastern North America: AAPG Bulletin, v. 54, p. 44-108, 1970.

Holbrook, W.S., and Kelemen, B., Large igneous province on the United States Atlantic margin and implications for magmatism during continental breakup: Nature, v. 364, p. 433-436, 1993.

Janney, P.E. and Castillo, P.R., Geochemistry of the oldest Atlantic oceanic crust suggests mantle plume involvement in the early history of the central Atlantic Ocean, Earth and Planetary Science Letters, v. 192, p. 291-302, 2001.

Keen, M.J., Possible edge effect to explain magnetic anomalies off the eastern seaboard of the U.S.: Nature, v. 222, p. 72-74, 1969.

McHone, J.G., Non-plume magmatism and rifting during the opening of the central Atlantic Ocean, Tectonophysics, v. 316, p. 287-296, 2000.
Mittelstaedt, E., Ito, G and Behn M.D., Mid-ocean ridge jumps associated with hotspot magmatism, Earth and Planetary Science Letters, V. 266, issues 3-4, p. 256-270, 2008.

Motazedian, D., and Atkinson, G., *Ground-Motion relations for Puerto Rico*, Geological Soc. America, Special Paper 385, p. 61–80, 2005.

Nomade, S., Knight, K.B., Beutel, E., Renne, P.R., Verati, C., Feraud, G., Marzoli, A., Youbi, N., and Bertrand, H., Chronology of the Central Atlantic Magmatic Province: Implications for the Central Atlantic rifting processes and the Triassic-Jurassic biotic crisis, Palaeogeography, Paleoclimatology, Paleoecology, v. 244, p. 326-344, 2007.

Wyer, P., and Watts, A.B., Gravity anomalies and segmentation at the East Coast, USA continental margin, Geophysical Journal International, v. 166, p. 1015-1038, 2006.

ASSOCIATED COLA REVISIONS:

None

ASSOCIATED ENCLOSURES:

None

SRP Section: 02.05.01 - Basic Geologic and Seismic Information

QUESTIONS from Geosciences and Geotechnical Engineering Branch 2 (RGS2)

NRC RAI Number: 02.05.01-11 (eRAI 6024)

FSAR Section 2.5.1.1.1.3.2 "Principal Tectonic and Structural Features" states that the site region has generally recorded only sedimentary processes since Mesozoic rifting, with the exception of tectonic activity associated with the collision of the Greater Antilles Arc with the Bahamas Platform during Cretaceous to Eocene time. The staff notes that this suggests that there has been no tectonic activity in the site region since the end of the Eocene (~34 Ma). However, the north coast of Cuba, the Walkers Cay fault, the Santaren Anticline, and the Straits of Florida normal faults all occur within the site region and show evidence for post-Eocene tectonic activity.

In order for the staff to fully understand site region specific geology, and in support of 10 CFR 100.23, please address the following: Update this discussion to clarify the timing and location of all tectonic features in the site region and place into the regional tectonic setting.

FPL RESPONSE:

This RAI mentions four structures or groups of structures: the Walkers Cay fault, the Santaren Anticline, the Straits of Florida normal faults, and structures along the north coast of Cuba. Each is addressed below, with a brief discussion of its activity and regional tectonic setting. Updated FSAR discussions are presented in additional RAIs that are specific to each structure, as referenced below.

As discussed in FSAR Subsection 2.5.1.1.1.3.2.2, the Walkers Cay fault is located north of the Little Bahama Bank. Sheridan et al. (FSAR Reference 2.5.1-307) indicate that the Walkers Cay fault may represent a reactivation of buried Mesozoic normal faults within the basement of the Bahama platform. As noted in the response to RAI 02.05.01-14, the interpretation of seismic reflection profiles and mapping of strands of the Walkers Cay fault up to or near the seafloor, documents Pliocene slip and suggests possible Quaternary activity on this fault.

The Santaren Anticline is located along the southern margin of the Bahama Platform and was active up until the Miocene (FSAR Subsection 2.5.1.1.1.3.2.2.). Although Masaferro et al. (FSAR Reference 2.5.1-479) calculated a non-zero fold uplift rate of 0.05 millimeters/year for a Quaternary bed that thinned over the crest of the anticline, since 20 Ma, the calculated fold uplift rates are so low that they are essentially indistinguishable from zero (See RAI 02.05.01-15 for a discussion). As discussed in the FSAR and response to RAI 02.05.01-15, the Santaren Anticline does not have a clear tectonic mechanism, though some authors interpret it as related to the collision of the Greater Antilles Arc with the Bahamas platform (FSAR 2.5.1 References 501and 479).

As described in FSAR Subsection 2.5.1.1.1.3.2.2 and RAI Response 2.5.1-16, the Straits of Florida normal faults were primarily active in the Eocene and acted to thin the overthickened wedge of foreland material shed off the colliding Greater Antilles arc (FSAR 2.5.1 References 221 and 482) (FSAR Figure 2.5.1-229). These structures were active in the Eocene and show very little evidence for younger deformation (Figure 2.5.1-209) though some may have been reactivated in response to far-field effects of collision in

central and southern Cuba during the Miocene (FSAR Reference 2.5.1-484). In summary, these faults are clearly related to the collision of the Greater Antilles arc.

Some structures in northern Cuba exhibit the potential for post-Eocene deformation, and it is possible that some have been active in the Quaternary, although evidence for Quaternary activity on any Cuban fault within the site region is not definitive (see RAI 02.05.01-21). For example, small-scale maps indicate the Pinar fault crosscuts strata as young as lower-to-middle Miocene (FSAR Reference 2.5.1-846). Cotilla-Rodriguez et al. (FSAR Reference 2.5.1-494) suggest the Pinar fault is inactive, but others, including Garcia et al. (FSAR Reference 2.5.1-489), suggest instead that it is active. As suggested by Cotilla-Rodriguez et al. (FSAR Reference 2.5.1-494), other potentially active faults in Cuba within the site region include the Hicacos, Nortecubana, and Las Villas faults. A full discussion of the age uncertainty of the Hicacos, Nortecubana, Las Villas, and Pinar faults is provided in the response to RAI 02.05.01-21.

The statement in the FSAR that generally no tectonic deformation has occurred since the Eocene in the site region outside of the Greater Antilles arc collision will be revised in a future COLA revision to specifically mention the Eocene and younger structures discussed in this RAI. The statement in the FSAR indicates that generally no tectonic deformation has occurred since the Eocene in the site region outside of the Greater Antilles arc collision. The Santaren Anticline and Walkers Cay fault are structures that may have been active in the Miocene or later and have uncertain relationships with the regional tectonic setting. The specifics of those uncertainties are further addressed in RAI Responses 02.05.01-14 and -15. Hence, they are rare exceptions to that general rule and are described as such in the FSAR. The structures along the coast of Cuba and the Straits of Florida normal faults are both probably related to the collision of the Greater Antilles arc with the Bahamas platform. While the Straits of Florida normal faults are predominantly Eocene in age, structures along the coast of Cuba are treated as potentially Quaternary in age (RAI 02.05.01-21).

This response is PLANT SPECIFIC.

References:

None

ASSOCIATED COLA REVISIONS:

The following paragraph of FSAR Subsection 2.5.1.1.1.3.2 will be revised in a future COLA revision as shown below:

2.5.1.1.1.3.2 Principal Tectonic and Structural Features

The site region is covered by a thick sequence of sedimentary rocks and deposits that obscure any Precambrian to Paleozoic tectonic features associated with the formation of Pangea (Figures 2.5.1-240, 2.5.1-242, and 2.5.1-201). In fact, this region has generally recorded only sedimentary processes since Mesozoic rifting, with the exception of the **possible** tectonic activity associated with ~~the collision of the Greater Antilles Arc with the Bahama Platform during Cretaceous to Eocene time~~ **the Cuban fold and thrust belt, possibly active faults in northern Cuba, adjacent Straits of Florida normal faults, the Santaren anticline, and the Walker's Cay fault.** The Florida Platform has been a site of stable carbonate platform deposition continually since the Cretaceous. Variations in

sediment thickness are interpreted as a series of arches, uplifts, basins, or embayments from geophysical or borehole data (Reference 413). Generally, these arches and basins are sedimentary responses to minor warping, regional tilting, sedimentary compaction, or sea level changes and are not considered associated with faulting or tectonic events (Reference 413). In some cases, the highs or lows seen in the stratigraphy may be mimicking Mesozoic paleotopography. The Bahama Platform is also largely undeformed, but does include sparse post-rift faulting or deformation, generally adjacent to the Cuban orogen. The EPRI (Reference 456) earthquake catalog and the updated earthquake catalog completed for the Units 6 & 7 site investigation (Subsection 2.5.2.1) indicate that north of Cuba and the northern Caribbean seismic source model (Subsection 2.5.2.4.4.3) earthquakes are sparsely and randomly distributed within the site region and that none of the earthquakes can be associated with a known geologic structure (Subsection 2.5.2.3).

FSAR Figure 2.5.1-229 will be revised in a future COLA revision to include a label for the Straits of Florida normal faults as shown below:

Figure 2.5.1-229 Regional Tectonic Features

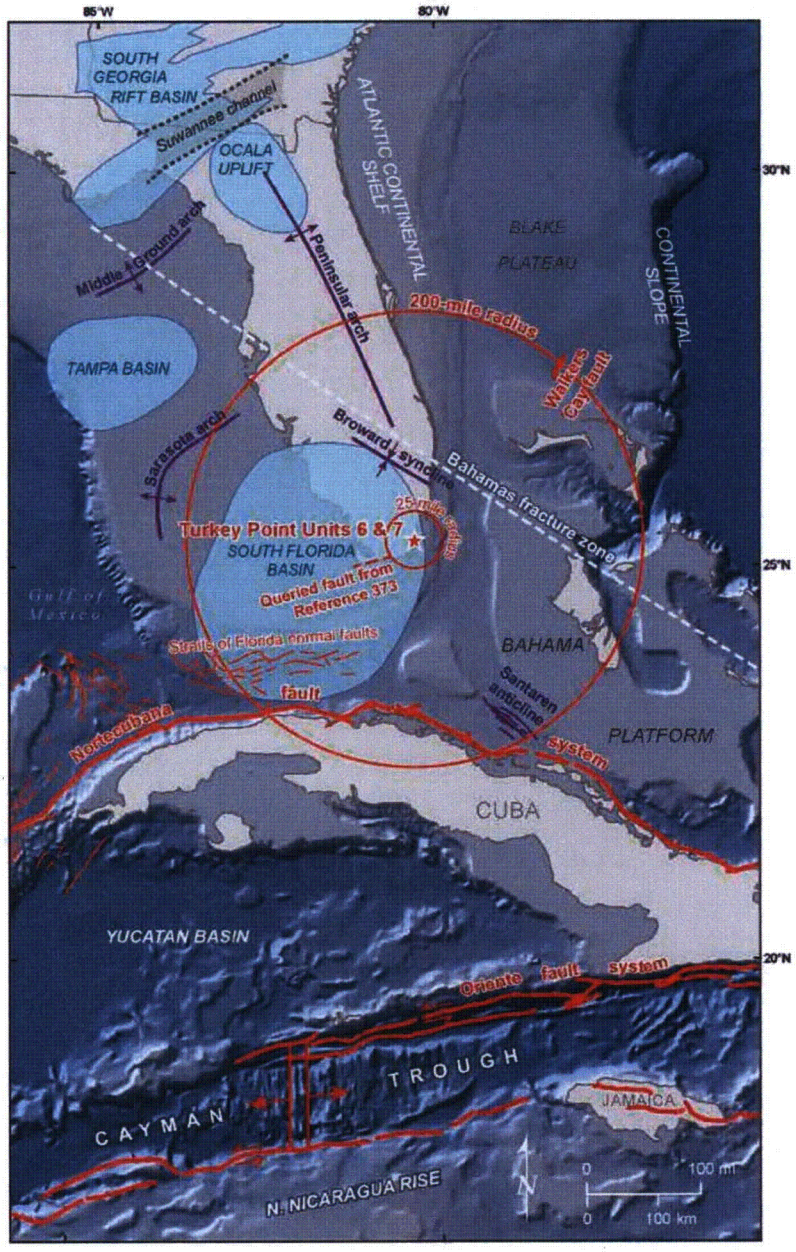

Sources: ~~**FSAR Section 2.5.1.3**~~ **References** ~~**2.5.1-**~~**822, 482, 823, 457, 212, and 421**

ASSOCIATED ENCLOSURES:

None

NRC RAI Letter No. PTN-RAI-LTR-041

SRP Section: 02.05.01 - Basic Geologic and Seismic Information

QUESTIONS from Geosciences and Geotechnical Engineering Branch 2 (RGS2)

NRC RAI Number: 02.05.01-12 (eRAI 6024)

FSAR Section 2.5.1.1.1.3.2.1, "Structures of the Florida Peninsula and Platform" states that occasional variations in pre-Miocene stratigraphy recorded in boreholes due to erosion-based paleo-topography or karst have sometimes been interpreted as possible faulting; for example, the queried fault in Figure 2.5.1-234 (between wells Park W-2404 and Gulf W-3510) appears to displace the base of the Long Key and Arcadia Formations at approximately 100 m and coincides with nearly a doubling in thickness of the Long Key Formation on the downthrown (southern) side. The staff notes that the fault juxtaposes the Long Key Formation against the Arcadia Formation and the Arcadia Formation against the Avon Park Formation. Cunningham et al., 1998 (Reference 373) also provides a structural contour map of the top of the Arcadia formation and a map of net thickness of Miocene-to-Pliocene siliciclastic sand that appears to be consistent with faulting (Figure 17 of Cunningham et al., 1998).

In order for the staff to fully understand site region geology and in support of 10 CFR 100.23, please address the following:

a) Substantiate your interpretation with specific evidence that the stratigraphic relations across the queried fault shown in Figure 2.5.1-234 and depicted in Reference 373 are a result of paleo-topographic or karst processes, rather than tectonic offset.
b) If the queried fault is indeed a fault, please discuss the timing and spatial extent of faulting and update the FSAR discussion accordingly.

FPL RESPONSE:

a) Substantiate your interpretation with specific evidence that the stratigraphic relations across the queried fault shown in Figure 2.5.1-234 and depicted in Reference 373 are a result of paleo-topographic or karst processes, rather than tectonic offset.

Introduction

Cunningham et al. (1998; FSAR Reference 2.5.1-373) provide three depictions of a postulated fault in southern Florida based on borehole data: a cross-section between widely spaced boreholes (Figure 1 [Figure 5 of Cunningham et al. (1998)]); structure contours on the top of the Oligocene-Miocene-age Arcadia Formation (Figure 2 [Figure 17B of Cunningham et al. (1998)]); and contoured thickness of Miocene-Pliocene siliciclastic sands (Figure 3 [Figure 17A of Cunningham et al. (1998)]).

Figure 1 is a modified version of FSAR Figure 2.5.1-234 that shows a cross-section across southern Florida (Figure 5 of Cunningham et al. [1998]). This cross-section was developed with data from eight wells in southern Florida. Between the southernmost two wells, Cunningham et al. (1998) postulate the existence of a fault that cuts up through Avon Park Formation, Suwannee Limestone, and Oligocene-Miocene-age Arcadia Formation, and potentially places the Arcadia Formation in fault contact with the lower portion of the overlying Miocene-Pliocene Long Key Formation. Alternatively, the Long Key Formation may be interpreted as deposited across a paleoscarp. Cunningham et al. (1998) label the postulated fault on this cross-section with two question marks,

indicating the speculative nature of this fault. It should also be noted that Figure 1 includes a variable horizontal scale, which necessarily results in variable vertical exaggeration throughout the cross section. Some of the greatest vertical exaggeration is in the vicinity of the postulated fault.

Figures 17A and 17B of Cunningham et al. (1998) show a dashed and queried fault on two contour maps based on well data: a structure contour map of the top of the Arcadia Formation (Figure 2) and an isopach map of Miocene-Pliocene siliciclastic sediments (Figure 3). The vertical surface projection of the queried fault shown on their contour maps (Figures 2 and 3) roughly corresponds to the location of the queried fault shown on their cross-section (Figure 1). The structure contour map of the top of the Arcadia Formation shows a circular low south of the trace of the fault, controlled by one well, Gulf W-3510, which is approximately 90 - 100 meters lower than the elevation indicated by contours north of the fault (Figure 2). The isopach map of Miocene-Pliocene siliciclastic sediments is contoured to indicate an elongate high in thickness located south of the trace of the fault (Figure 3). Both of the stratigraphic anomalies used to demarcate the fault are mostly limited to the one well south of the fault and do not include data from the wells in the Florida Keys, located more than 40 kilometers to the south. For example, the wells in the Florida Keys have Mio-Pliocene thicknesses similar to the wells north of the fault, rather than the one well immediately south of the structure (Figure 3).

Stratigraphic Data

The two wells on either side of the fault are the Everglades Park well W-2404, which drilled through the top of the Arcadia Formation northeast of the queried fault at a depth of approximately 125 meters, while to the southwest the Gulf Oil well W-3510 drilled through the top of the Arcadia Formation at a depth of approximately 225 meters. Hence, Cunningham et al.'s (1998) cross-section shows approximately 100 m of vertical separation of the top of the Oligocene-Miocene-age Arcadia Formation over a distance of approximately 18 km. As common practice in oil and gas exploration, two of the critical wells were originally logged to obtain geologic information on potential reservoirs within the Cretaceous stratigraphic section. However, Cunningham et al. (1998) use cuttings and logs archived by the Florida Geologic Survey (FGS website, 2012) to reinterpret the stratigraphy of southern Florida. Unfortunately, well W-3510, one of the key wells for the interpretation of the postulated fault, has no sampling of the Arcadia Formation from 231 - 356 meters in depth, and no samples from 375 - 505 m (FGS website, 2012).

Two Hypotheses

Although Cunningham et al. (1998) show a postulated fault in their Figures 5, 17A, and 17B (reproduced in this response as Figures 1 through 3), their figure captions do not describe the queried fault, and no specific discussion of the queried fault is provided in the text of the paper. Cunningham et al. (1998) do, however, discuss the possibility of the existence of either a "tectonically produced low" or "erosional paleotopography" (pp. 254-255):

> "A net thickness map of coarse-grained siliciclastics shows that maximum current strength for transport of the siliciclastics occurred along a corridor from west of Lake Okeechobee to the Florida Keys (Fig. 17A). This corridor of maximum current strength corresponds to a low mapped on a structural contour map on the top of the Arcadia Formation (Figure 17B). This suggests that an accumulation of the coarse-grained siliciclastics was focused within a tectonically produced low or erosional paleotopography at the top of the Arcadia. Testing this hypothesis is an objective of the SFDP [South Florida Drilling Project]. The SFDP will map the thickness of the

> Arcadia Formation in southern Florida and core the top of the Arcadia to establish whether the top of the Arcadia Formation has been eroded or the Arcadia has been structurally lowered."

FPL interprets this text to indicate that Cunningham et al. (1998) consider both paleotopography and tectonic causes as equally plausible explanations for elevation variations of the top of the Arcadia Formation within southern Florida. However, FPL notes that this paragraph does not specifically describe the postulated fault on their figures. The first sentence of the paragraph on their pages 254 and 255 states that "maximum current strength for transport of the siliciclastics occurred along a corridor from west of Lake Okeechobee to the Florida Keys (Fig. 17A)". This corridor of maximum current strength, further interpreted by Cunningham et al. (1998) in the second sentence of the paragraph as a "low mapped on the structural contour map on the top of the Arcadia Formation (Figure 17B)" extends *from west of Lake Okeechobee to the Florida Keys,* and hence, a regional low oriented approximately north-south that crosses the southern portion of the Florida peninsula (similar to the grey dashed line on Figure 17B showing the "coarse-sand channel") (Figures 2 (yellow line) and 3). Without specific discussion of the queried fault drawn in Cunningham et al.'s (1998) Figures 5 and 17, FPL interprets the symbology in the figures and the general discussion on their pages 254-255 to indicate that the queried fault is offered as a speculative potential cause of thickness variations, with paleotopography being an alternate, and equally viable, possible explanation. FPL emphasizes that the Cunningham et al. (1998) paper only presents the queried structure as a possibility and is not positively identifying a fault in southern Florida.

Paleotopography

The queried fault on Cunningham et al.'s (1998) Figure 5 (FSAR Figure 2.5.1-234) is drawn to explain thickness and stratigraphic variations. These variations may instead be related to paleotopography, indeed, the top of the Arcadia Formation is known to have significant paleotopographic variation. On Key Largo, relief on the top of the Arcadia Formation as large as 40 meters was found between borings only a few kilometers apart (Warzeski et al., 1996). Futhermore, in Cunningham et al.'s (1998) Figure 4 (Figure 4), the elevation of the top of the Arcadia Formation varies by approximately 100 meters between wells W-3174 and W-17086 (88 km apart), by 50 meters between wells W-17156 and W12554 (56 km apart), and by 25 m between wells W-3011 and W-17157 (2 km apart). The slope required to achieve this latter elevation variation, 0.7 degrees, is actually greater than the slope required to achieve the elevation variation observed in the Arcadia Formation between the Everglades Park and Gulf Oil wells, where the queried fault is depicted in Figure 5 of Cunningham et al. (1998) (approximately 100 meters over 18 kilometers of distance, or a 0.3 degree slope). Numerous other examples exist throughout southern Florida of steeper paleotopographic slopes on the top of the Arcadia Formation that are not associated with faulting. In addition, the down-to-the-south separation depicted on the postulated fault in Figure 1 is consistent with, and may, in part, be attributed to the regional southward dip of the strata towards the South Florida Basin in the area (e.g., Miller, 1986; Figure 6). Similarly, the increase in the thickness of clastics south of the fault is consistent with thickness variations seen throughout southern Florida associated with proximity to the "coarse sand channel" (Figure 2).

The top of the Arcadia Formation is a known regional unconformity, which allows for the possibility of geologic thickness variations without requiring or indicating faulting (see discussion in FSAR Subsection 2.5.1.1.1.2.1.1). For example, "A distinct regional unconformity and subaerial exposure surface at the top of the Arcadia Formation separates the Long Key and Arcadia Formations" (Warzeski et al., 1996)." A cross-section presented by Warzeski et al. (1996) depicts 90 meters of

relief on the top of the Arcadia Formation surface in southern Florida, while the thickness of the Arcadia Formation varies from 200 meters in the central portion of the Florida peninsula to between 0 and 20 meters farther east (Missimer, 2001). A SFDP study in southern Florida determined that intensification of marine currents increased the erosion of marine carbonates and led to a significant time hiatus (more than 4 m.y.) following deposition of the Arcadia Formation (Guertin et al., 2000) and the influence of Arcadia Formation paleotopography on highs in subsequent carbonate and clastic deposition in southernmost Florida has been recognized (McNeil et al., 2004; FSAR Reference 2.5.1-395).

The karst-influenced paleotopography of the Arcadia Formation is detailed in Hine et al. (2009). While using borings at a much finer spacing than Cunningham study, the Hine study documents karst sub-basins with as much as 100 meters of relief over distances of kilometers to tens of kilometers on the top of the Arcadia Formation in west-central Florida. They attribute this relief to a mid to late Miocene sea-level lowstand that caused dissolution in the deeper carbonates, such as the Arcadia Formation, and formed paleotopographic depressions and non-tectonic deformation in the Arcadia Formation (Hine et al., 2009).

Faulting

Elevation variations on the top of the Arcadia Formation are hypothesized by Cunningham et al. (1998) to be the result of either faulting or erosion. Cunningham et al.'s (1998) postulated fault is depicted in their Figures 5, 17a, and 17b. FPL interprets the use of question marks on Cunningham et al.'s (1998) postulated fault as indicating those authors' uncertainty regarding the existence of this structure, and FPL interprets Cunningham et al.'s (1998) use of a dashed line in the map view to indicate where the queried fault, if it exists, is approximately located.

Alternative interpretations of well data in southern Florida, often including the three wells closest to the postulated fault, provide evidence for unfaulted Eocene to Pliocene stratigraphy in the same location (e.g., Miller, 1986; Warzeski et al., 1996; Guertin et al., 2000; Cunningham et al., 2001). For example, Figure 2 from Guertin et al. (2000) provides a stratigraphic correlation diagram across the projection of the queried fault from Cunningham et al. (1998) and interprets no faulting (Figure 5). This diagram also displays similar relief between boreholes on the top of the Arcadia to the north. Two of the co-authors of Guertin et al. (2000) also are co-authors on the Cunningham et al. (1998) publication. Likewise, the regional north-south-oriented cross-section shown in Scott (2001) intersects the projection of the queried fault and does not indicate faulting in the area (Figure 6).

As shown in Cunningham et al. (1998) Figure 17B (Figure 2), there are three wells adjacent to the queried structure: Gulf Oil W-3510 south of the postulated fault and W-1115 and W-2404 north of it. The Gulf Oil well W-3510 appears to control the set of structure contours used to delineate the area of faulting (Figure 2). Other published contour maps of the same well data use dashed contours and question marks to indicate uncertainty in contouring such sparse data in the Florida Bay area (Figures 7 and 8). A later publication, Cunningham et al. (2001), also provides interpretations of unfaulted Miocene to Pliocene stratigraphy in the same location (Figure 9) as the postulated fault from Cunningham et al. (1998). Although focused on central Florida, regional maps presented in Cunningham et al (2003) do not depict the queried fault from Cunningham et al (1998) in the same location.

Preferred Interpretation

In summary, Cunningham et al. (1998) present a dashed and queried fault as one of two possible explanations for stratigraphic variations in southern Florida. Subsequent publications by the same authors and the SFDP (e.g., Guertin et al., 2000; Cunningham et al., 2001; Cunningham et al., 2003; Hine et al., 2009) have not shown the existence of this fault in southern Florida, nor have these publications continued the postulation of the fault originally presented in Cunningham et al. (1998) (Figures 5 and 9). Because of (1) other subsequent publications excluding this fault interpretation, (2) the uncertainties associated with the tectonic interpretation of Cunningham et al. (1998), and (3) data supporting a non-tectonic origin for other similar stratigraphic variations in the region, it is more likely that paleotopography is the cause of the stratigraphic variation seen in the boreholes. Additionally, multiple alternate interpretations of well data in the area do not support the presence of faulting at the location of the queried structure presented by Cunningham et al. (1998).

b) If the queried fault is indeed a fault, please discuss the timing and spatial extent of faulting and update the FSAR discussion accordingly.

Constraints on Length of the Postulated Fault

If Cunningham et al.'s (1998) queried structure is a tectonic fault, the map indicates that the approximately located structure is between 50 and 60 kilometers long (30 - 36 miles) (Figures 2 and 3). At its nearest approach, the eastern end of the queried fault is approximately 41 kilometers (25 miles) west of the Turkey Point Units 6 and 7 site.

Constraints on Age of Most-Recent Slip on the Postulated Fault

Cunningham et al. (1998) provide no discussion of the age of most-recent slip on their postulated fault. Based on the depiction of the queried fault in Figure 5 of Cunningham et al. (1998), the fault tips out at the base of the Arcadia Formation and the Arcadia formation is potentially in fault contact with the lower portion of the overlying Miocene-Pliocene Long Key Formation (Figure 1). The depiction of potentially folded strata within the Long Key Formation (Figure 1) could be interpreted to suggest syntectonic deposition. Thus, one could interpret that movement on the postulated fault is as young as Miocene-Pliocene.

Alternatively, the Long Key Formation could be interpreted as being draped over a pre-existing paleoscarp of the Oligocene-Miocene Arcardia Formation, thus post-dating slip on the postulated fault. Post-Miocene movement on the postulated fault is only suggested by Figure 17A of Cunningham et al. (1998). In this figure, Cunningham et al. draw the dashed and queried fault on an isopach map of Miocene-Pliocene siliciclastic sands (Figure 3). According to this interpretation, the postulated fault was last active during the Miocene to Pliocene, and is not a Quaternary-active structure.

In contrast, Figures 3 and 5 of Warzeski et al. (1996) depict unfaulted Miocene and younger strata in a structural contour map of the Plio-Pleistocene boundary, along with an isopach map of the Miocene Peace River Formation that indicates continuous stratigraphy across the projection of the postulated fault (Figure 7 and 8). Cunningham et al. (2001) present contour maps of Miocene and Pliocene units (e.g., Figure 9) that do not show faulting in the location of the postulated fault from Cunningham et al. (1998). Similarly, surficial maps and cross sections near the eastern portion of the postulated fault do not indicate faulting in the Pliocene and younger units (Green et al., 1996; FSAR Reference 2.5.1-830)

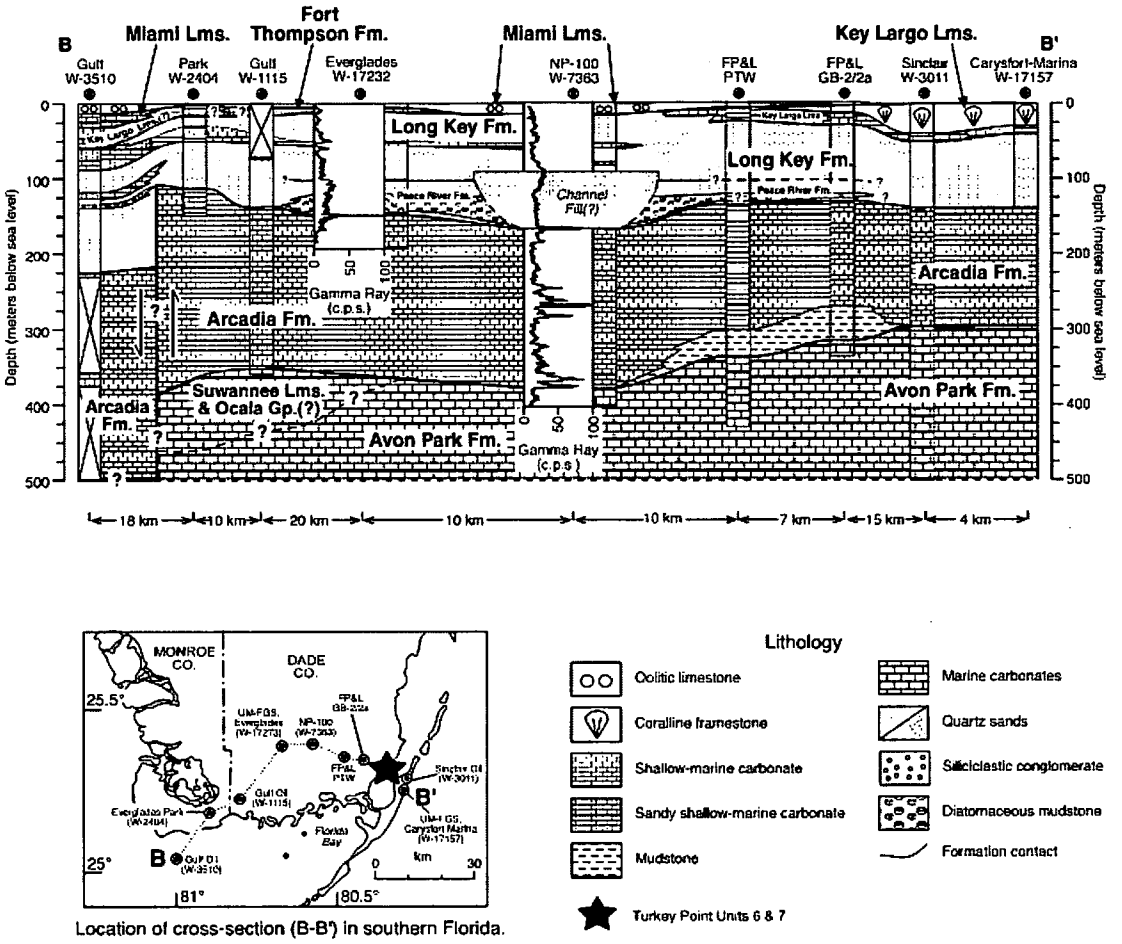

Figure 1. Figure 5 from Cunningham et al (1998); Stratigraphic correlation diagram across southern Florida.

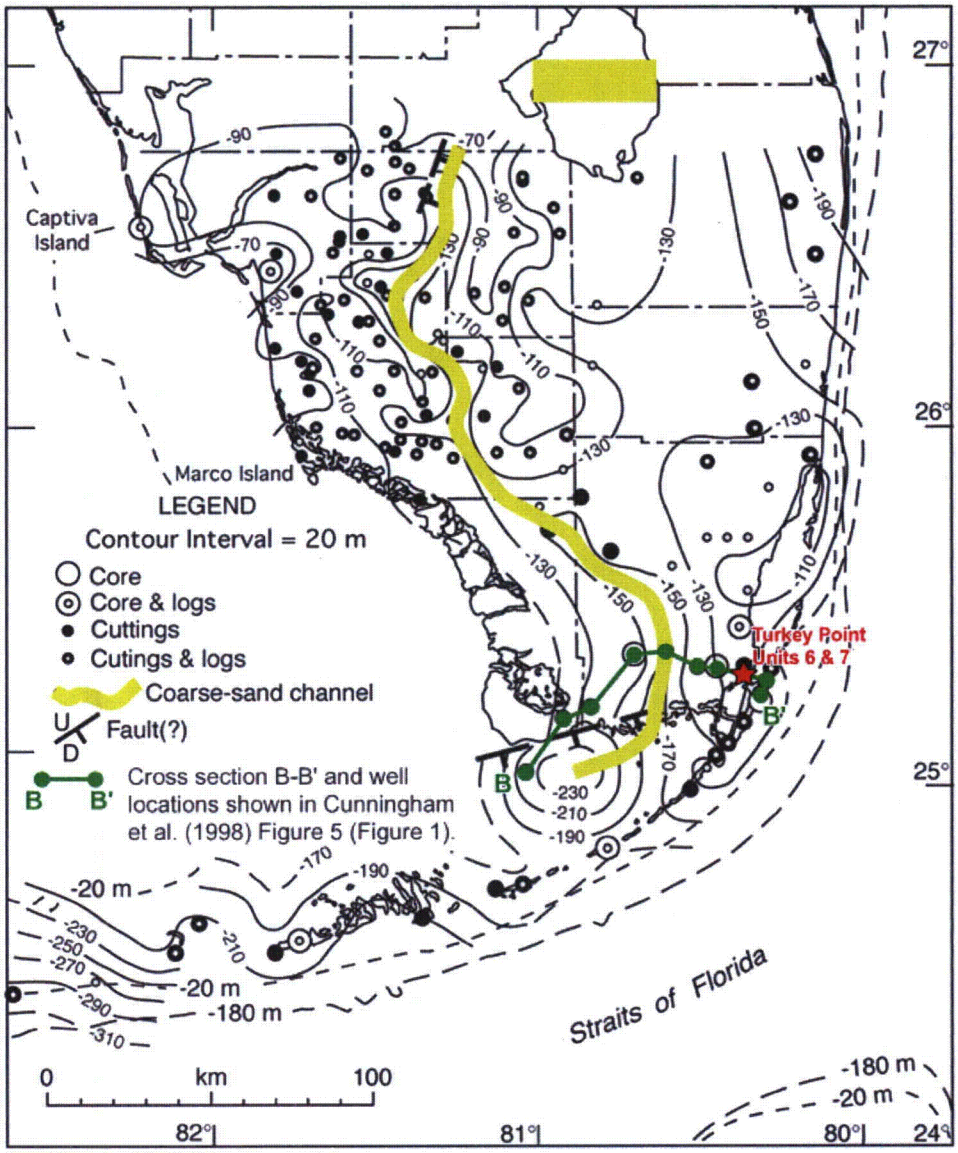

Figure 2. Figure 17b from Cunningham et al (1998); Structure contour map of the top of the Oligiocene-Miocene Arcadia formation.

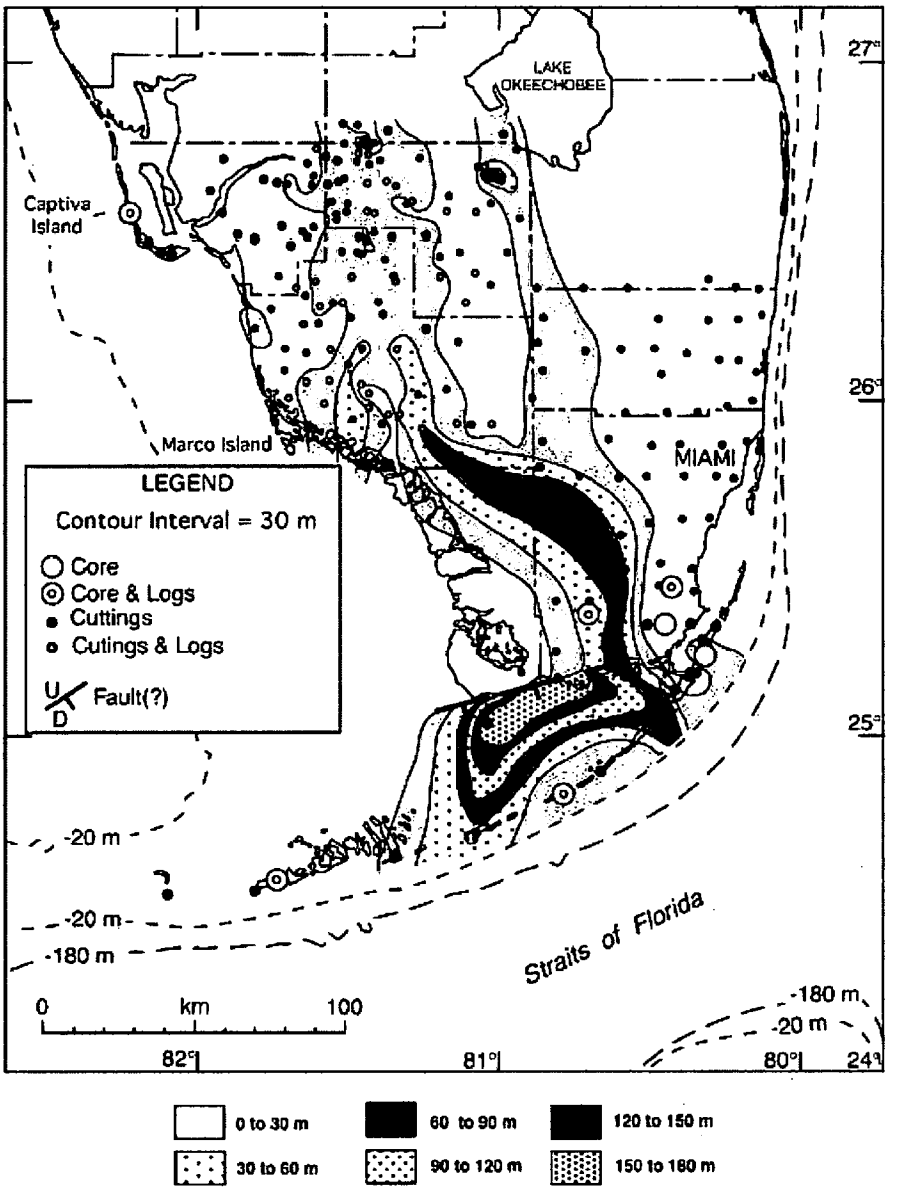

Figure 3. Figure 17a from Cunningham et al (1998); Isopach map of Mio-Pliocene siliciastic sands.

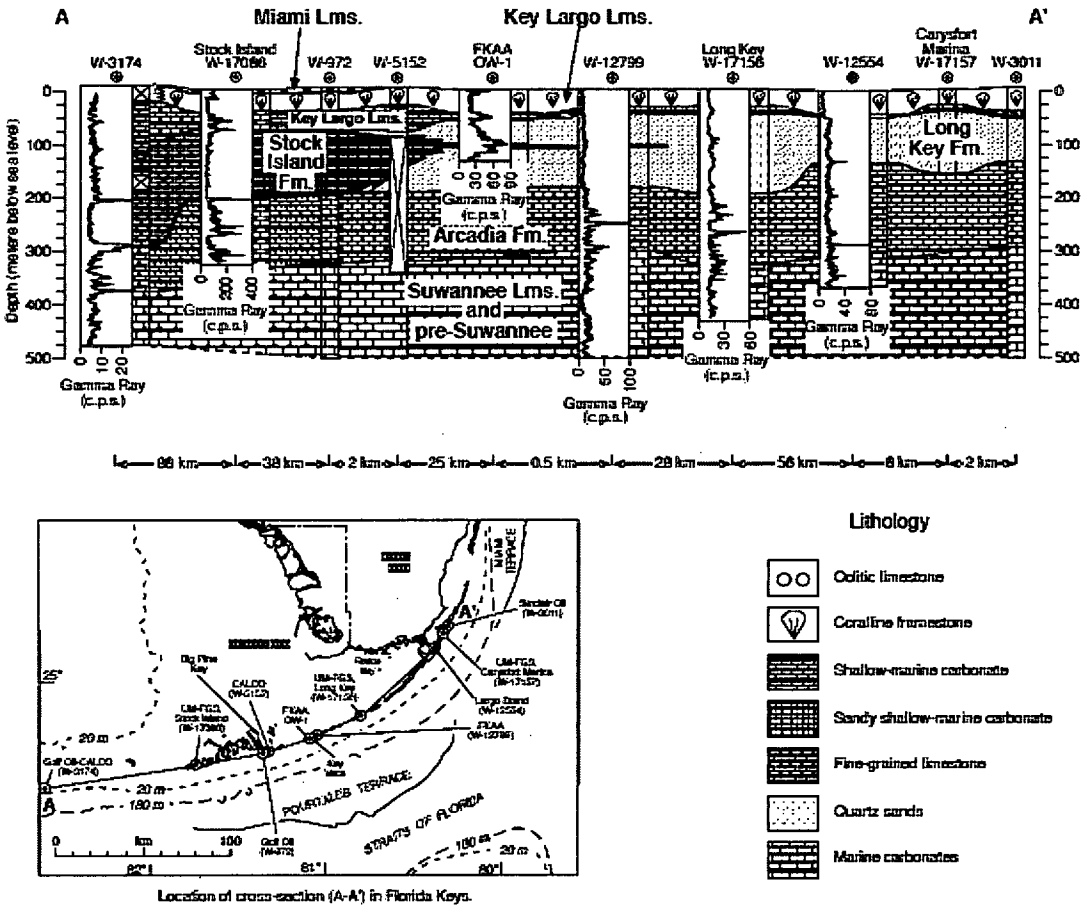

Figure 4. Figure 4 from Cunningham et al (1998); Stratigraphic correlation diagram along the Florida Keys.

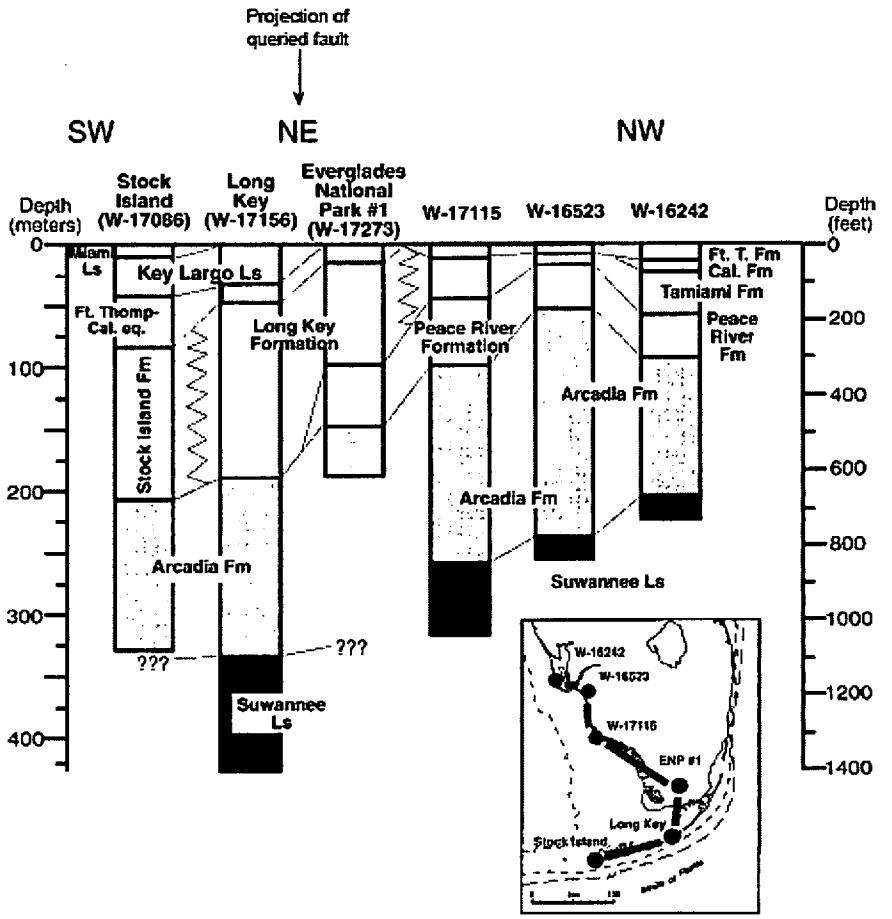

Figure 5. Figure 2 from Guertin et al (2000); Stratigraphic correlation diagram across southern Florida.

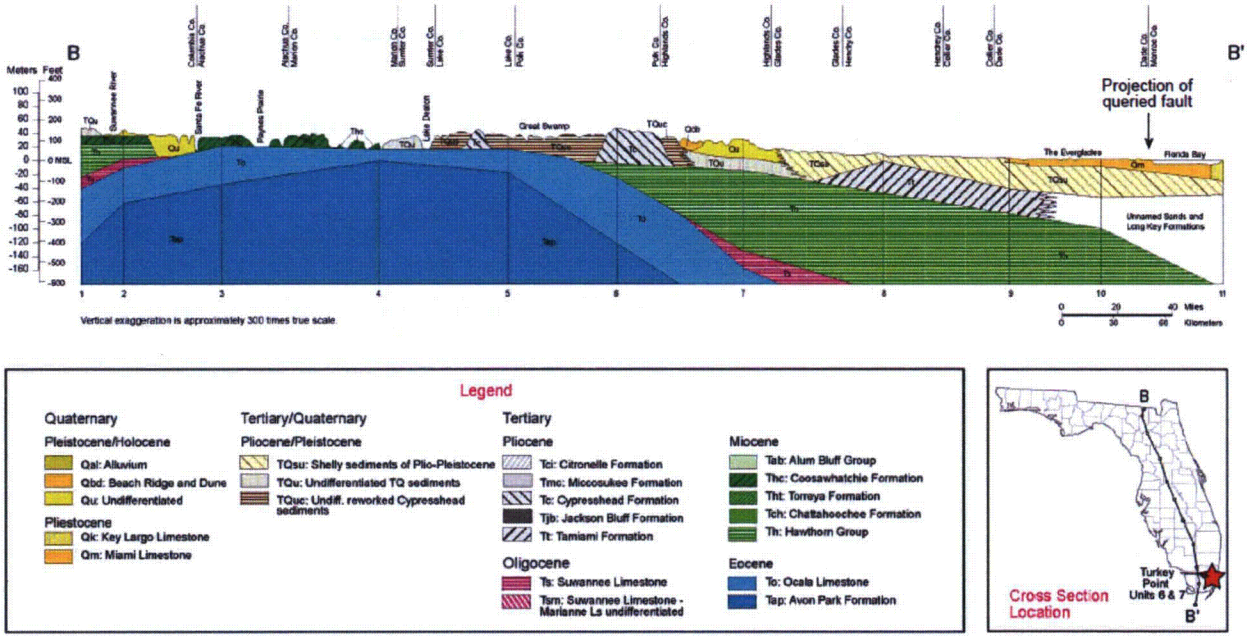

Figure 6. Figure 3 from Scott (2001); Regional north-south cross section.

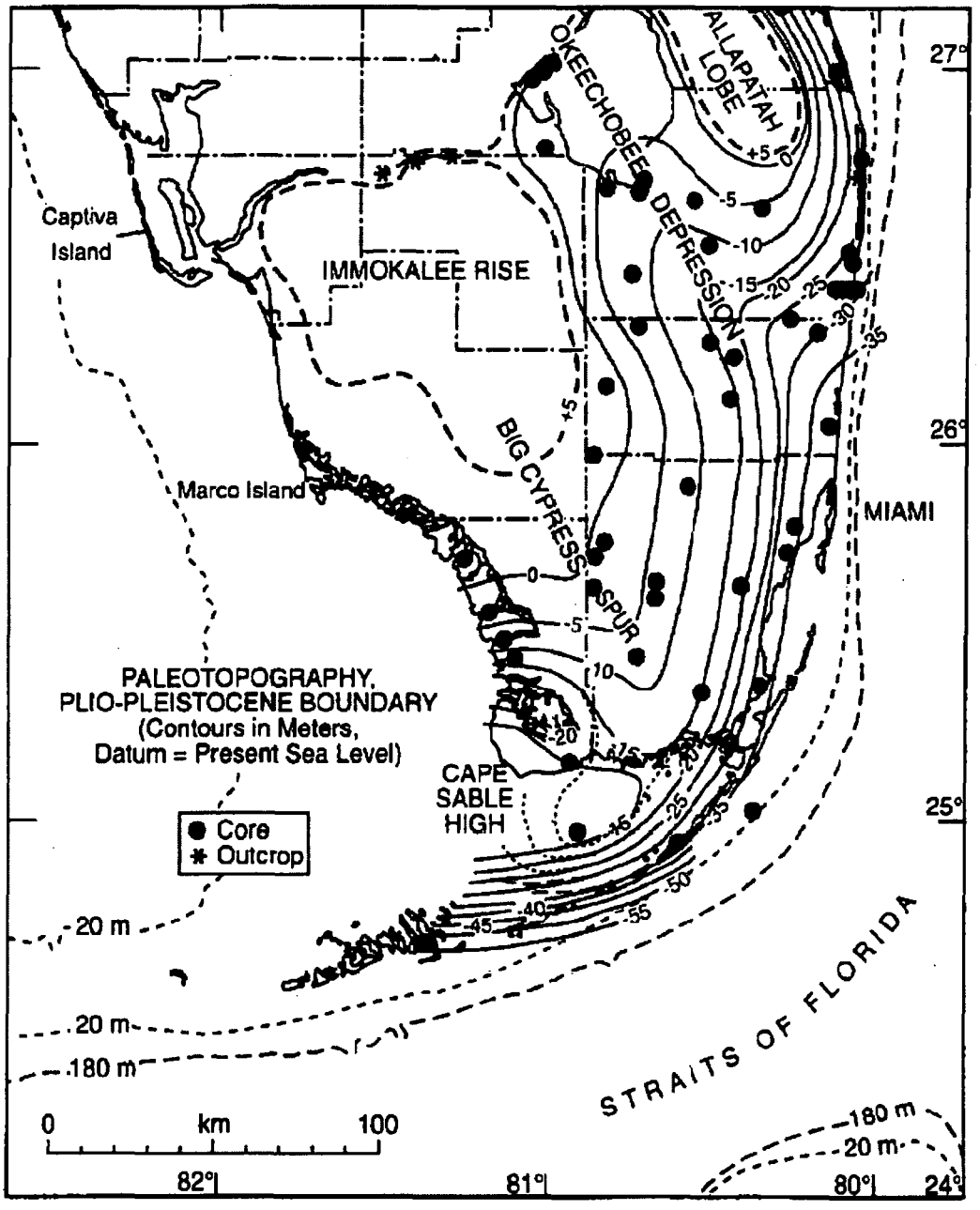

Figure 7. Figure 3 from Warzeski et al (1996); Paleotopography of Plio-Pleistocene boundary.

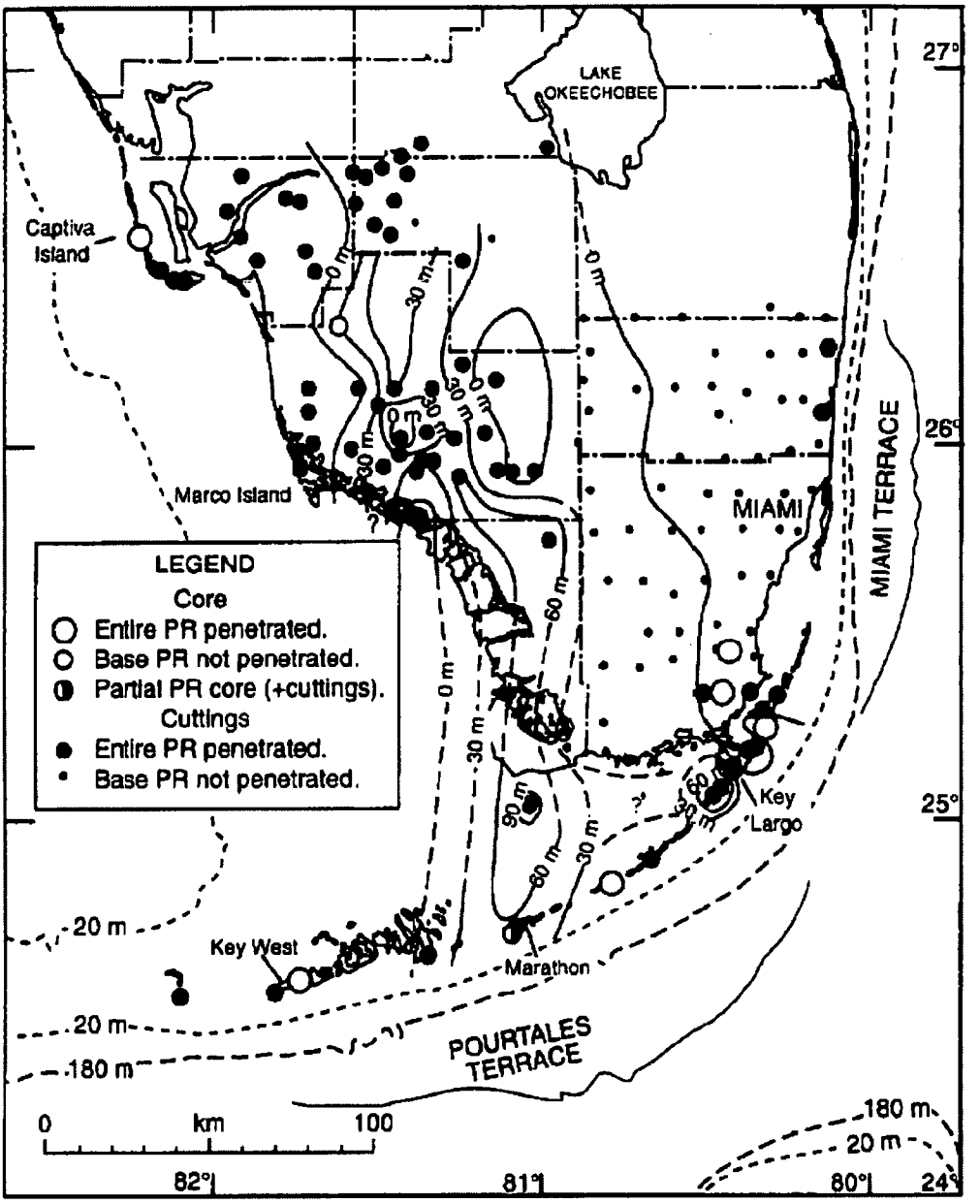

Figure 8. Figure 5 from Warzeski et al (1996); Isopach map of Miocene Peace River formation.

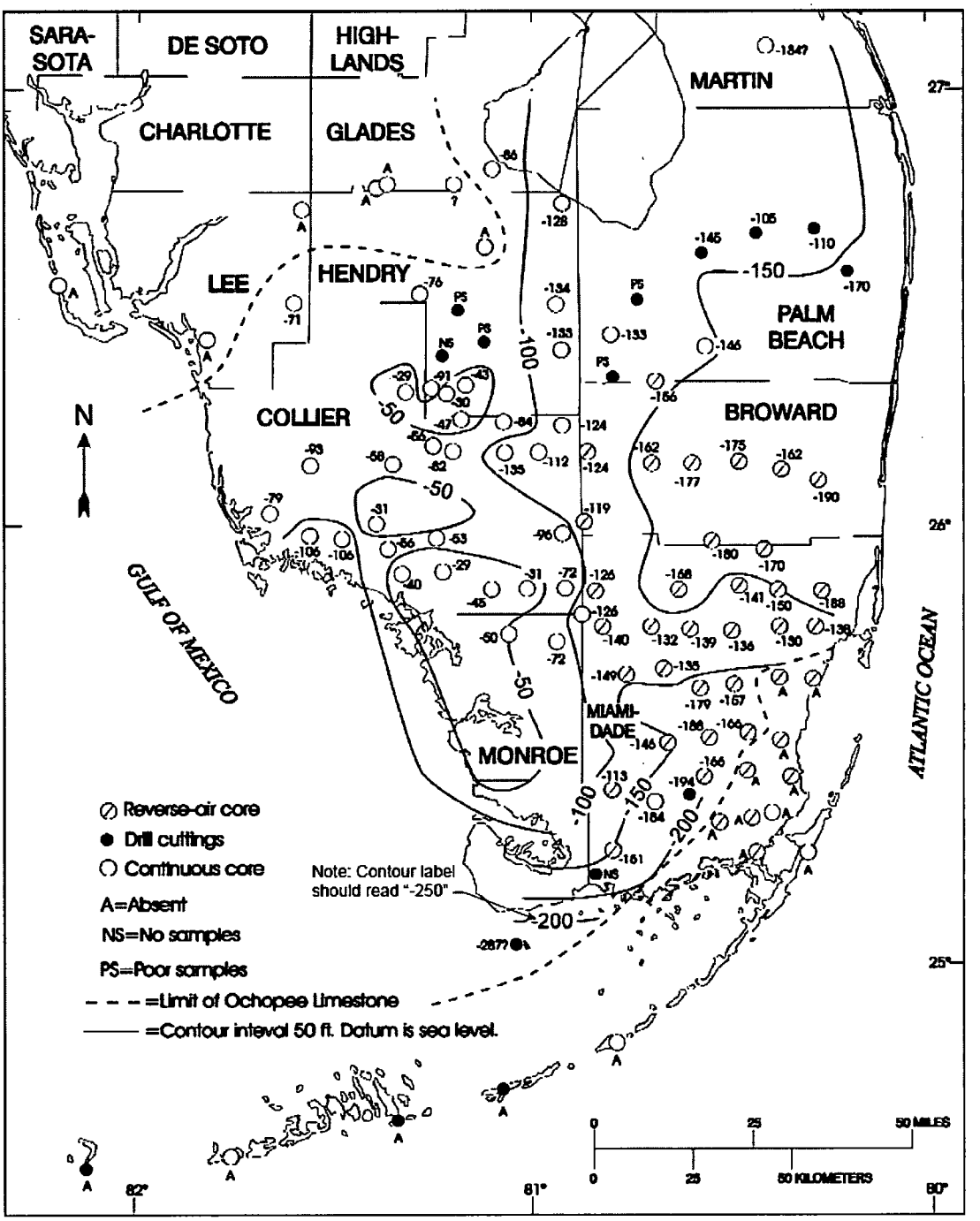

Figure 9. Figure 8 from Cunningham (2001); Structure contour map of the limestone within the Pliocene Tamiami formation.

This response is PLANT SPECIFIC.

References:

Cunningham, K. J., Bukry, D., Sato, T., Barron, J. A., Guertin, L. A., Reese, R. S., 2001, Sequence stratigraphy of a south Florida carbonate ramp and bounding siliciclastics (Late Miocene-Pliocene); Florida Geological Survey Special Publication 49, p. 35-66.

Cunningham, K. J., Locker, S. D., Hine, A. C., Bukry, D., Barron, J. A., Guertin, L. A., 2003, Interplay of late Cenozoic siliciclastic supply and carbonate response on the southeast Florida platform: Journal of Sedimentary Research, v. 73, p. 31-46.

Florida Geological Survey (FGS) website, Lithologic database, http://publicfiles.dep.state.fl.us/FGS/WEB/lithologic/sfwmd2.zip, accessed 5/2/2012.

Guertin, L. A., Missimer, T. M., McNeill, D. F., 2000, Hiatal duration of correlative sequence boundaries from Oligocene-Pliocene mixed carbonate/siliciclastic sediments of the south Florida Platform: Sedimentary Geology, v. 134, p. 1-26.

Hine A. C., Suthard, B. C., Locker, S. D., Cunningham, K. J., Duncan, D. S., Evans, M., Morton, R. A., 2009, Karst sub-basins and their relationship to the transport of Tertiary siliciclastic sediments on the Florida Platform: International Association of Sedimentologists Special Publication: v. 41, p. 179-197.

McNeil, D. F., Cunningham, K. J., Guertin, L. A., Anselmetti, F. S., 2004, Depositional themese of mixed carbonate-siliciclastics in the south Florida neogene: Application to ancient deposits, in Integration of outcrop and modern analogs in reservoir modeling: AAPG Memoir 80, p. 23-43.

Miller, J. A., 1986, Hydrogeologic framework of the Floridan Aquifer system in Florida and parts of Georgia, Alabama, and South Carolina: USGS Professional Paper 1403-B, 91 p.

Missimer, T. M., 2001, Siliciclastic facies belt formation and the Late Oligocene to Middle Miocene partial drowning of the southern Florida platform, Gulf Coast Association of Geological Societies Transacations, v. LI, p. 229-238.

Scott, T., 2001, Geologic map of the state of Florida, Florida Geological Survey Open File Report 80.

Warzeski, E. R., Cunningham, K. J., Ginsburg, R. N., Anderson, J. B., Ding, Z. D., 1996, A Neogene mixed siliciclastic and carbonate foundation for the Quaternary carbonate shelf, Florida Keys, Journal of Sedimentary Research, V. 66, p. 788-800.

ASSOCIATED COLA REVISIONS:

A paragraph regarding the queried fault will be added to the FSAR Subsection 2.5.1.1.1.3.2.1. in a future COLA revision.

Queried Fault from Cunningham et al.

Cunningham et al. (Reference 373) postulate that a fault or paleotopography could be responsible for elevation variations in the Arcadia formation in southwestern Florida (Figure 2.5.1-229). The queried structure is between 50 and 60 kilometers long (30–37 miles) (Figure 2.5.1-229), and at its nearest approach, the eastern end of the queried fault is approximately 41 kilometers (25 miles) west of the Turkey Point Units 6 & 7 site.

Figure 2.5.1-234 shows a cross section across southern Florida that was developed with data from eight wells in southern Florida, with variable horizontal scale between pairs of wells, and, thus, with variable vertical exaggeration. Between the southernmost two wells, Cunningham et al. (Reference 373) postulate the existence of a fault that cuts up through Avon Park Formation, Suwannee Limestone, and Oligocene-Miocene-age Arcadia Formation, and potentially places the Arcadia Formation in fault contact with the lower portion of the overlying Miocene-Pliocene Long Key Formation. Alternatively, the Long Key Formation may be interpreted as deposited across a paleoscarp. Reference 373 labels the postulated fault on this cross section with two question marks, indicating the speculative nature of this fault.

In cross section, the postulated fault cuts units as young as the Miocene Arcadia formation, and although the Miocene to Pliocene Long Key Formation and the Pleistocene Key Largo are depicted as unfaulted, they have thickness and elevation differences across the structure (Figure 2.5.1-234). Higherrup, section above the queried fault tip, Cunningham et al. (Reference 373) cross section shows marine carbonate stringers that could be interpreted as deformed by slip on the underlying fault. Alternatively, these marine carbonate stringers could represent deposition draped across a paleoscarp and thus could post-date slip on the underlying postulated fault.

Although the postulated fault in Figure 2.5.1-234 would not represent a Quaternary faulting hazard for the site if it existed, in detail the thickness and stratigraphic variations may instead be related to paleotopography. Indeed, the top of the Arcadia Formation is known to be an erosional unconformity with significant paleotopographic variation. For example, "A distinct regional unconformity and subaerial exposure surface at the top of the Arcadia Formation separates the Long Key and Arcadia Formations" (Reference 393). A cross section presented by Reference 393 depicts 90 meters (295 feet) of relief on the top of the Arcadia Formation surface in southern Florida, while the thickness of the Arcadia Formation varies from 200 meters (656 feet) in the central portion of the Florida peninsula to between 0 and 20 meters (0 and 66 feet) farther east (Reference 394). A study in southern Florida determined that intensification of marine currents

increased the erosion of marine carbonates and led to a significant time hiatus (more than 4 m.y.) following deposition of the Arcadia Formation (Reference 934) and the influence of Arcadia Formation paleotopography on highs in subsequent carbonate and clastic deposition in southernmost Florida has been recognized (Reference 395).

On Key Largo, relief on the top of the Arcadia Formation as large as 40 meters (131 feet) was found between borings only a few kilometers apart (Reference 393). Furthermore, in other cross sections presented by Reference 273, the elevation of the top of the Arcadia Formation varies by approximately 100 meters (328 feet) between wells W-3174 and W-17086 (88 kilometers or 55 miles apart), by 50 meters (164 feet) between wells W-17156 and W-12554 (56 kilometers or 35 miles apart), and by 25 meters (82 feet) or 1.2 miles between wells W-3011 and W-17157 (2 kilometers apart), all interpreted without faulting. The slope required to achieve this latter elevation variation, 0.7 degree, is actually greater than the slope required to achieve the elevation variation observed in the Arcadia Formation between the Everglades Park and Gulf Oil wells, where the queried fault is depicted in Figure 2.5.1-234 (approximately 100 meters [328 feet] over 18 kilometers [11 miles] of distance, or a 0.3-degree slope). Numerous other examples exist throughout southern Florida of steeper paleotopographic slopes on the top of the Arcadia Formation that are not associated with faulting. In addition, the down-to-the-south separation depicted on the postulated fault in Figure 2.5.1-234 is consistent with, and may, in part, be attributed to the regional southward dip of the strata towards the South Florida Basin in the area (References 377 and 389).

The karst-influenced paleotopography of the Arcadia Formation is detailed in Reference 936. While using borings at a much finer spacing than Cunningham study, the Hine study documents karst sub-basins with as much as 100 meters (328 feet) of relief over distances of kilometers to tens of kilometers on the top of the Arcadia Formation in west-central Florida. They attribute this relief to a mid- to late-Miocene sea level lowstand that caused dissolution in the deeper carbonates, such as the Arcadia Formation, and formed paleotopographic depressions and non-tectonic deformation in the Arcadia Formation (Reference 936).

Alternative interpretations of well data in southern Florida, often including the three wells closest to the postulated fault, provide evidence for unfaulted Eocene to Pliocene stratigraphy in the same location (References 389, 393, 934, 935). For example, Reference 934 provides a stratigraphic correlation diagram across the projection of the queried fault from Cunningham et al. (Reference 373) and interprets no faulting. This diagram also displays similar relief between boreholes on the top of the Arcadia to the north. Likewise, the regional north-south-oriented cross section shown in Figure 2.5.1-233 intersects the projection of the queried fault and does not indicate faulting in the area.

As shown in Figure 2.5.1-381, there are three wells adjacent to the queried structure: Gulf Oil W-3510 south of the postulated fault and W-1115 and W-2404 north of it. The Gulf Oil well W-3510 appears to control the set of structure contours used to delineate the area of faulting (Figures 2.5.1-234 and 2.5.1-381). Yet, other

published contour maps of the same well data use dashed contours and question marks to indicate uncertainty in contouring such sparse data in the Florida Bay area (Reference 393). A later publication (Reference 935) also provides interpretations of unfaulted Miocene to Pliocene stratigraphy in the same location as the postulated fault from Reference 273.

In summary, numerous other sources using similar well data indicate unfaulted strata that gently dips to the south in this location, reflecting the influence of the South Florida Basin (References 389, 393, 396, and 827). The fault postulated by Reference 273 has not been documented in any subsequent investigations and numerous examples of paleotopographic variation in the top of the Arcadia support a non-fault-related origin for the stratigraphic variations seen in Figure 2.5.1-234

The following references will be included in FSAR Subsection 2.5.1.3 in a future COLA revision:

934. Guertin, L., T. Missimer, and D. McNeill, *Hiatal Duration of Correlative Sequence Boundaries from Oligocene-Pliocene Mixed Carbonate/Siliciclastic Sediments of the South Florida Platform: Sedimentary Geology,* Vol. 134, pp. 1–26, 2000.

935. Cunningham, K., D. Bukry, T. Sato, J. Barron, L. Guertin, and R. Reese, *Sequence Stratigraphy of a South Florida Carbonate Ramp and Bounding Siliciclastics (Late Miocene-Pliocene),* Florida Geological Survey, Special Publication 49, pp. 35–66, 2001.

936. Hine, A., B. Suthard, S. Locker, K. Cunningham, D. Duncan, M. Evans, and R. Morton, *Karst Sub-Basins and their Relationship to the Transport ofTertiary Siliciclastic Sediments on the Florida Platform,* International Association of Sedimentologists, Special Publication, Vol. 41, pp. 179–197, 2009.

The following figure will be revised in a future COLA revision:

Figure 2.5.1-229 Regional Tectonic Features

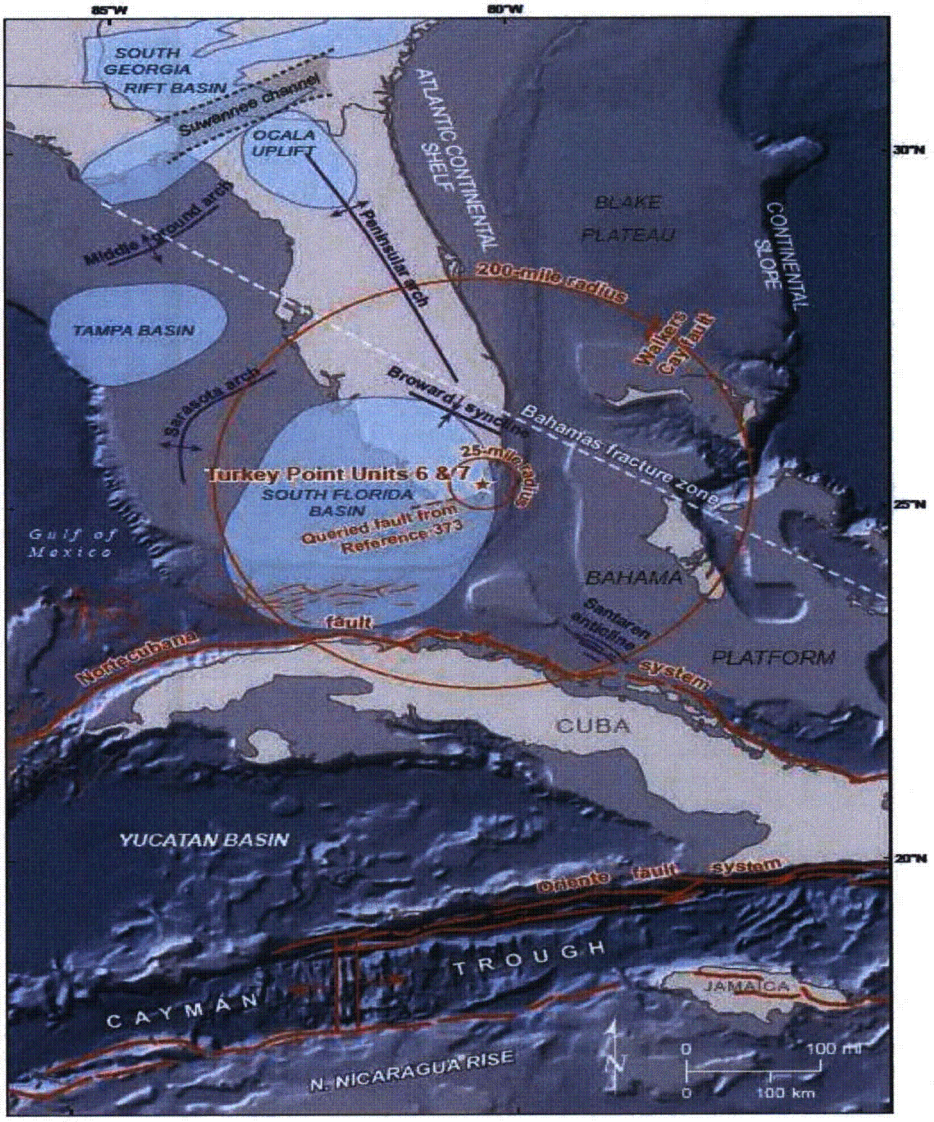

Sources: References 822, 482, 823, 457, 212, and 421

The following new figure will be included in FSAR Subsection 2.5.1 in a future COLA revision:

Figure 2.5.1-381 Structure Contour Map of the Top of the Oligiocene-Miocene Arcadia Formation

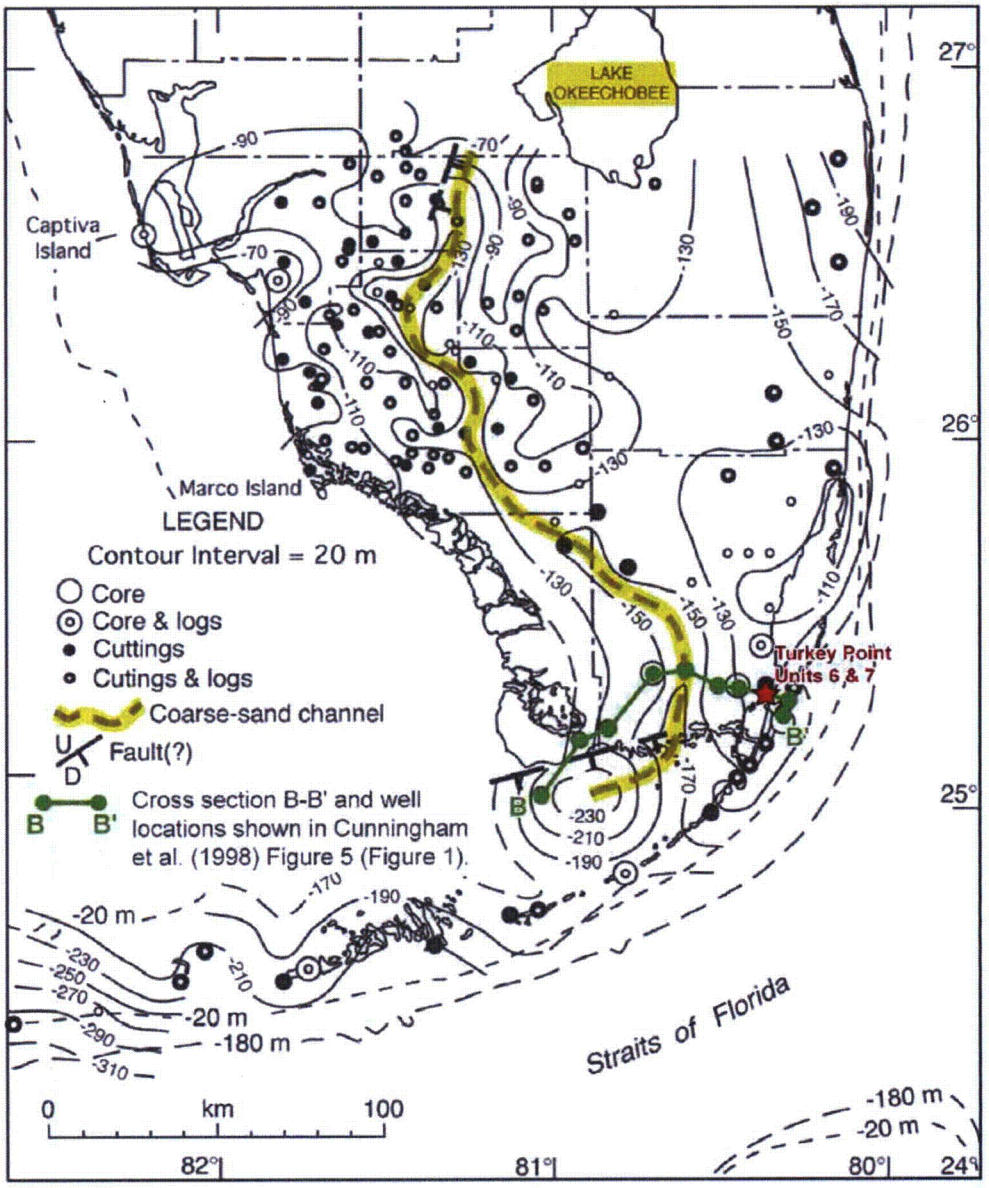

ASSOCIATED ENCLOSURES:

None

NRC RAI Letter No. PTN-RAI-LTR-041

SRP Section: 02.05.01 - Basic Geologic and Seismic Information

QUESTIONS from Geosciences and Geotechnical Engineering Branch 2 (RGS2)

NRC RAI Number: 02.05.01-13 (eRAI 6024)

FSAR Section 2.5.1.1.1.3.2.2 states with respect to Mesozoic Normal Faults of the Bahamas Platform, that the basement of the Bahamas Platform is depicted as a series of fault blocks with syn-tectonic Triassic to Jurassic strata, draped by undeformed Cretaceous strata. However, the staff notes that in FSAR Figure 2.5.1-264, Lower Cretaceous strata are faulted.

In order for the staff to evaluate the site region geology and in support of 10 CFR 100.23, please clarify the age of latest movement in light of faulted lower Cretaceous strata.

FPL RESPONSE:

The discussion of Mesozoic normal faults of the Bahamas Platform in FSAR Subsection 2.5.1.1.1.3.2.2 notes that normal faults cutting Cretaceous strata have been identified, but concludes the following: "More commonly, the basement of the Bahama Platform is depicted as a series of fault blocks with syn-tectonic Triassic to Jurassic strata, draped by undeformed Cretaceous strata." Such undeformed Cretaceous strata are interpreted in the Straits of Florida (FSAR Figures 2.5.1-243, -263, and -272), the western Bahama Bank (FSAR Figure 2.5.1-268), the Great Bahama Bank (FSAR Figures 2.5.1-269 and -271), and the southeast Bahama Plateau (FSAR Figure 2.5.1-270), all of which are discussed in FSAR Subsection 2.5.1.1.1.3.2.2.

Sheridan et al. (1988) (FSAR Subsection 2.5.1 Reference 307) interpret Lower Cretaceous strata (Albian-Aptian) as faulted, but Upper Cretaceous strata (Cenomanian to Conacian and Santorinian to lower Paleocene) strata are unfaulted (right panel of FSAR Figure 2.5.1-264), consistent with the statement in the FSAR. The statement in Subsection 2.5.1.1.1.3.2.2 of the FSAR will be revised to provide clarification.

This response is PLANT SPECIFIC.

References:

None

ASSOCIATED COLA REVISIONS:

The first and second paragraphs of FSAR Subsection 2.5.1.1.1.3.2.2 will be revised as shown below in a future revision of the FSAR:

2.5.1.1.1.3.2.2 Bahama Platform Tectonic and Structural Features

Structures of the Bahama Platform

The Bahama Platform, like the Florida Platform, is best characterized by continuous, horizontal carbonate deposition, rarely interrupted by faulting or other deformation (Figure 2.5.1-245). Because the platform is largely submerged, all information about potential structures is gained from interpretations of seismic lines, and therefore is subject to limitations. The vast majority of seismic lines inspected and available to this study confirm the unfaulted nature of Cretaceous and younger strata across the Bahama Platform and southern Florida Platform (Figures ~~2.5.1-262,~~ 2.5.1-263, 2.5.1-268, 2.5.1-269, 2.5.1-270, 2.5.1-271, and 2.5.1-272). However, a few exceptions to this exist, such as the ~~normalfault~~ **deformation** associated with **the** Santaren **a**nticline **(Figure 2.5.1-278)** ~~and in~~ **normal faults in** the Straits of Florida (Figure 2.5.1-273)**, the Walkers Cay fault (Figure 2.5.1-275), and the eastern Bahama Platform (right panel of Figure 2.5.1-264).** ~~These younger features are generally associated with, and in close proximity to, the Tertiary Cuban orogen.~~

Mesozoic Normal Faults of the Bahama Platform

As described above, the openings of the Gulf of Mexico and Atlantic Ocean led to the development of Mesozoic normal faults that extended the basement beneath the Florida and Bahama Platforms. No detailed maps of the entire subsurface Bahama Platform exist, but limited mapping of such faults has been done in conjunction with large-scale seismic surveys. For example, ~~Austin et al. (Reference 432) identify seven normal faults cutting a Cretaceous horizon in the Exuma Sound, and~~ a seismic line in the Straits of Florida identified several minor normal faults cutting **strata above a mid-Cretaceous shallow-water carbonate platform at a depth of 940 meters (3084 feet) below the seafloor** ~~a Cretaceous horizon~~ (Figure 2.5.1-274). More commonly, the basement of the Bahama Platform is depicted as a series of fault blocks with **syntectonic** Triassic to Jurassic strata, draped by undeformed **Lower and/or Upper** Cretaceous strata. ~~(Figures2.5.1-264and 2.5.1-242~~ **In the eastern Bahama Platform, Sheridan et al. (Reference 307) interpret normal faults cutting Lower Cretaceous strata that are draped by unfaulted Upper Cretaceous (Santonian or Cenomanian) strata (right panel of Figure 2.5.1-264). On Figure 2.5.1-263, a north-south seismic line located east of the site indicates normal faulted basement of Paleozoic to Jurassic strata draped by unfaulted Upper Jurassic to Lower Cretaceous strata. Similarly, the seismic line interpretation on Figure 2.5.1-243 indicates faulted basement covered by undeformed Upper Jurassic and younger strata. On Figures 2.5.1-268 and 2.5.1-269, flat unfaulted Lower Cretaceous and younger strata cover the Bahama Platform.**

The notes for FSAR Figure 2.5.1-270 will be revised as shown below in a future revision of the FSAR:

Notes:

~~(a)~~ Seismic line OBC-8B, C, 48-trace, 24-fold; four air guns of 6000 cubic inches total volume, fired at 500 psi in 25-second intervals; data not deconvolved or migrated.

~~(b)~~ Interpretation of line OBC-8B, C Identification of reflectors seaward of escarpment is based on correlation with DSDP Site 99. Modified from: Reference ~~794~~ **687**

Reference 2.5.1- 794 in FSAR Subsection 2.5.1.3 will be revised as shown in a future revision of the FSAR:

794. Schlager, W., **R**. Buffler, **D.** Angstadt, and **R.** Phair, 32. *Geologic History of the Southeastern Gulf of Mexico*," Initial Reports DSDP, 77, **R.** Buffler **W.** Schlager, **J.** Bowdler, **P.** Cotillon, **R**. Halley et al. (eds.), Washington D.C., U.S. Government Printing Office, pp. 715-738, 1984.

ASSOCIATED ENCLOSURES:

None

NRC RAI Letter No. PTN-RAI-LTR-041

SRP Section: 02.05.01 - Basic Geologic and Seismic Information

QUESTIONS from Geosciences and Geotechnical Engineering Branch 2 (RGS2)

NRC RAI Number: 02.05.01-14 (eRAI 6024)

FSAR Section 2.5.1.1.1.3.2.2, "Bahamas Platform Tectonic and Structural Features" states with respect to Walkers Cay Fault, that although strata above the Oligocene horizon have been interpreted as both faulted and unfaulted, Harwood and Towers (1988) indicated that the Walkers Cay fault has minimal effect on middle Miocene and younger strata. In addition the FSAR states that because of the minor deformation of Miocene and younger strata, the Walkers Cay fault is concluded to be a Tertiary structure, and consequently, not a capable tectonic structure.

In order for the staff to understand the geologic setting of the TPNPP site and In support of 10 CFR 100.23 please address the following:

1) Label Walkers Cay fault on FSAR Figure 2.5.1-276.

2) Explain the basis for Harwood and Towers (1988) conclusion within the limits of resolution for marine seismic reflection data.

3) Discuss the earlier interpretation of fault offset to the sea floor in light of the Austin et al 1988 a and b papers.

4) Discuss site-survey profiles LBB-17 and LBB-18 of ODP Leg 101, which show the Walkers Cay fault displacing the seafloor(see Austin et al., 1988 *a* and *b)*.

   a. Austin, J. A., Jr., Schlager, W., et al, 1988, Proceedings of the Ocean Drilling Program, Scientific Results (1988) 101: 455-472. Paper number 29, by the "Leg 101 Scientific Party." Copyright 1988, Ocean Drilling Program.

   b. Austin, J. A., Jr., Schlager, W., et al., 1988, Proceedings of the Ocean Drilling Program, Scientific Results (1988) 101: 455-472. Paper number 26, by Austin et al." Copyright 1988, Ocean Drilling Program.

FPL RESPONSE:

This response is divided into three parts. The first part of this response describes available geologic data for the Walkers Cay fault. The second part of this response addresses items 1 through 4 specified in the RAI. The third part of this response describes the results of a sensitivity calculation performed to assess the potential impact on the probabilistic seismic hazard analysis (PSHA) for the Turkey Point Units 6 & 7 site if the Walkers Cay fault were to be included as a capable fault source.

Available Geologic Data for the Walkers Cay Fault

The Walkers Cay fault was initially identified by Mullins and Van Buren (1981) (FSAR 2.5.1 Reference 474) north of Little Bahama Bank based on seismic reflection data. As later mapped by Van Buren and Mullins (1983) (FSAR 2.5.1 Reference 791), the fault is a 33-km-long structure that strikes north-northeast (FSAR Figure 2.5.1-275 and Figure 1). In contrast, Austin et al. (1988b) (FSAR 2.5.1 Reference 785) depict a broad zone of faulting by mapping the northwest and southeast boundaries of the zone, but do not map the extent

of any individual strands within the zone. These boundaries of the Walkers Cay fault zone are defined as having a more easterly strike than the fault of Van Buren and Mullins (1983) (FSAR 2.5.1 Reference 791) and a similar length (Figure 1). The spatial coincidence of the faulting expressed in Oligocene- to Cretaceous-age strata with a magnetic anomaly has been used to interpret the Walkers Cay fault as a basement-involved structure (Mullins and Van Buren 1981; Sheridan et al. 1988) (FSAR 2.5.1 References 474 and 307).

In the vicinity of the Walkers Cay fault, five seismic reflection lines with variable levels of interpretation have been reproduced in the published literature. Each of these five lines is described in the paragraphs below. Mullins and Van Buren (1981) (FSAR 2.5.1 Reference 474) and Van Buren and Mullins (1983) (FSAR 2.5.1 Reference 791) present two air gun seismic reflection profiles (Profile 4 and Profile E) in their reports about this structure (Figure 1). Shortly thereafter, the Ocean Drilling Program (ODP) Leg 101 conducted another seismic survey of the north slope of Little Bahama Bank and these data are discussed in several publications (e.g., Austin et al. 1986a; Austin et al. 1986b; Harwood and Towers 1988 [FSAR 2.5.1 Reference 476]; Austin et al. 1988a, 1988b [FSAR 2.5.1 Reference 785]). Three published seismic lines from that work (Lines LBB-13, LBB-17 and LBB-18) depict the Walkers Cay fault or a splay of the fault (Figure 1). In at least one of those lines (Line LBB-18), Austin et al. (1988b, p. 401) (FSAR 2.5.1 Reference 785) interpret a normal fault "believed to be the Walkers Cay normal fault" as extending up to the seafloor, suggesting possible Quaternary activity. Normal faulting is reportedly visible on lines LBB-5, LBB-6, and LBB-15 (Harwood and Towers 1988) (FSAR 2.5.1 Reference 476), but these seismic lines have not been reproduced in any of the publications from ODP Leg 101.

Profile 4

Profile 4 is oriented north-northeast (Figure 1) and an interpretation provided by Van Buren and Mullins (1983) (FSAR 2.5.1 Reference 791) shows the fault as a solid line up to the boundary between NLBB-1 and NLBB-2 (late Oligocene), and as a dashed-line above this boundary (Figure 2). The dashed extension of the fault extends upward approximately halfway through the Late Oligocene to Recent section, and Van Buren and Mullins (1983) (FSAR 2.5.1 Reference 791) draw short, unfaulted reflectors above the dashed upward termination of the fault (Figure 2). The fault does not appear to extend upward to the seafloor, but the exact location in the section of its upward termination is not clear. As described by Mullins and Van Buren (1981) (FSAR 2.5.1 Reference 474), the late Oligocene reflector (NLBB-2) is displaced vertically by as much as 75 to 100 meters.

Profile E

Profile E is oriented west-northwest (Figure 1) and the Van Buren and Mullins (1983) (FSAR 2.5.1 Reference 791) interpretation depicts four fault strands that, presumably, collectively represent the Walkers Cay fault. The westernmost fault strand is shown as a solid line, with three fault strands to the east shown as dashed lines (Figure 3). As in Profile 4, the westernmost fault is shown as solid up to the boundary between NLBB-1 and NLBB-2 (late Oligocene), and as a dashed line above that boundary. These four fault strands do not appear to be drawn to the seafloor, and are not described as extending to the seafloor by Van Buren and Mullins (1983) (FSAR 2.5.1 Reference 791) (Figure 3). The data

resolution near the surface, however, may preclude any definitive assessment of the fault tips.

LBB-17

Seismic line LBB-17 is oriented north-northeast (Figure 1). Austin et al. (1988b) (FSAR 2.5.1 Reference 785) illustrate the location of the Walkers Cay fault with two leader lines beneath a monocline and do not draw the fault in this seismic line (Figure 4). Austin et al. (1988b, p. 395) (FSAR 2.5.1 Reference 785) state, "This normal fault is well defined on LBB-17, particularly where it offsets sequence G. Sequences A-F do not appear to be offset, but thickening of sequences A-E across the upward continuation of the fault trace implies continuing differential subsidence across this feature" and possible synsedimentary movement on the fault. The exact upward termination of deformation in section LBB-17 is not clear, however, the uppermost reflectors above 1.5 seconds appear parallel and unfaulted across the structure (Figure 4). Based on the poor resolution of the seismic reflection data as presented in Figure 4, however, the possibility of deformation extending upward to the seafloor cannot be precluded at that location. No statements are made by the authors regarding the magnitude of offset or thickening, nor do they address the thickness of the Quaternary section at this location. Based on three nearby ODP borings, however, the Quaternary section is very thin, with measured thicknesses ranging from 3.6 m to 18.2 m (Figure 1b).

LBB-18

Seismic line LBB-18 is oriented north-northeast, parallel to, and west of, seismic line LBB-17 (Figure 1). The interpreted version of seismic line LBB-18 from Harwood and Towers (1988) (FSAR 2.5.1 Reference 476) is shown in the upper panel of Figure 5, which depicts a normal fault extending upward to the seafloor at approximately 700 hrs. This unnamed fault is possibly the Walkers Cay fault, although Harwood and Towers (1988, p. 266) (FSAR 2.5.1 Reference 476) indicate that it is "a minor splay." The lower left panel of Figure 5 shows Austin et al.'s (1988b) (FSAR 2.5.1 Reference 785) interpretation of the portion of seismic line LBB-18 that includes this same normal fault strand. Austin et al. (1988b, p. 401) (FSAR 2.5.1 Reference 785) state, "This fault may still be active, as it appears to offset the seafloor." No statements regarding the amount of offset in Quaternary strata, or the thickness of the Quaternary section, are provided by Austin et al. (1988b) (FSAR 2.5.1 Reference 785) or Harwood and Towers (1988) (FSAR 2.5.1 Reference 476). Previous publications on analysis of cores (Austin et al. 1986a, 1986b, 1986c), however, indicate that three borings along LBB-18 demonstrate the Quaternary section ranges from 3.6 m to 18.2 m in thickness (Figure 1b).

LBB-13

Seismic line LBB-13 is oriented west-northwest (Figure 1). Austin et al. (1988b) (FSAR 2.5.1 Reference 785) interpret three fault strands from these data (Figure 6) but provide minimal description of these faults. No interpretation of this line was provided by the ODP publications (Austin et al., 1988b; Harwood and Towers, 1988) (FSAR 2.5.1 References 785 and 476). The seismic line shows clear offset in three relatively narrow zones at the top of an Early Cretaceous bed (unit G), with the majority of displacement occurring on the westernmost fault splay, which is located nearest the mapped trace of the Walkers Cay fault from Van Buren and Mullins (1983) (FSAR 2.5.1 Reference 791) (Figure 1). Austin et

al. (1988b, p. 395) (FSAR 2.5.1 Reference 785) indicate that "all of the seismic sequences are faulted down to the east", with a maximum throw of 70 meters on one of the faults at the top of sequence G (early Cretaceous).

Responses to RAI Items 1 through 4

1) Label Walkers Cay fault on FSAR Figure 2.5.1-276.

FSAR Figure 2.5.1-276 is revised to label the fault strands that compose the Walkers Cay fault. Revised FSAR Figure 2.5.1-276 is provided in the Associated COLA Revisions section of this response.

2) Explain the basis for Harwood and Towers (1988) conclusion within the limits of resolution for marine seismic reflection data.

Harwood and Towers (1988, p. 266) (FSAR 2.5.1 Reference 476) conclude that the "Walkers Cay fault is visible on seismic profiles LBB 5, 6, 13, and 15, with a minor splay on LBB 18 (Figure 6), but throughout the area it has only a minimal effect on sediments younger than middle Miocene." As Harwood and Towers (1988) (FSAR 2.5.1 Reference 476) only present a subset of the seismic profiles collected for their study, it is difficult to re-examine their conclusion with respect to all profiles. In addition, they also do not quantify fault displacements in different age units. Of the five seismic reflection lines available, one (LBB-18) shows the Walkers Cay fault reaching the seafloor, but the majority of seismic lines (Profile E, Profile 4, LBB-13 and LBB-17) appear to show fault deformation terminating at 1.3 to 1.5s (two-way travel time) below the seafloor. The Harwood and Towers (1988) (FSAR 2.5.1 Reference 476) assessment that the Walkers Cay fault has "a minimal effect on sediments younger than middle Miocene" likely is due to: (1) the limited amount of deformation that can be observed in the shallower deposits of middle Miocene and younger age, and (2) the thin nature of post-Miocene deposits.

Harwood and Towers (1988) (FSAR 2.5.1 Reference 476) do not provide an explicit statement regarding the resolution of ODP seismic reflection data. Harwood and Towers (1988, p. 263) (FSAR 2.5.1 Reference 476) do, however, state that "seismic sedimentologic features are recognizable to a resolution of better than 10 m." FPL interprets this to indicate that one cannot observe disturbances in post-middle Miocene strata that are appreciably smaller than the resolution limit of the seismic data (approximately 10 m). If we assume the Walkers Cay fault has remained active to the present day and the vertical fault separation in the past ~5 Ma were twice the seismic data resolution (20 m), then the long-term vertical separation rate would be very low, on the order of 0.004 mm/yr.

In addition, the thickness of the Quaternary section, as measured in three ODP borings along profile LBB-18, ranges from 3.6 m to 18.2 m. This is similar to the resolution of the seismic data as described by Harwood and Towers (1988) (FSAR 2.5.1 Reference 476), which makes it difficult to accurately assess the presence or absence of Quaternary deformation on the Walkers Cay fault.

3) Discuss the earlier interpretation of fault offset to the sea floor in light of the Austin et al 1988 a and b papers.

The earliest descriptions of the Walkers Cay fault (Mullins and Van Buren 1981; Van Buren and Mullins 1983) (FSAR 2.5.1 References 474 and 791) do not describe or graphically depict the Walkers Cay fault as cutting the seafloor. In both of those studies, the authors do not map the Walkers Cay fault upward to the seafloor on either Profile E or Profile 4 (Figures 2 and 3). Although the authors speculate that the fault appears to extend "possibly even to the seafloor" (Mullins and Van Buren 1981, p. 226) (FSAR 2.5.1 Reference 474) they state that "movement along the Walkers Cay Fault occurred during the Cenozoic (post-late Oligocene time)" (Mullins and Van Buren 1981, p. 226) (FSAR 2.5.1 Reference 474). Additionally, a three-dimensional schematic rendering of the Little Bahama slope shows the Walkers Cay fault as not reaching the seafloor, but instead terminating upward within the Late Oligocene to Recent section (Figure 7). In both publications, the authors refer to the fault as a "Cenozoic" feature. Thus, the information provided in Mullins and Van Buren (1981) and Van Buren and Mullins (1983) (FSAR 2.5.1 References 474 and 791) does not demonstrate nor preclude Quaternary (Pleistocene or even Holocene) activity on the Walkers Cay fault.

The more recent publications on the Walkers Cay fault include Austin et al. (1988a), Austin et al. (1988b) (FSAR 2.5.1 Reference 785), and Harwood and Towers (1988) (FSAR 2.5.1 Reference 476). In seismic line LBB-18, a normal fault is interpreted by Austin et al (1988b) (FSAR 2.5.1 Reference 785) as reaching the seafloor (Figure 5), and, depending on the age of the strata at the seafloor, could represent evidence for Quaternary fault activity. In LBB-17, however, Austin et al. (1988b) (FSAR 2.5.1 Reference 785) depict brittle faulting up through sequence G. Overlying seismic sequences A-F "do not appear to be offset, but thickening of sequences A-E across the upward continuation of the fault trace implies continuing differential subsidence across this feature" (Austin et al. 1988b, p. 395) (FSAR 2.5.1 Reference 785). FPL notes that this could be caused by non-brittle faulting or differential compaction, and that the uppermost reflector(s) representing the youngest strata appear flat and thus do not indicate thickening across the Walkers Cay at the time of their deposition. FPL interprets LBB-13 to show faulting at depth, and folding of decreasing amplitude upward, with several overlying parallel and unfaulted reflectors at the top of section (Figure 6). The uppermost obvious folding above the Walkers Cay fault on LBB-13 appears to be within seismic sequence D, or Eocene to early Miocene strata, according to correlations with ODP Site 627 presented in Austin et al. (1988a) (Figure 8). Similarly, the uppermost folding associated with the Walkers Cay fault on LBB-17 appears to occur below the seafloor, and possibly within pre-Quaternary sediments, given that the Quaternary section in this region is typically less than approximately 20 m thick (discussed in part 4 below).

Harwood and Towers (1988) (FSAR 2.5.1 Reference 476) present the only summary of all available timing information on the Walkers Cay fault from the ODP Leg 101 publications. Harwood and Towers (1988, p. 266) (FSAR 2.5.1 Reference 476) state the "Walkers Cay fault is visible on seismic profiles LBB 5, 6, 13, and 15, with a minor splay on LBB 18 (Figure 6), but throughout the area it has only a minimal effect on sediments younger than middle Miocene." This conclusion is consistent with the conclusions of Mullins and Van Buren (1981) and Van Buren and Mullins (1983) (FSAR 2.5.1 References 474 and 791).

The primary difference between the earlier and later studies is the interpertation of seafloor offset in a minor splay of the Walkers Cay fault in LBB-18, discussed in detail below.

4) Discuss site-survey profiles LBB-17 and LBB-18 of ODP Leg 101, which show the Walkers Cay fault displacing the seafloor.

As described above, ODP Leg 101 seismic line LBB-18 depicts a normal fault extending from above the carbonate platform top (sequence G) to the seafloor (Austin et al. 1988b) (FSAR 2.5.1 Reference 785) (Figure 5). This is the only profile in which any author has described faulting to the seafloor. No statements regarding the amount of offset in Quaternary strata are provided in Austin et al. (1988a) or Austin et al. (1988b) (FSAR 2.5.1 Reference 785).

Regarding profile LBB-17 (Figure 4), as stated above, Austin et al. (1988b) (FSAR 2.5.1 Reference 785) depict brittle faulting within sequence G, and deformation continuing upwards as monoclinal folding in the upper stratigraphy (Figure 4). Austin et al. (1988b, p. 401) (FSAR 2.5.1 Reference 785) attribute the fold in seismic reflection sequences A-F to "synsedimentary movement". The monocline appears to be the result of tectonic deformation that extends upward through at least the D-E boundary, which would argue for tectonic activity at least into the late Paleocene-early Eocene (Austin et al., 1986b). They do not suggest that the fault extends to the seafloor in this profile. There appear to be flat-lying, undeformed reflectors between 1.5 seconds (two-way travel time) and the seafloor.

Borehole data in the vicinity of these seismic profiles indicate that the Quaternary section is limited to a thin veneer. At ODP sites 627, 628, and 630, analysis of cores found that planktonic foraminifers associated with Pleistocene sediments are limited to approximately the uppermost 15.5 m, 3.6 m, and 18.2 m, respectively (Figure 1) (Austin et al. 1986a, 1986b, 1986c). There is no indication of abrupt thinning or thickening of layers in the seismic profiles that would suggest these observations are spatial anomalies. Furthermore, these thicknesses are in agreement with regional mapping (Reed et al., 2005) that indicates Neogene (Pliocene or Miocene) strata are within 20 m of the seafloor in this area. Thus, to determine if the Walkers Cay fault is a Quaternary structure, seismic data would need to resolve displacement within approximately the uppermost 20 m of seafloor sediments.

In summary, on only one of the five presented seismic lines that cross the Walkers Cay fault (LBB-18) do the authors interpret a fault reaching the seafloor (Figure 5) (Austin et al. 1988b) (FSAR 2.5.1 Reference 785). This is consistent with the summary of seismic lines collected in ODP Leg 101 that states that "throughout the area it [the Walkers Cay fault] has only a minimal effect on sediments younger than middle Miocene" (Harwood and Towers 1988, p. 266) (FSAR 2.5.1 Reference 476). The possibility of Quaternary slip on the Walkers Cay fault cannot be precluded by the available data.

Hazard Sensitivity Calculation for the Walkers Cay Fault

As described above, at least one strand of the Walkers Cay fault may extend upward to the seafloor, but it is unclear whether the Walkers Cay fault extends upward into Quaternary deposits and thus may be a capable tectonic source. Based on the available data, possible faulting of the seafloor and Quaternary activity on the Walkers Cay fault cannot be precluded. For this reason, a hazard sensitivity calculation was performed to assess the potential impact of a Walkers Cay fault source on the probabilistic seismic hazard analysis (PSHA) for the Turkey Point Units 6 & 7 site. The Walkers Cay fault lies northeast of the site and straddles the 200-mile site region boundary (Figure 1).

Seismic Source Characterization for the Walkers Cay Fault

The Walkers Cay fault is included as a discrete fault source in a hazard sensitivity calculation. The input parameters for the Walkers Cay fault source are described below:

Probability of Activity: For the purpose of the hazard sensitivity calculation, it is assumed that the Walkers Cay fault is a capable tectonic source with a probability of activity of 1.0.

Source Location and Geometry: Van Buren and Mullins (1983) (FSAR 2.5.1 Reference 791) map the Walkers Cay fault as an approximately 33-km-long, north-northeast-striking, steeply dipping structure. At its nearest point, the Walkers Cay fault is located approximately 300 km from the Turkey Point Units 6 & 7 site. Alternatively, Austin et al. (1988b) (FSAR 2.5.1 Reference 785) map the Walkers Cay fault zone at approximately the same distance from Turkey Point Units 6 & 7 and as a broad northeast-striking zone that could include a fault of up to 24 km in length (Figures 1 and 9). For the purpose of the hazard sensitivity calculation, the geometry of the Walkers Cay fault source is simplified after the 33-km-long mapped depiction of Van Buren and Mullins (1983) (FSAR 2.5.1 Reference 791) and is assumed to have a vertical dip angle and a rupture depth from 0 to 15 km depth.

Maximum Magnitude Assessment: The characteristic magnitude for the Walkers Cay fault source is based on the empirical surface rupture length-magnitude regression from Wells and Coppersmith (1994) (FSAR 2.5.1 Reference 662) for all fault types, assuming a surface rupture length equal to the 33 km mapped length of the fault from Van Buren and Mullins (1983) (FSAR 2.5.1 Reference 791). This regression provides a median value of M_w 6.8. Uncertainty associated with this value is accounted for in the hazard sensitivity calculation by allowing earthquakes of 0.2 magnitude units larger or smaller than the characteristic event. The characteristic magnitude distribution [and weights] assigned to the Walkers Cay fault source is: M_w 6.6 [0.2], 6.8 [0.6], 7.0 [0.2].

Slip Rate Assessment: There are no data with which to directly determine the late Quaternary slip rate on the Walkers Cay fault. There are, however, data and observations that can be used to constrain possible slip rate values for the Walkers Cay fault source, including:

- Published literature describing the Walkers Cay fault does not provide description of any possible fault scarps in the seafloor in the vicinity of the Walkers Cay fault.

- Published literature indicates a relatively thin Quaternary section in the vicinity of the Walkers Cay fault (Figure 1). Specifically, borehole data from ODP sites 627, 628, and 630 indicate Quaternary sediments are limited to approximately the uppermost 15.5 m, 3.6 m, and 18.2 m, respectively (Figure 1). Moreover, regional mapping by Reed et al. (2005) indicates Neogene (Pliocene or Miocene) strata are within 20 m of the seafloor in the vicinity of the Walkers Cay fault.
- There is no indication in the seismic reflection data (e.g., Van Buren and Mullins 1983; Austin et al. 1988b; Harwood and Towers 1988) (FSAR 2.5.1 References 791, 785, and 476) of abrupt thickening of young layers (post-Miocene) in the vicinity of the Walkers Cay fault that might indicate thickening of Quaternary basin geometry.
- The lack of observed bathymetric expression in the vicinity of the Walkers Cay fault, coupled with the observation of only a thin veneer of Quaternary deposits across the region, suggests the lack of significant vertical separation associated with the fault in Quaternary time. As discussed in part 2 of this response, a vertical separation rate greater than 0.004 mm/yr should be resolvable in the data published by Harwood and Towers (1988) (FSAR 2.5.1 Reference 476).Van Buren and Mullins (1983) (FSAR 2.5.1 Reference 791) indicate up to 100 m of vertical separation of the 30 Ma boundary between NLBB-1 and NLBB-2 across the Walkers Cay fault (Figure 2). The time period over which this separation occurred is not clear, but if it occurred since 15 Ma (half-way up through NLBB-1 on Figure 2), this results in a vertical separation rate of 0.0067 mm/yr since that time. If this vertical separation occurred since 10 Ma (two-thirds of the way up through NLBB-1 on Figure 2), this results in a vertical separation rate of 0.01 mm/yr since that time.
- Austin et al. (1988b) (FSAR 2.5.1 Reference 785) provide structure contour maps with 20-m contour intervals for the top of Sequence D (latest early Miocene) and the top of Sequence G (early Cretaceous) (Figure 9). Major perturbations in these contours that would be indicative of significant fault offset since those times are not apparent, suggesting that the total amount of vertical separation across the Walkers Cay fault likely is on the order of tens of meters or less.
- The table below indicates, for different assumed vertical separation rates, the expected total vertical separation in Quaternary time. For example, assuming a vertical separation rate of 0.01 mm/yr yields 18-26 m of vertical relief that should be expressed as either scarps in the seafloor or thickening of Quaternary sediments.
- Austin et al (1988b) (FSAR 2.5.1 Reference 785) desribe at least one strand of the Walkers Cay fault as normal, but the published literature does not provide clear geometry, including dip, kinematic information, or the ratio of horizontal to vertical slip on the Walkers Cay fault. The table below shows, for assumed horizontal to vertical ratios of 1:1 and 5:1, the expected slip rates that correspond to different vertical separation rates on a vertically dipping fault plane.

Assumed vertical separation rate (mm/yr)	Total vertical separation (m) in Quaternary (1.8 Ma)*	Total vertical separation (m) in Quaternary (2.6 Ma)*	Slip rate (mm/yr) if horizontal to vertical slip ratio = 1:1	Slip rate (mm/yr) if horizontal to vertical slip ratio = 5:1
0.001	1.8	2.6	0.0014	0.0051
0.005	9	13	0.0071	0.026
0.01	18	26	0.014	0.051
0.05**	90	130	0.071	0.26
0.10**	180	260	0.14	0.51

** At present, the Quaternary Period is defined as spanning from approximately 2.6 Ma to present (Gibbard et al. 2009). At the time of publication of Austin et al. (1988b) (FSAR 2.5.1 Reference 785) and Van Buren and Mullins (1983) (FSAR 2.5.1 Reference 791), the Quaternary Period was defined as spanning from approximately 1.8 Ma to present.*

*** Note that these vertical separation rates would produce total vertical separations that are not supported by geologic data, as discussed in the text.*

Taken together, the data and observations described above are used to constrain a conservative representation of the modeled slip rate distribution for the Walkers Cay fault source for hazard sensitivity calculation purposes, as follows:

- The upper bound on the modeled slip rate distribution is set at 0.05 mm/yr. This is based on the assessment that, even assuming a high horizontal to vertical slip ratio, any greater Quaternary slip rate likely would have resulted in several tens of meters of vertical relief that would be recognized in bathymetric and/or seismic reflection data. This suggests that slip rates of 0.05 mm/yr and larger on the Walkers Cay fault are not supported by the presently available data.
- The median value of modeled slip rate is set at 0.01 mm/yr. This is based on the assessment that the Walkers Cay fault could have been active throughout the Quaternary at this rate and remain unobserved in the bathymetry and/or seismic reflection data. Assuming a moderate fault dip and relatively low horizontal to vertical slip ratios, consistent with the inference that the Walkers Cay fault has mostly normal slip, a slip rate of 0.01 mm/yr likely would result in vertical separations of 10 to 20 m at the base of the Quaternary section.
- The lower bound on the modeled slip rate distribution is set at 0.001 mm/yr. This is based on the possibility that the Walkers Cay fault is slipping at a very low rate, not likely to be detectable within the limits of available data, yet is still a capable tectonic source.

The potential for erosion of Quaternary sediments is a complicating factor for estimating Quaternary slip rates on the Walkers Cay fault. Structure contour data and vertical separation observed from seismic reflection lines limit the total vertical separations across the fault. This uncertainty is accounted for in the broad distribution of slip rates assigned the the Walkers Cay fault. The slip rate distribution in mm/yr [and weights] assigned to the Walkers Cay fault source for hazard sensitivity calculation is: 0.001 [0.2], 0.01 [0.6], 0.05 [0.2]. This slip rate distribution accounts for the possibility of some horizontal component of fault slip and captures uncertainty in possible fault dip. The largest weight in this distribution is accorded to a slip rate of 0.01 mm/yr, which appears to represent a limiting rate beyond which there would be a significant likelihood that vertical separations of the seafloor and Quaternary deposits would be sufficiently large to be observable within the presently available data.

Recurrence Model: For the purpose of the hazard sensitivity calculation, a characteristic earthquake recurrence model (Youngs and Coppersmith 1985), but with no contribution from an exponential portion of the recurrence curve at lower magnitudes, is assumed for the Walkers Cay fault source.

Results and Conclusions from the Hazard Sensitivity Calculation

Walkers Cay fault hazard is calculated using the Midcontinent crustal model and non-rifted coefficients from the EPRI 2004 attenuation relations. The Midcontinent crustal model generates higher hazard curves than the Gulf Coast crustal model and is therefore a more conservative model to this sensitivity calculation.

Figures 10 and 11 show 1 and 10 Hz mean hazard curves, respectively, for the Walkers Cay fault (Midcontinent, non-rifted coefficients (MIDC)), the FSAR total mean hazard, and the FSAR total + Walkers Cay. The table below shows the sensitivity of total mean hazard to the Walkers Cay fault source:

Frequency	10^{-4} MAFE amplitudes, g			MAFE at FSAR 10^{-4} amplitude		
	FSAR	FSAR + Walkers Cay	% Diff	FSAR	FSAR + Walkers Cay	% Diff
1 Hz	0.0343	0.0344	0.3%	1.000E-04	1.007E-04	0.7%
10 Hz	0.0822	0.0826	0.5%	1.000E-04	1.010E-04	1.0%

As shown in the table above, adding the Walkers Cay fault to the FSAR total hazard results in 10^{-4} MAFE (mean annual frequency of exceedance) amplitudes that are 0.3% higher at 1 Hz and 0.5% higher at 10 Hz (comparison along the x-axis), and annual frequencies of exceedance, at the FSAR 10^{-4} MAFE amplitudes, that are 0.7% higher at 1 Hz and 1.0% higher at 10 Hz (comparison along the y-axis). As such, the results of the hazard sensitivity calculation based on the conservative seismic source characterization of the Walkers Cay fault indicate that further consideration of the Walkers Cay fault for the Turkey Point Units 6 & 7 site hazard is unwarranted due to its insignificant contribution to hazard. Therefore, no updates to the PSHA presented in the FSAR are required to account for the Walkers Cay fault.

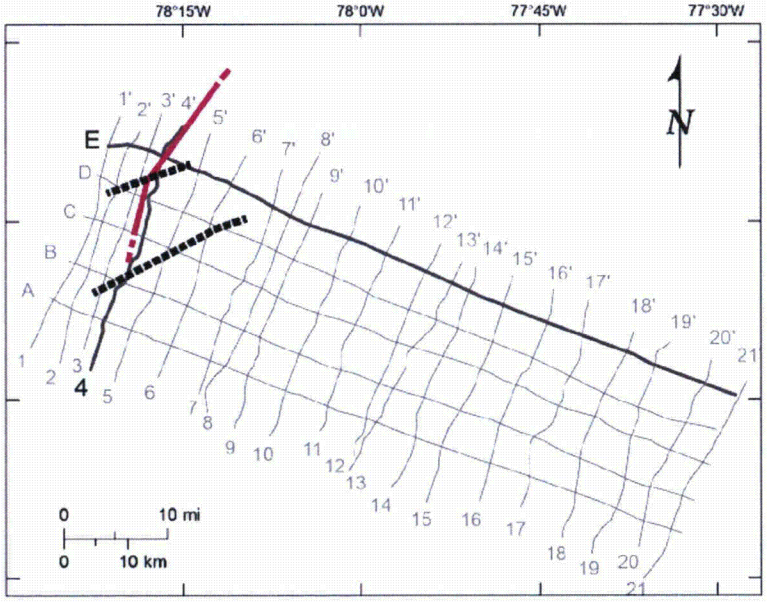

(a) Survey grid and pink fault line from Van Buren and Mullins (1983) (FSAR 2.5.1 Reference 791), dashed lines representing margins of faulting from Austin et al. (1988b) (FSAR 2.5.1 Reference 785).

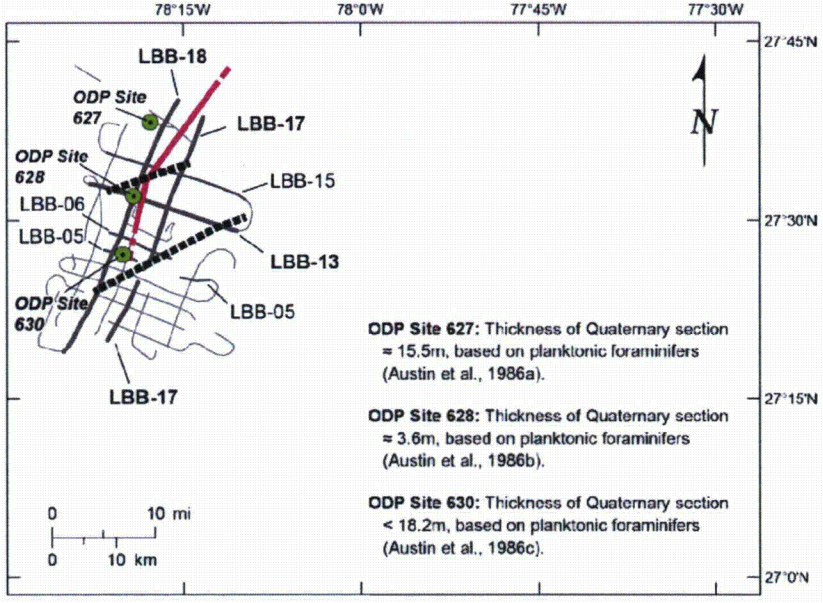

(b) Survey grid and dashed lines representing margins of faulting from Austin et al. (1988b) (FSAR 2.5.1 Reference 785), pink fault line from Van Buren and Mullins (1983) (FSAR 2.5.1 Reference 791).

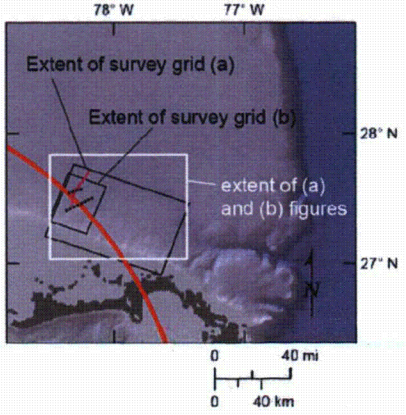

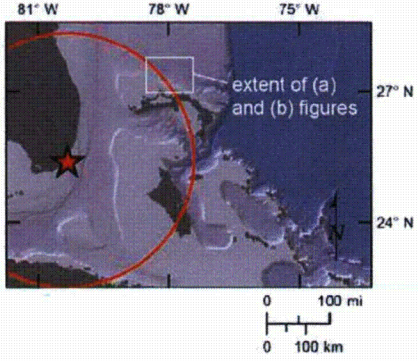

Figure 1 Comparison of mapped depictions of the Walkers Cay fault based on seismic reflection data (modified from Van Buren and Mullins's (1983) (FSAR 2.5.1 Reference 791) Figures 2 and 13, and Austin et al.'s (1988b) (FSAR 2.5.1 Reference 785) Figures 3 and 9.

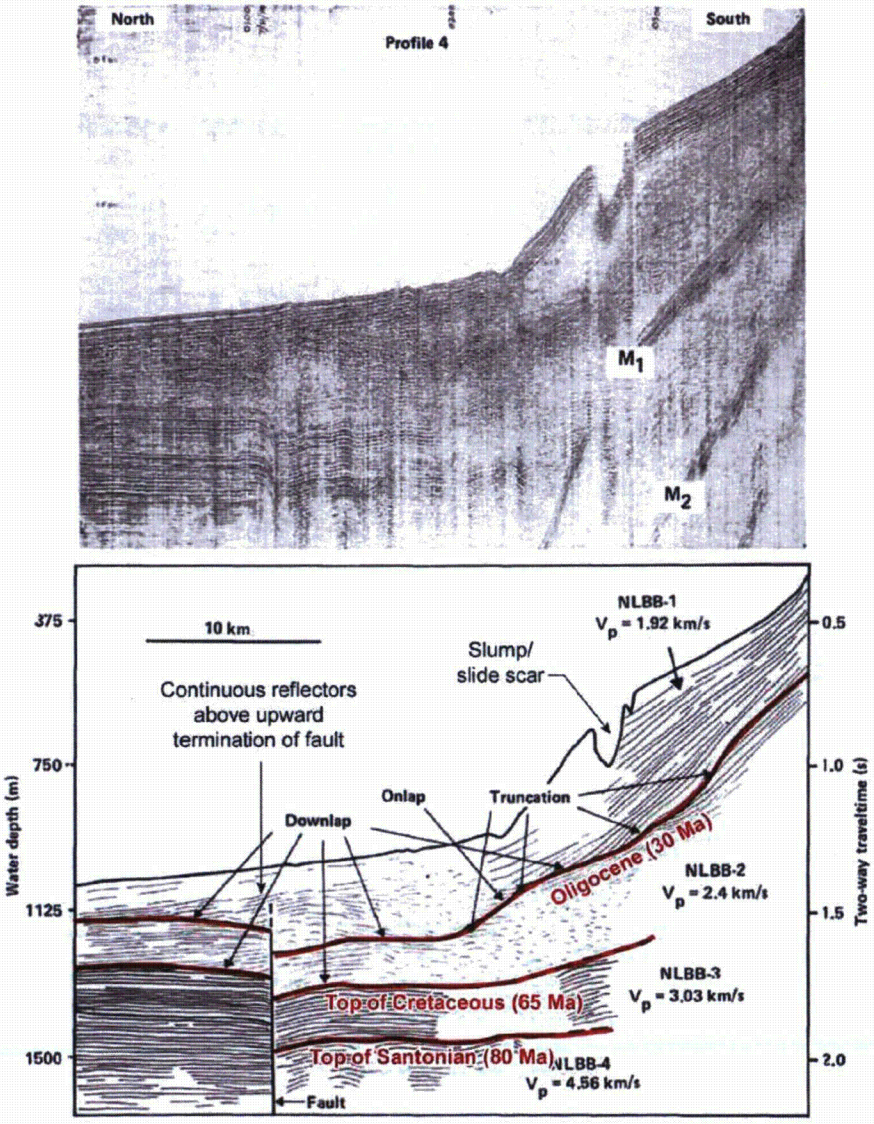

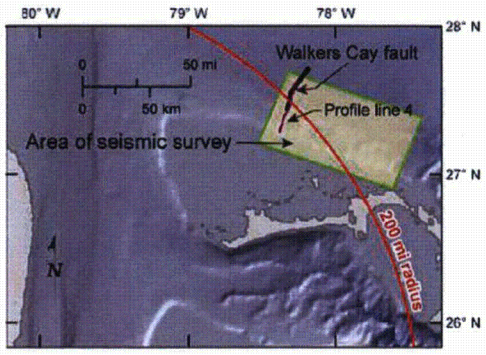

Figure 2 Interpretation of the Walkers Cay fault Profile 4 (modified from Van Buren and Mullins's (1983) (FSAR 2.5.1 Reference 791) Figures 4 and 14).

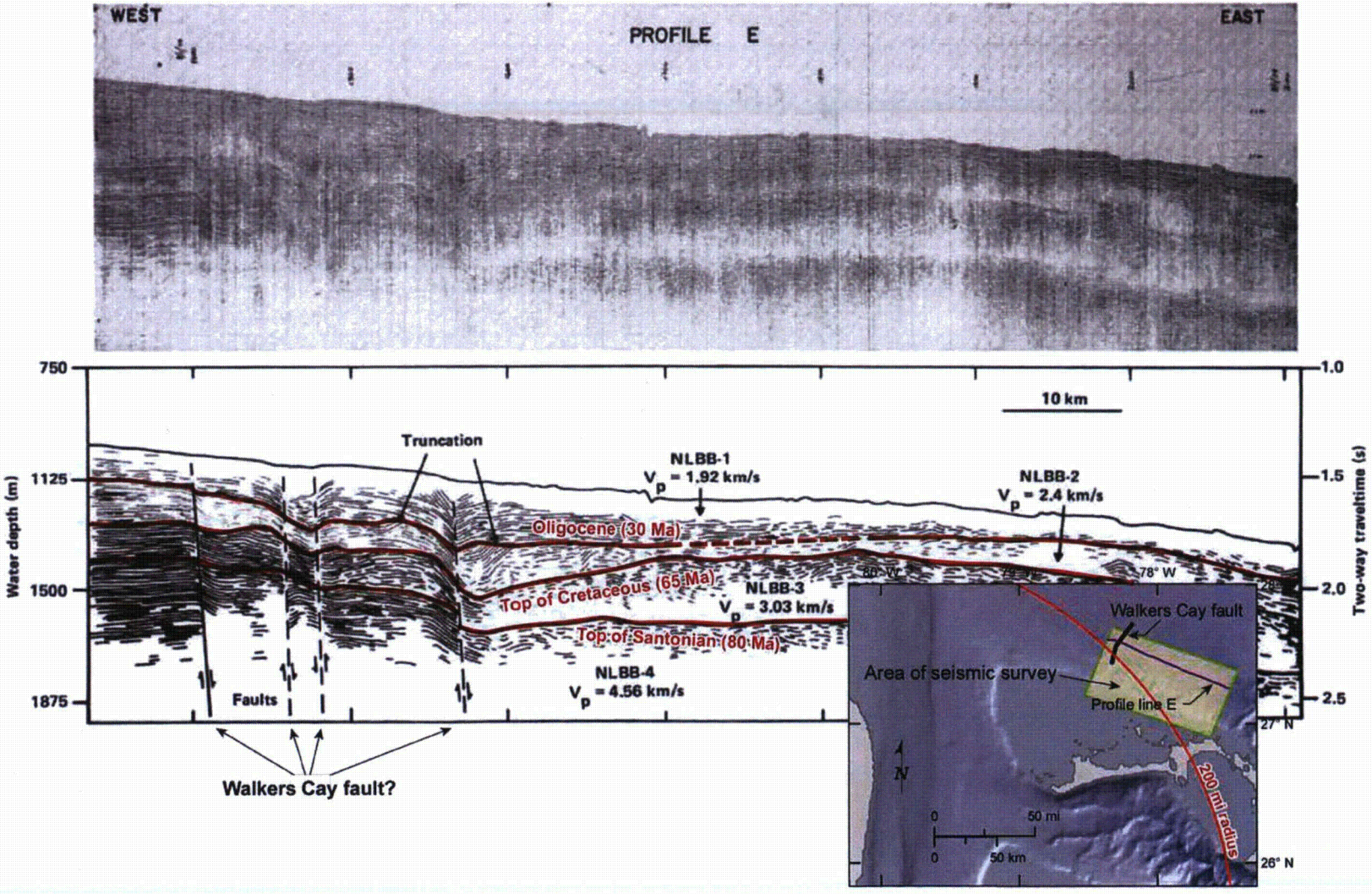

Figure 3 Interpretation of Profile E (modified from Van Buren and Mullins's (1983) (FSAR 2.5.1 Reference 791) Figure 5).

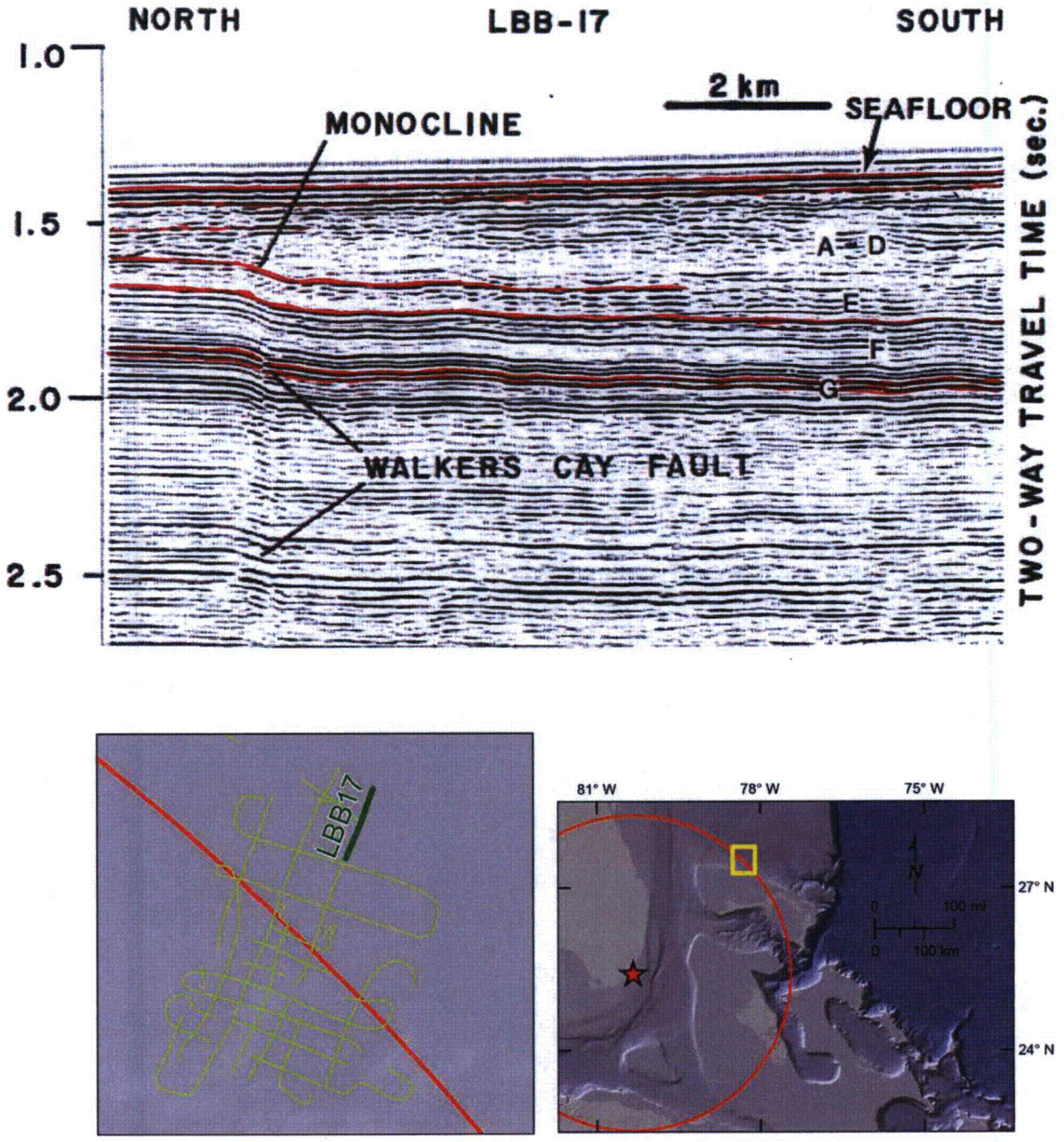

Figure 4 Interpretation of LBB-17 (modified from Austin et al.'s (1988b) (FSAR 2.5.1 Reference 785) Figure 6).

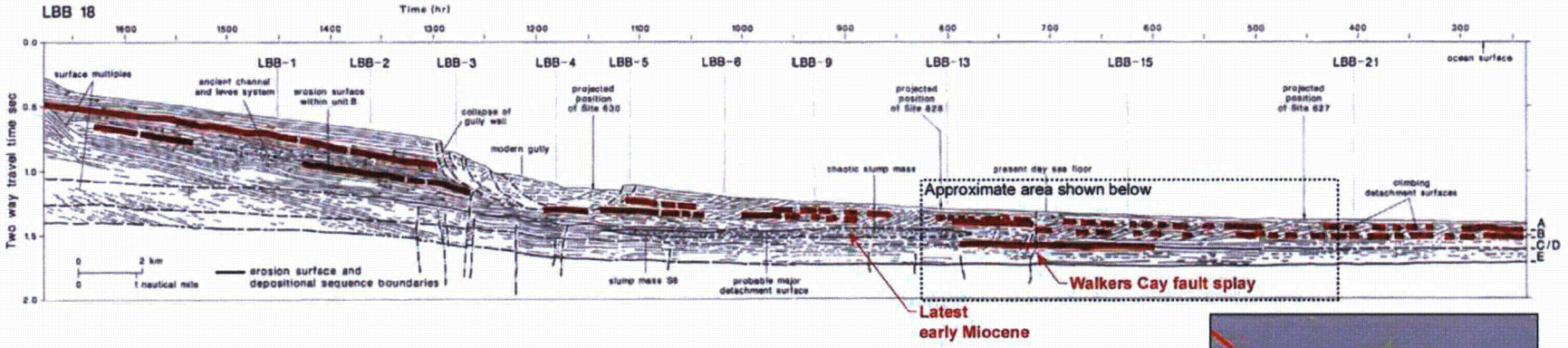

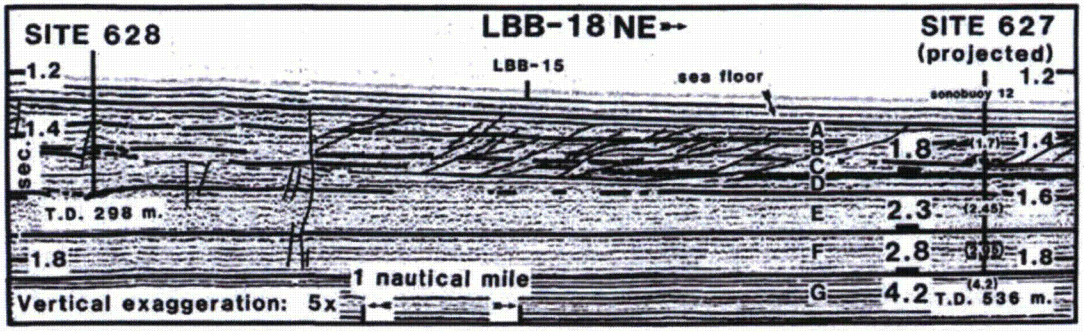

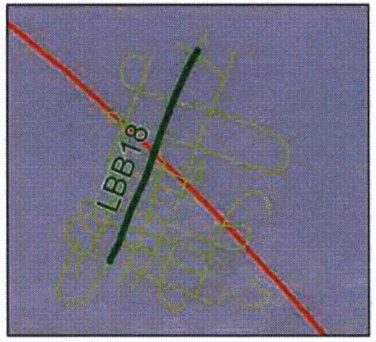

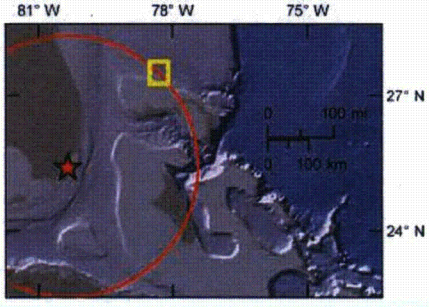

Figure 5 Interpretation of LBB-18. Uppermost cross-section modified from Harwood and Towers' (1988) (FSAR 2.5.1 Reference 476) Figure 6. Lower left cross-section from Austin et al.'s (1988b) (FSAR 2.5.1 Reference 785) Figure 5.

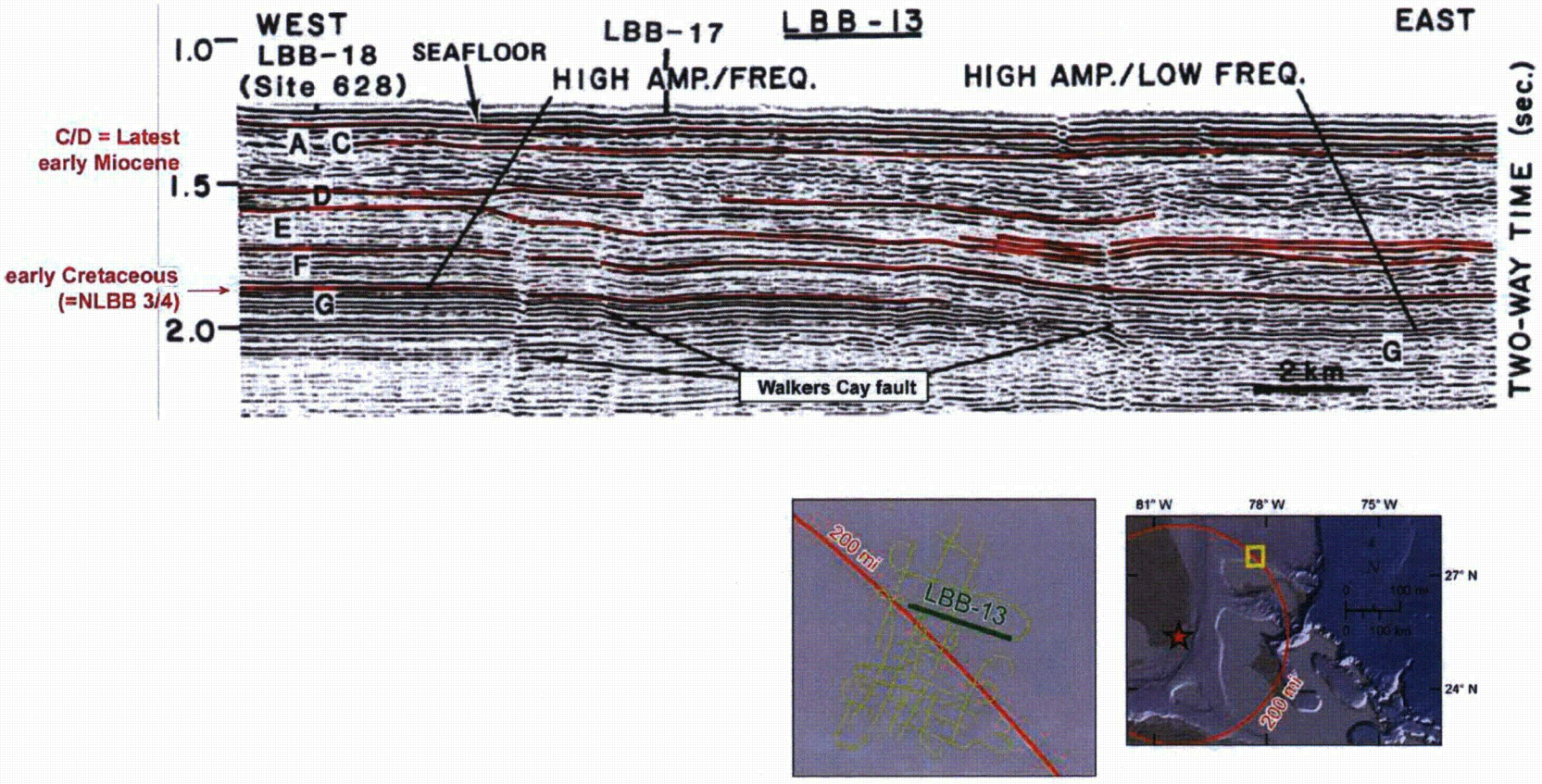

Figure 6 Interpretation of LBB-13 (modified from Austin et al.'s (1988b) (FSAR 2.5.1 Reference 785) Figure 7).

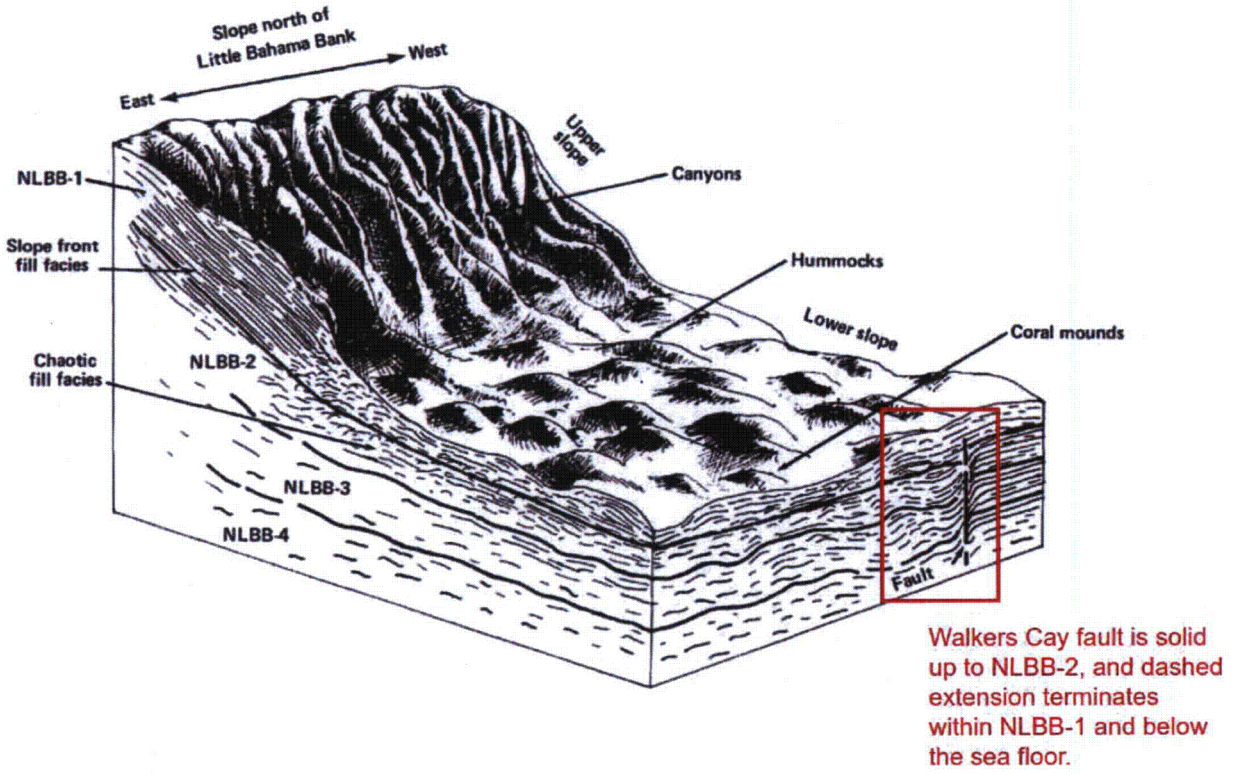

Figure 7 Schematic block diagram depicting surface morphology (exaggerated) and seismic stratigraphic units north of the Little Bahama Bank. View is looking to the southwest from the Blake Plateau. No scale is implied (modified from Van Buren and Mullins's (1983) (FSAR 2.5.1 Reference 791) Figure 14).

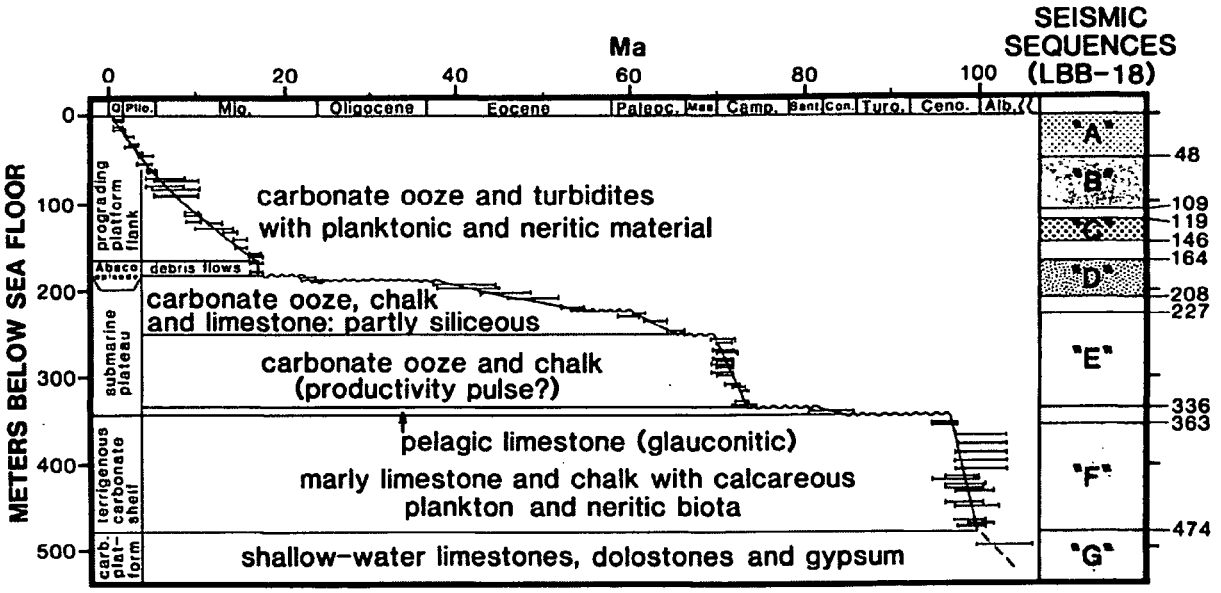

Figure 8 Correlation between seismic stratigraphy and ODP site 627 (modified from Austin et al.'s (1988a) Figure 8).

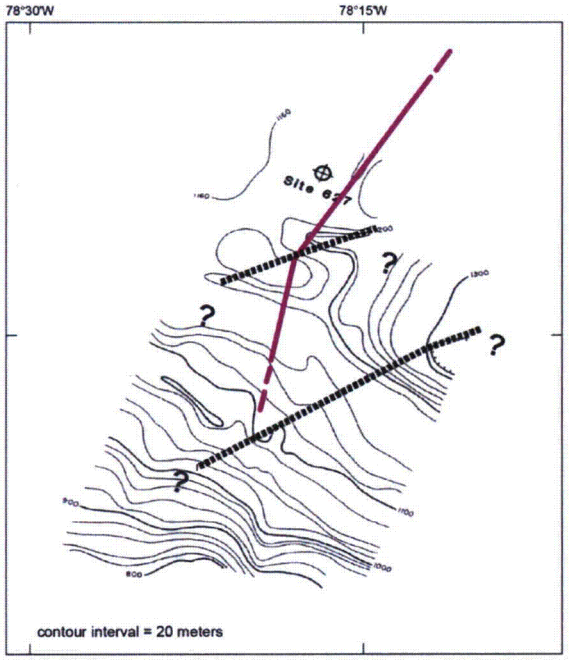

(a) Structure contours on the top of Sequence D and queried boundaries of faulting from Austin et al. (1988b) (FSAR 2.5.1 Reference 785), pink fault line from Van Buren and Mullins (1983) (FSAR 2.5.1 Reference 791). Contours indicate meters below sea level.

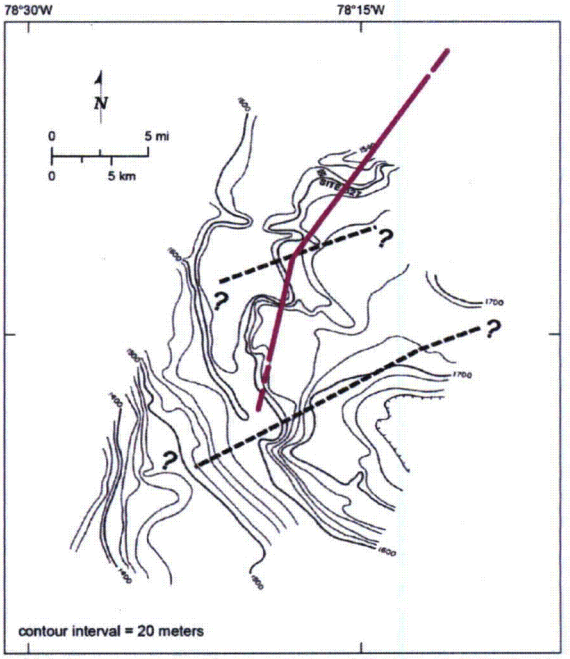

(b) Structure contours on the top of Sequence G (uppermost Albian) and queried boundaries of faulting from Austin et al. (1988b) (FSAR 2.5.1 Reference 785), pink fault line from Van Buren and Mullins (1983) (FSAR 2.5.1 Reference 791). Contours indicate meters below sea level.

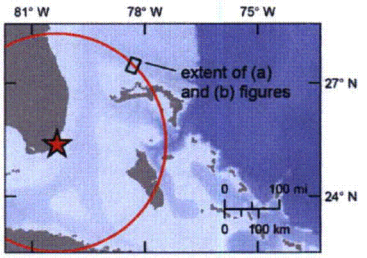

Figure 9 Structure contour maps in the vicinity of the Walkers Cay fault (modified from Van Buren and Mullins's (1983) (FSAR 2.5.1 Reference 791) Figure 13 and Austin et al.'s (1988b) (FSAR 2.5.1 Reference 785) Figures 8 and 9).

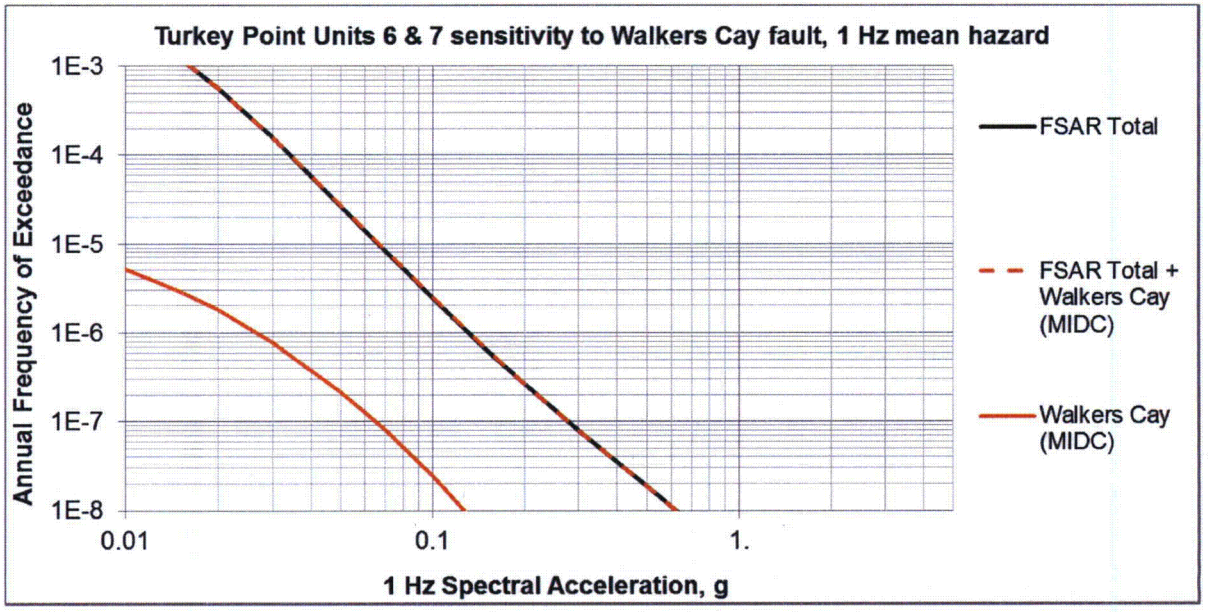

Figure 10 FSAR total 1 Hz mean hazard sensitivity to Walkers Cay fault source.

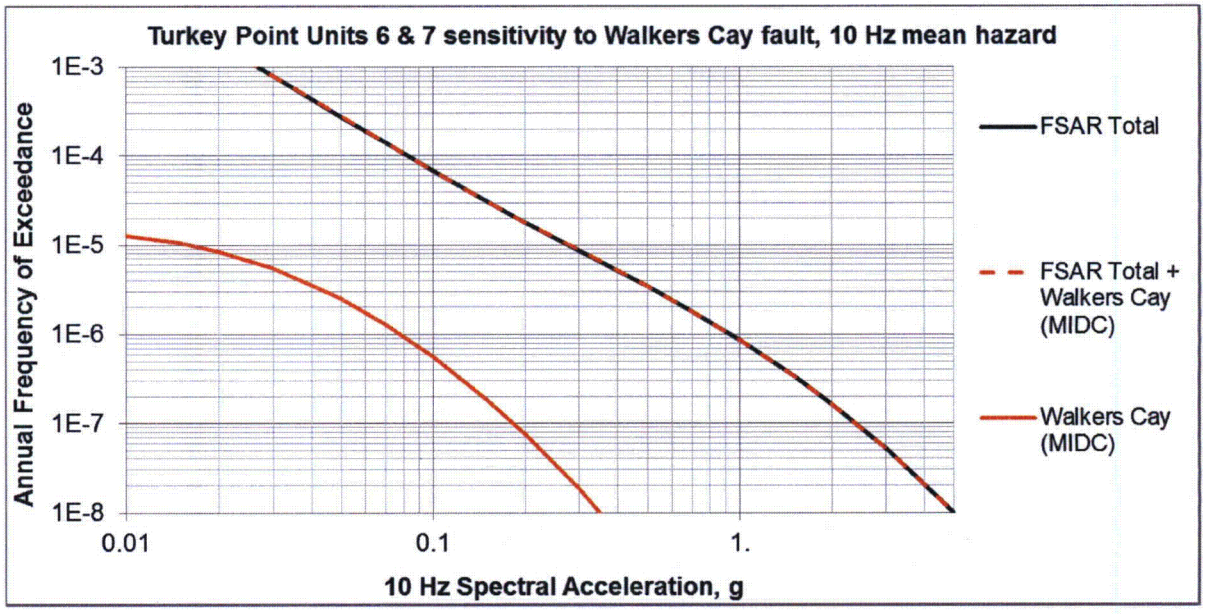

Figure 11 FSAR total 10 Hz mean hazard sensitivity to Walkers Cay fault source.

This response is PLANT SPECIFIC.

References:

Austin, J.A., Jr., Schlager, W., Palmer, A. A., et al., 1986a, Proceedings of the Ocean Drilling Program, Initial Results (Part A), 101: 6, Site 627: Southern Blake Plateau: P. 111-212.

Austin, J. A., Jr., Schlager, W., Palmer, A. A., et al., 1986b, Proceedings of the Ocean Drilling Program, Initial Results (Part A), 101: 7, Site 628: Little Bahama Bank, p. 213-271.

Austin, J. A., Jr., Schlager, W., Palmer, A. A., et al., 1986c, Proceedings of the Ocean Drilling Program, Initial Results (Part A), 101: 8, Site 629 and 930: Little Bahama Bank, p. 271-340.

Austin, J. A., Jr., Schlager, W., et al, 1988a, Proceedings of the Ocean Drilling Program, Scientific Results, 101: 29, Leg 101: An Overview, p. 455-472.

Gibbard, P.L., Head, M.J., and Walker, J.C., 2009. *Formal ratification of the Quaternary System/Period and the Pleistocene Series/Epoch with base at 2.58 Ma*, Journal of Quaternary Science, v. 25, no. 2, p. 96-102.

Reed, J.C., Wheeler, J.O., and Tucholke, B.E., 2005, Decade of North American Geology, Geologic Map of North America, The Geological Society of America, Boulder, Colorado.

Youngs, R.R. and Coppersmith, K.J., 1985, Implications of fault slip rates and earthquake recurrence models to probabilistic seismic hazard estimates, Bulletin of the Seismological Society of America, v. 75, no. 4, p. 939-964.

ASSOCIATED COLA REVISIONS:

The third paragraph of FSAR Subsection 2.5.1.1.1.3.2.2 will be revised as shown below in a future FSAR revision:

Walkers Cay Fault

~~The Walkers Cay fault is mapped just north of Little Bahama Bank (approximately 198 miles or 320 kilometers from the Units 6 & 7 site) (Figure 2.5.1-229) in a series of seismic reflection profiles (Reference 474). However, different seismic studies have depicted different geometries for the estimated trace of the fault and its location should be considered uncertain. Originally, the youngest offset on the structure was interpreted as the top of a seismic sequence correlated as Oligocene, with 75 to 100 meters (250 to 330 feet) of offset (Reference 474) (Figure 2.5.1-275). Later work with a more detailed seismic study indicated that the youngest sequence offset by the fault is the top of an Early Cretaceous (Albian) shallow water carbonate platform, and that overlying strata thicken across the trace of the fault, indicating continuing differential subsidence (Reference 432) (Figure 2.5.1-346). However, some seismic profiles indicate that the Walkers Cay fault, or a similar normal fault, may extend to the seafloor (Figures 2.5.1-276 and 2.5.1-277). Regional summaries assign a Cretaceous to middle Tertiary age for this structure and interpret it as indicating some late-stage reactivation of Mesozoic normal faults cutting basement (Reference 307). While strata above the Oligocene horizon have been interpreted as both faulted and unfaulted (e.g., References 475 and 432), Harwood and Towers (Reference 476) indicate that the Walkers Cay fault has only a minimal effect on middle Miocene and younger strata. Because of the minor deformation of Miocene and younger strata, the Walkers Cay fault is concluded to be a Tertiary structure, and thus, not considered a capable tectonic structure.~~

The Walkers Cay fault was initially identified by Mullins and Van Buren (Reference 474) north of Little Bahama Bank based on seismic reflection data. As later mapped by Van Buren and Mullins (Reference 791), the fault is a 33-kilometer-long (21-mile-long) structure that strikes north-northeast (Figures 2.5.1-275 and 2.5.1-366). In contrast, Austin et al. (Reference 785) depict a broad zone of faulting by mapping the northwest and southeast boundaries of the zone, but do not map the extent of any individual strands in the zone. These boundaries of the Walkers Cay fault zone are defined as having a more easterly strike than the fault of Van Buren and Mullins (Reference 791) and a similar length (Figure 2.5.1-366). The spatial coincidence of the faulting expressed in Oligocene- to Cretaceous-age strata with a magnetic anomaly has been used to interpret the Walkers Cay fault as a basement-involved structure (References 307 and 474).

In the vicinity of the Walkers Cay fault, five seismic reflection lines with variable levels of interpretation have been reproduced in the published literature. Mullins and Van Buren (Reference 474) and Van Buren and Mullins (Reference 791) present two air gun seismic reflection profiles (Profile 4 and Profile E) in their reports about this structure (Figure 2.5.1-366). Shortly thereafter, the Ocean Drilling Program (ODP) Leg 101 conducted another seismic survey of the north slope of Little Bahama Bank and these data are discussed in several publications (References 476, 785, 937, 938, and 940). Three published seismic lines from that work (Lines LBB-13, LBB-17 and LBB-18) depict the Walkers Cay fault or a splay of the fault (Figure 2.5.1-366). In at least one of those lines (Line LBB-18), the authors interpret a normal fault "believed to be the Walkers Cay normal fault" as extending up to the seafloor, suggesting possible Quaternary activity (Reference 785,) (Figure 2.5.1-367). Normal faulting is reportedly visible on lines LBB-5, LBB-6, and LBB-15 (Reference 476), but these seismic lines have not been reproduced in any of the publications from ODP Leg 101.

Borehole data in the vicinity of these seismic profiles indicate that the Quaternary section is limited to a thin veneer. At ODP sites 627, 628, and 630, analysis of cores found that planktonic foraminifers associated with Pleistocene sediments are limited to approximately the uppermost 15.5 meters (50.9 feet), 3.6 meters (11.8 feet), and 18.2 meters (59.7 feet), respectively (Figure 2.5.1-366) (References 937, 938, 939). There is no indication of abrupt thinning or thickening of layers in the seismic profiles that would suggest these observations are spatial anomalies. Furthermore, these thicknesses are in agreement with regional mapping (Reference 941) that indicates Neogene (Pliocene or Miocene) strata are within 20 meters (66 feet) of the seafloor in this area. Thus, to determine if the Walkers Cay fault is a Quaternary structure, seismic data would need to resolve displacement within approximately the uppermost 20 meters (66 feet) of seafloor sediments.

In summary, on only one of the five interpreted seismic lines that cross the Walkers Cay fault (LBB-18) do the authors interpret a fault reaching the seafloor (Figure 2.5.1-367) (Reference 785). This is consistent with the summary of seismic lines collected in ODP Leg 101 that states that "throughout the area it [the Walkers Cay fault] has only a minimal effect on sediments younger than middle Miocene" (Reference 476). The possibility of Quaternary slip on the Walkers Cay fault cannot be precluded by the available data. For this reason, a hazard sensitivity calculation for a Walkers Cay fault source is presented in Subsection 2.5.2.4.4.3.4.

Several new paragraphs will be inserted into a new FSAR Subsection 2.5.2.4.4.3.4 to describe the hazard sensitivity studies for the Walkers Cay fault, Cuba faults, and Cuba areal source zone. The text below for the Walkers Cay fault will be added in a future FSAR revision:

2.5.2.4.4.3.4 Hazard Sensitivity Calculations

Hazard sensitivity calculations were performed to assess the significance of certain aspects of the PSHA for the Turkey Point Units 6 & 7 site. Calculations were performed to assess the potential impact of: (1) the Walkers Cay fault, (2) several faults within Cuba, and (3) different approaches to modeling the Cuba areal source zone.

2.5.2.4.4.3.4.1 Walkers Cay Fault Hazard Sensitivity Calculation

The Walkers Cay fault lies northeast of the Turkey Point Units 6 & 7 site and straddles the 200-mile site region boundary (Figure 2.5.1-366). Subsection 2.5.1.1.1.3.2.2 describes geologic and seismic reflection data for the Walkers Cay fault. Based on the available data that suggest possible faulting of the seafloor, Quaternary activity on the Walkers Cay fault cannot be precluded. For this reason, a hazard sensitivity calculation was performed to assess the potential impact of a Walkers Cay fault source on the PSHA for the Turkey Point Units 6 & 7 site.

The geometry of the Walkers Cay fault source is based on the mapping of Mullins and Van Buren (Reference 355). For the purposes of the hazard sensitivity calculation, the Walkers Cay fault is assumed to have a vertical dip angle and a rupture depth from 0 – 15 kilometers (0-9 miles). The characteristic magnitude for the Walkers Cay fault source is based on the empirical surface rupture length-magnitude regression from Wells and Coppersmith (Reference 334) for all fault types, assuming a surface rupture length equal to the 33-kilometer (21-mile) mapped length of the fault. This regression provides a median value of M_w 6.8. Uncertainty associated with this value is accounted for in the hazard sensitivity calculation by allowing earthquakes of 0.2 magnitude units larger or smaller than the characteristic event. The characteristic magnitude distribution [and weights] assigned to the Walkers Cay fault source is: M_w 6.6 [0.2], 6.8 [0.6], 7.0 [0.2].

There are no data with which to directly determine the late Quaternary slip rate on the Walkers Cay fault. There are, however, data and observations that can be used to constrain possible slip rate values for the Walkers Cay fault source. The slip rate distribution in millimeters/year [and weights] assigned to the Walkers Cay fault source for the hazard sensitivity calculation is: 0.001 [0.2], 0.01 [0.6], 0.05 [0.2]. The largest weight in this distribution is accorded to a slip rate of 0.01 millimeters/year, which

appears to represent a limiting rate beyond which there would be a significant likelihood that vertical separations of Quaternary and Pliocene deposits would be sufficiently large to be observable within the presently available data. Also, the lack of perturbations observed in structure contours of Miocene- and Cretaceous-age contacts in the vicinity of the Walkers Cay fault suggests that the total amount of vertical separation across the fault likely is on the order of tens of meters or less.

For the purpose of the hazard sensitivity calculation, a characteristic earthquake recurrence model (Reference 356) but with no contribution from an exponential portion of the recurrence curve at lower magnitudes is assumed for the Walkers Cay fault source. Walkers Cay fault hazard is calculated using the Mid-continent crustal model and non-rifted coefficients from the EPRI 2004 attenuation relations.

The results of the sensitivity study indicate that adding the Walkers Cay fault to the total hazard results in 10^{-4} mean annual frequency of exceedance (MAFE) amplitudes that are 0.3 percent higher at 1 Hz and 0.5 percent higher at 10 Hz, and annual frequencies of exceedance, at the FSAR 10^{-4} MAFE amplitudes, that are 0.7 percent higher at 1 Hz and 1.0 percent higher at 10 Hz. As such, the results of the hazard sensitivity calculation based on the conservative seismic source characterization of the Walkers Cay fault indicate that further consideration of the Walkers Cay fault for the Turkey Point Units 6 & 7 site hazard is unwarranted due to its insignificant contribution to site hazard.

New references will be included in a future revision of FSAR Subsection 2.5.1.3:

937. Austin, J., Jr., W. Schlager, A. Palmer, et al., Proceedings of the Ocean Drilling Program, Initial Results (Part A), 101: 6, Site 627: Southern Blake Plateau: pp. 111-212, 1986.

938. Austin, J., Jr., W. Schlager, A. Palmer, et al., Proceedings of the Ocean Drilling Program, Initial Results (Part A), 101: 7, Site 628: Little Bahama Bank, pp. 213-271, 1986.

939. Austin, J. Jr., W. Schlager, A. Palmer, et al., Proceedings of the Ocean Drilling Program, Initial Results (Part A), 101: 8, Site 629 and 630: Little Bahama Bank, pp. 271-340, 1986.

940. Austin, J. Jr., W. Schlager, et al, Proceedings of the Ocean Drilling Program, Scientific Results, 101: 29, Leg 101: An Overview, pp. 455-472, 1988a.

941. Reed, J., J. Wheeler, and B. Tucholke, *Decade of North American Geology, Geologic Map of North America,* The Geological Society of America, Boulder, Colorado, 2005.

A New reference will be included in a future revision of FSAR Subsection 2.5.2.7

356. Youngs, R. and K. Coppersmith, *Implications of Fault Slip Rates and Earthquake Recurrence Models to Probabilistic Seismic Hazard Estimates*, Bulletin of the Seismological Society of America, Vol. 75, No. 4, pp. 939-964, 1985

FSAR Figure 2.5.1-276 will be replaced with the following revised figure in a future revision of the FSAR:

Figure 2.5.1-276 Seismic Line and Interpretation Across the Walkers Cay Fault

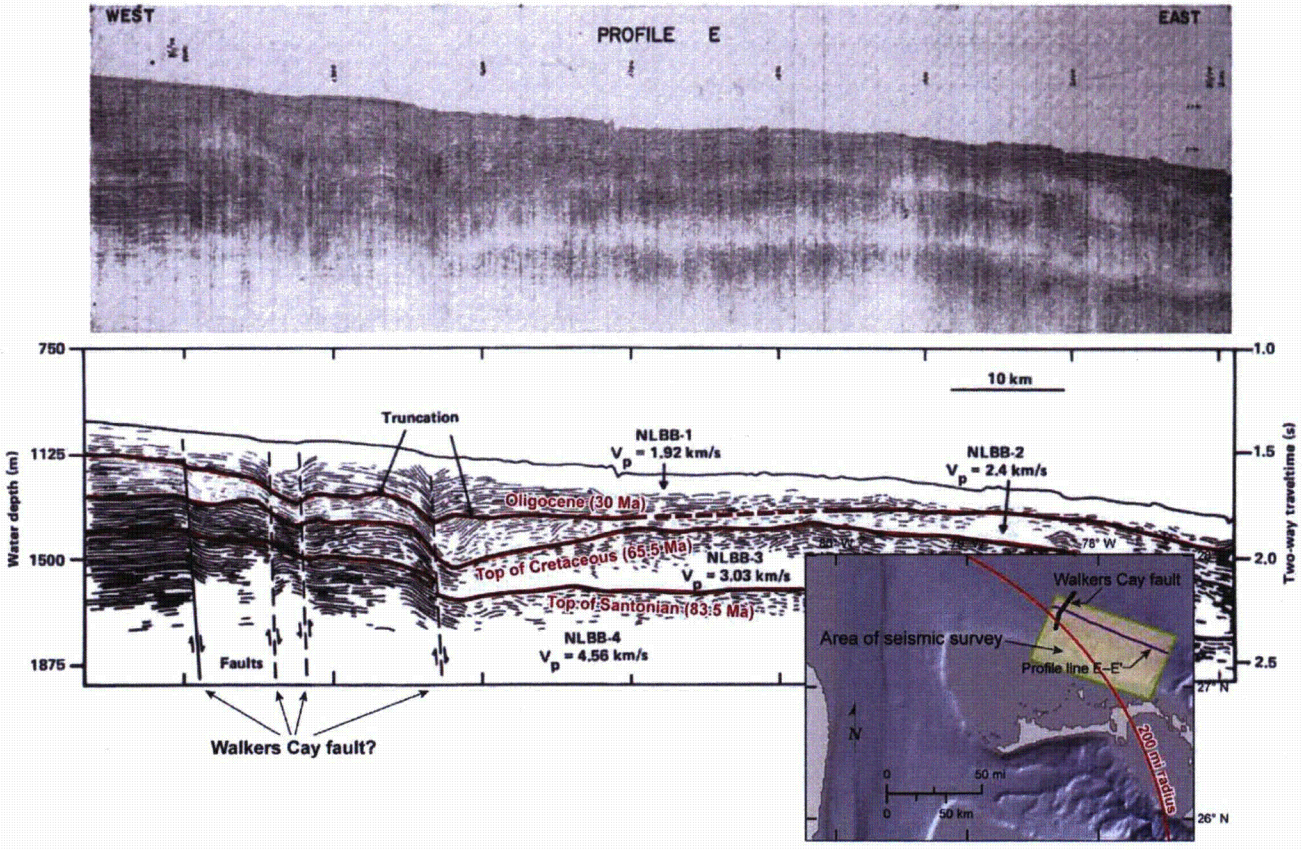

Figure 2.5.1-366 will be added as a new figure in a future revision of the FSAR:

Figure 2.5.1-366 Mapped Depictions of the Walkers Cay Fault Based on Seismic Data

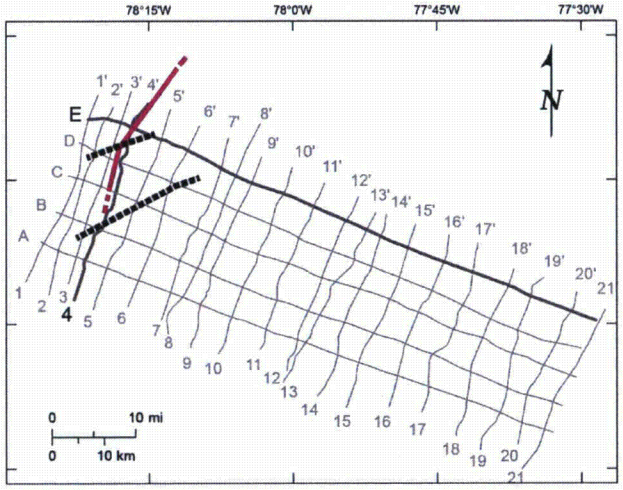

(a) Survey grid and pink fault line from Van Buren and Mullins 1983, dashed lines representing margins of faulting from Austin et al. 1988b

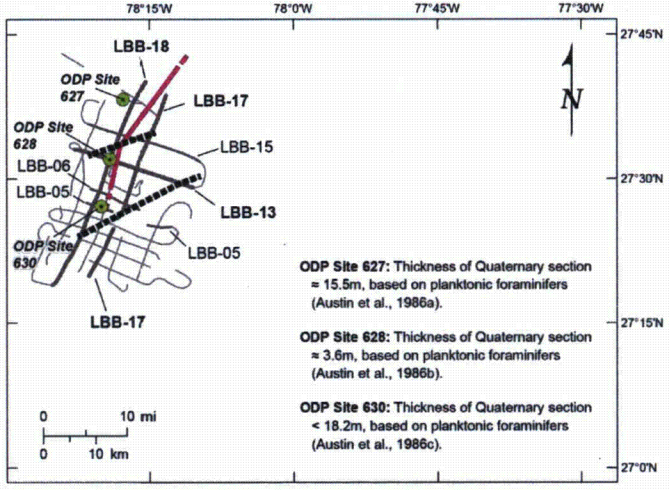

(b) Survey grid and dashed lines representing margins of faulting from Austin et al. 1988b, pink fault line from Van Buren and Mullins 1983

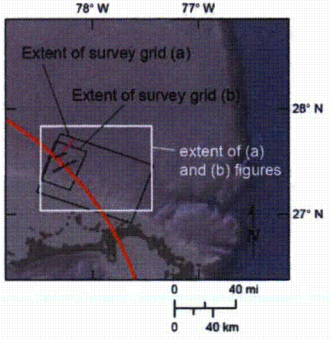

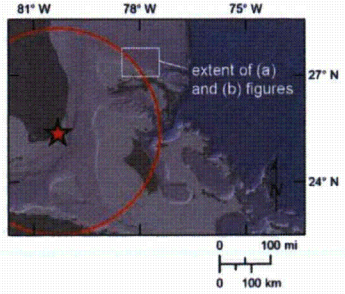

Source: References 474 and 791

Figure 2.5.1-367 will be added as a new figure in a future revision of the FSAR:

Figure 2.5.1-367 Interpretation of the Walkers Cay fault in Seismic Line LBB-18

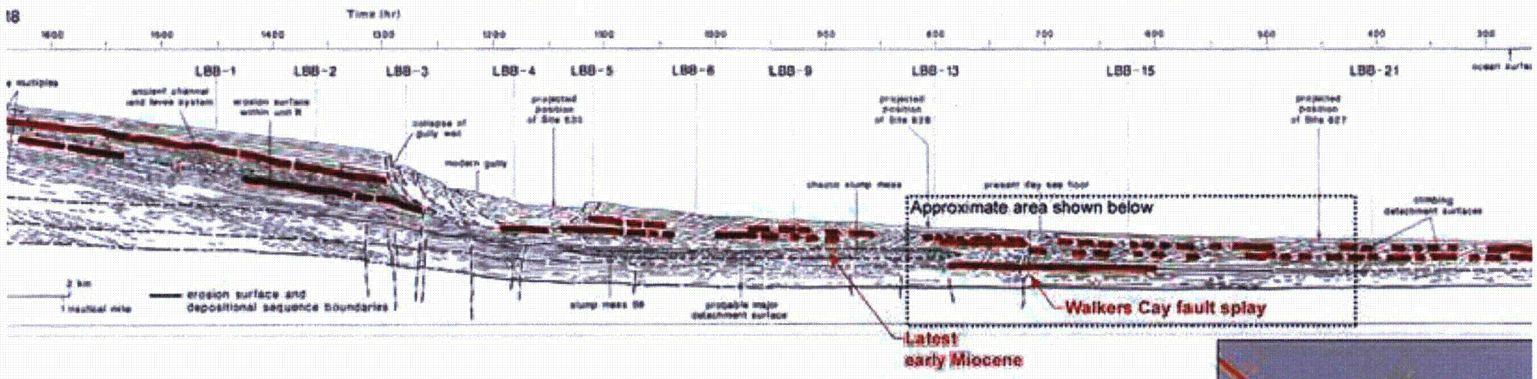

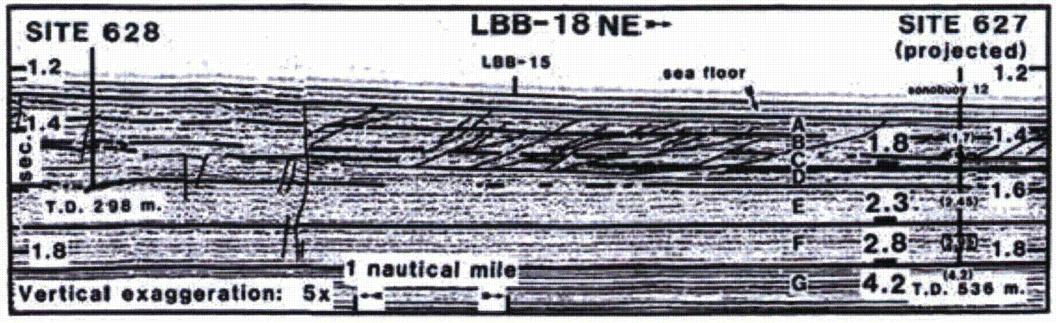

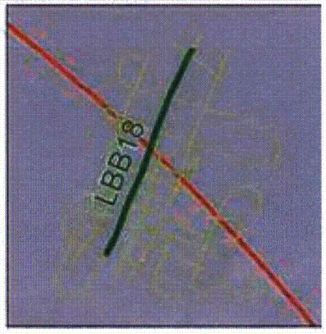

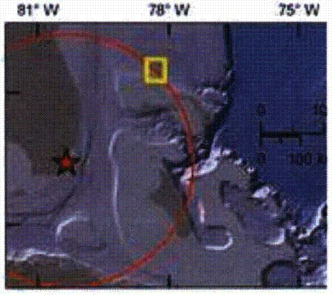

Source: References 476 and 785

ASSOCIATED ENCLOSURES:

None

NRC RAI Letter No. PTN-RAI-LTR-041

SRP Section: 02.05.01 - Basic Geologic and Seismic Information

QUESTIONS from Geosciences and Geotechnical Engineering Branch 2 (RGS2)

NRC RAI Number: 02.05.01-15 (eRAI 6024)

FSAR Section 2.5.1.1.1.3.2.2 states, with respect to the Santaren Anticline, that stratigraphic analysis (References 477 and 479) used to infer Pliocene or potential Quaternary activity on the structure, suggests this structure is Tertiary in age and predominantly active during the Eocene, with diminishing activity throughout the Miocene. The staff notes that References 477, 479, and 501 present evidence that the Santaren Anticline (within the 200 mi radius of the site) is cored by a thrust fault and is undergoing present-day shortening.

In order for the staff to determine the potential for activity on this structure and in support of 10 CFR 100.23 please address the following questions:

a) In light of evidence for ongoing deformation (References 477, 479, and 501), discuss the present day rates of shortening calculated across the anticline (see also Masaferro et al, 1999).

b) Plot regional seismicity on a close-up view of the Santaren Anticline and comment whether the Santaren Anticline is a capable tectonic structure.

c) Provide a discussion regarding the possibility that the Santaren Anticline and the Nortecubana fault system are linked.

[a] Masaferro, J.L., Poblet, J., Bulnes, M., Eberli, G.P., Dixon, T.H., and McClay, K., 1999, Palaeogene-Neogene/present day(?) growth folding in the Bahamian foreland of the Cuban fold and thrust belt: Journal of the Geological Society of London, v. 156, Part 3, 617–631.

FPL RESPONSE:

a) In light of evidence for ongoing deformation (References 477, 479, and 501), discuss the present-day rates of shortening calculated across the anticline (see also Masaferro et al., 1999).

Part (a) of this response summarizes data and interpretations presented in the literature pertaining to the Santaren anticline. Specifically, part (a) of this response addresses evidence in the literature for: (1) ongoing deformation; (2) calculations of present day rates of shortening; and (3) the possible existence of a thrust fault that cores the Santaren anticline. For the purposes of this response, the terms "ongoing" and "present day" are understood to refer to any activity in the Quaternary period.

Ball et al. (1985)

Based on seismic reflection, gravity, and magnetic data collected from the southwest edge of the Bahama Platform, Ball et al. (1985) (FSAR Reference 2.5.1-501) interpret subsurface geology and structures associated with the northern edge of the Bahama-Cuba collision zone. Ball et al. (1985) (FSAR Reference 2.5.1-501) identify the Santaren anticline as an approximately 10-km-wide, 70-km-long, northwest-trending structure (FSAR Figure 2.5.1-

343). Ball et al. (1985) (FSAR Reference 2.5.1-501) resolve regional thinning of upper Cretaceous beds from north to south across the Santaren anticline, with the largest magnitude of thinning (up to a factor of four) occurring off the anticline's southern flank within uppermost Cretaceous and lower Cenozoic carbonate beds (p. 1285) (Figure 1). Ball et al. (1985) (FSAR Reference 2.5.1-501, pp. 1,285-1,287) conclude "these thinning relationships indicate that the structure was initiated during the Late Cretaceous and that maximum topographic relief occurred in the early Cenozoic. Late Cenozoic expression could be a result of differential compaction of thick, semiconsolidated sediments on the structure's flanks." Ball et al. (1985) (FSAR Reference 2.5.1-501, p. 1,292) reiterate "the [Santaren anticline] appears to have been formed in the Late Cretaceous and early Cenozoic."

Ball et al. (1985) (FSAR Reference 2.5.1-501, pp. 1,290-1,292) also provide a structural interpretation of the Santaren anticline in their Figure 9b (Figure 1), noting "Deep terminations occur, below 4 km depth, in inferred basinal sediments beneath the anticline, 3 km north of the zone of dip and thickness variation. Some major dislocation related to faults may have caused the aberrant dips and local thickness variations. However, the regional thinning was caused by southward onlap of basinal carbonates on shallow-water carbonate material. Subsequent compressional tectonism produced the anticline." Based on the previously quoted age determinations, the location of the anticline, the interpreted asymmetry of the anticline, and the interpretation of a fault below 4 km depth, Ball et al. (1985) (FSAR Reference 2.5.1-501, p. 1,294) state "We speculate that this structure is a hanging-wall anticline marking the northern limit of thrusting in the Cuban arc."

These data and interpretations are not used by Ball et al. (1985) (FSAR Reference 2.5.1-501) to provide evidence of ongoing deformation or to calculate present day rates of shortening across the Santaren anticline. Ball et al. (1985) (FSAR Reference 2.5.1-501, p. 1287) specifically note that "late Cenozoic expression" (which presumably refers to the interpretation of thinned Paleogene strata, the youngest strata that are discussed) may not be related to tectonic processes, but may instead be the result of differential compaction. Ball et al. (1985) (FSAR Reference 2.5.1-501) do not calculate shortening rates for the Santaren anticline. Furthermore, it should be noted that the location of the steeply dipping fault dashed in Ball et al.'s (1985) (FSAR Reference 2.5.1-501) Figure 9b (Figure 1) is kinematically incompatible with the location of the Santaren anticline. As drawn, at least half of the interpreted hanging-wall anticline is actually on the footwall of the dashed fault.

Masaferro et al. (1999)

Masaferro's Ph.D. dissertation (1997) (FSAR Reference 2.5.1-477) is the source for seismic reflection data that are analyzed in subsequent peer-reviewed publications, including Masaferro et al. (1999) (FSAR Reference 2.5.1-426) and Masaferro et al. (2002) (FSAR Reference 2.5.1-479). Masaferro et al. (1999) (FSAR Reference 2.5.1-426) combine these seismic reflection data with well logs acquired during the Ocean Drilling Project (ODP) to provide a more detailed stratigraphic and structural analysis of the Santaren anticline, relative to the analysis conducted by Ball et al. (1985) (FSAR Reference 2.5.1-501). Using the geometries and inferred ages of growth strata associated with the Santaren anticline, Masaferro et al. (1999) (FSAR Reference 2.5.1-426, p. 630) reinterpret the Santaren anticline "as a detachment fold involving limb rotation and perhaps tangential-longitudinal strain", expressly stating that the fold geometry imaged in their seismic

reflection data "argues against a fault-bend and/or fault propagation fold" (p. 623-624) as suggested by Ball et al. (1985) (FSAR Reference 2.5.1-501). Masaferro et al. (1999) (FSAR Reference 2.5.1-426, p. 630) conclude the Santaren anticline experienced fold growth "from the Mid-Eocene to Pliocene and perhaps to the present day", although they note that "the youngest beds might be post-tectonic." Masaferro et al. (1999) (FSAR Reference 2.5.1-426) calculate vertical fold growth rates of between 0.006 mm/yr and 0.014 mm/yr for the last 19 million years before present (Ma), and a fold shortening rate of 0.001 mm/yr over the same time period.

The data and interpretations of Masaferro et al. (1999) (FSAR Reference 2.5.1-426) do not conclusively provide evidence for ongoing tectonic deformation (as suggested by the queried reference to present day folding in the title of the reference) and they do not calculate present-day rates of shortening. As noted above, Masaferro et al. (1999) (FSAR Reference 2.5.1-426) allow for the youngest beds to be post-tectonic, although "youngest" is not defined. The present-day rate of shortening is not directly stated by Masaferro et al. (1999) (FSAR Reference 2.5.1-426), however, this rate can be calculated using data from their youngest two horizons in their Table 5. Masaferro et al. (1999) (FSAR Reference 2.5.1-426) calculate a change in cumulative shortening of 1 m between deposition of horizon M (cumulative shortening of 785 m) and horizon N (cumulative shortening of 786 m), over an interval of the past 3.6 Ma (their Table 5). This corresponds to a mid-Pliocene shortening rate of 0.0003 mm/yr. However, the calculation of cumulative shortening is dependent on a number of assumptions and uncertainties. Masaferro et al. (1999) (FSAR Reference 2.5.1-426) note that these errors are not quantifiable, but suggest each cumulative shortening value has an associated error of ±10%. Thus, the calculation of a present-day shortening rate relies on the ability to detect a difference of 1 m between two values that may each vary by ±78 m. Viewed another way, calculation of a shortening rate relies on the ability of Masaferro et al. (1999) (FSAR Reference 2.5.1-426) to resolve a difference in horizon bed length of 1 m in horizons that are approximately 11 km long, or a 0.009% change in horizon length. This is likely beyond the resolution of the data.

Masaferro et al.'s (1999) (FSAR Reference 2.5.1-426) interpretation of the Santaren anticline as a detachment fold (in the context of Epard and Groshong, 1995; Homza and Wallace, 1995; Poblet and McClay, 1996) (References 2, 3, and 4) directly contradicts the idea that the anticline might be cored by a steeply dipping thrust fault, as proposed by Ball et al. (1985) (FSAR Reference 2.5.1-501), because a detachment fold is interpreted as resulting from movement along a horizontal detachment surface.

Masaferro et al., 2002

Masaferro et al. (2002) (FSAR Reference 2.5.1-479) build on the analysis presented in Masaferro et al. (1999) (FSAR Reference 2.5.1-426) by identifying a number of additional subhorizons between the horizons originally identified in the 1999 manuscript. This allows Masaferro et al. (2002) (FSAR Reference 2.5.1-479) to model the temporal variability in sedimentation and fold-growth rates since Late Oligocene time; shortening amounts and rates are not discussed. Masaferro et al. (2002) (FSAR Reference 2.5.1-479) conclude that the geometry of Santaren anticline growth strata results from the interplay between sedimentation and tectonic fold uplift, and that sedimentation and fold-growth rates have been highly variable over time. In other words, the "evolution of the Santaren anticline consists of cycles that involved tectonically active periods separated by interruptions in

which the tectonic activity fell to zero" (FSAR Reference 2.5.1-479, p. 21). This is in contrast to the conclusion of Masaferro et al. (1999) (FSAR Reference 2.5.1-426), which proposes that the Santaren anticline experienced approximately constant, slow growth. Masaferro et al. (2002) (FSAR Reference 2.5.1-479) further suggest that the preponderance of tectonic growth of the Santaren anticline occurred prior to 20 Ma (i.e., prior to bed "E" in their figure 4C) (Figure 2). Since that time, the average fold uplift rate is approximately 0.03 mm/yr. Masaferro et al. (2002) (FSAR Reference 2.5.1-479, p. 21) conclude that, for the time period 6.2 Ma to present, "there were many lapses within this [time period] during which no tectonic uplift occurred" and that the greatest fold uplift rate since approximately 6.2 Ma occurred during or just before deposition of beds K2 and K3, which are assigned a Late Miocene age. Since deposition of beds K2 and K3, Santaren anticline fold uplift rates have been at or near zero (FSAR Reference 2.5.1-479, Table 4c) (Figure 2). The youngest interval for which a non-zero uplift rate was calculated was the interval between deposition of early Quaternary beds M2 and M3, which has a 0.05 millimeters per year (0.002 inches per year) fold uplift rate (FSAR Reference 2.5.1-479) (Figure 2).

The data and interpretations of Masaferro et al. (2002) (FSAR Reference 2.5.1-479) do suggest possible tectonic deformation in the Quaternary period. As stated above, Masaferro et al. (2002) (FSAR Reference 2.5.1-479) interpret the Santaren anticline to have experienced episodic tectonic growth and sedimentation since at least Oligocene time, with the most recent episode of tectonic uplift interpreted to have occurred in the early Quaternary (between deposition of beds M2 and M3, with a fold uplift rate of 0.05 mm/yr).

The calculation of present day rates of shortening is less straightforward. First of all, the tectonic activity that is interpreted to have occurred between deposition of early Quaternary beds M2 and M3 is followed by no tectonic activity between deposition of beds M3 and N (FSAR Reference 2.5.1-479, Figure 4c) (Figure 2). The absolute age of subhorizon M3 is not explicitly provided in FSAR Reference 2.5.1-479, however, ages are plotted in their Figure 3a. Using the scale provided, it is clear that the interval from deposition of bed M3 to deposition of bed N spans the period from approximately 1 Ma to present. It is reasonable to question the degree to which an early Quaternary rate would accurately characterize a structure that has exhibited no activity for the past 1 million years.

In addition, the episodic tectonic growth, indicated by some beds thinning across the anticline while others do not, could also be caused by variations in local sedimentation rate, variations in sea level, and erosion by bottom currents. Masaferro et al. (2002) (FSAR Reference 2.5.1-479) indicate that erosion by bottom currents and variations in sea level can be ruled out because strata in one location nearby do not exhibit such variations, however, other examples of Miocene and Pliocene erosional unconformities exist just to the north at Site 1007 (Eberli et al. 2002) (Reference 1).

Furthermore, the assumptions and uncertainties associated with fold uplift rates (which are based on differences in cumulative fold-crestal relief) are identical to those described above for shortening rates. Masaferro et al. (2002) (FSAR Reference 2.5.1-479) do not provide cumulative fold-crestal relief data for subhorizons M2 and M3, however, these values should logically fall between the values for horizons M and N, which are 1302 m and 1326 m, respectively (Masaferro et al. 1999, Table 4). This means that calculation of the M2-M3 fold uplift rate relies on the ability to discern less than 24 m of cumulative fold-crestal relief

between two values that each can vary by approximately +/- 130 m (Masaferro et al. 1999, Table 4). It is likely that the calculation of the early Quaternary 0.05 mm/yr fold uplift rate exceeds the resolution of the data.

Masaferro et al. (2002) (FSAR Reference 2.5.1-479) recognize previous interpretations of the Santaren anticline as a fault-related fold (i.e., Ball et al. 1985 (FSAR Reference 2.5.1-501)) or a detachment fold (Masaferro et al. 1999 (FSAR Reference 2.5.1-426)). Masaferro et al. (2002) (FSAR Reference 2.5.1-479) do not provide any additional discussion or interpretation of fold-growth models for the Santaren anticline.

b) Plot regional seismicity on a close-up view of the Santaren Anticline and comment whether the Santaren Anticline is a capable tectonic structure.

The Phase 2 earthquake catalog developed for the Turkey Point Units 6 & 7 site indicates that there is only one earthquake within 40 km of the Santaren anticline. This M_w 3.26 earthquake occurred on 06/02/1990 and is located approximately 8 km northwest of the northwestern-most mapped point along the Santaren anticline fold axis (Figure 3), FSAR Reference 2.5.1-426. The Phase 2 earthquake catalog is a declustered catalog that includes only independent events of M_w 3 and greater.

As discussed above, different structural frameworks have been suggested to explain the Santaren anticline. Ball et al. (1985) (FSAR Reference 2.5.1-501) suggest the Santaren anticline may be cored by a steeply dipping thrust fault, whereas Masaferro et al. (1999) (FSAR Reference 2.5.1-426) interpret the Santaren anticline as a detachment fold. Masaferro et al. (2002) (FSAR Reference 2.5.1-479) note these different interpretations but provide no further discussion of any postulated fault, nor do any faults appear in their interpreted cross-sections of the Santaren anticline. Thus, even if the Santaren anticline currently is undergoing shortening at a very low rate (<0.1 mm/yr), it is not clear that this shortening is accommodated by a seismogenic structure capable of producing vibratory ground motion or tectonic surface deformation.

Regardless of these structural interpretations, the issue of whether or not the Santaren anticline is a capable tectonic structure is addressed by data presented by Masaferro et al. (2002) (FSAR Reference 2.5.1-479). The calculated fold uplift rates for the Santaren anticline, as depicted in Figure 4c of FSAR Reference 2.5.1-479 (Figure 2), show no uplift since deposition of beds M2-M3. As detailed in part (a) of this response, this period of tectonic quiescence spans the period from approximately 1 Ma to present. The fact that FSAR Reference 2.5.1-479 depicts no uplift in the most recent 1 million years would therefore support the conclusion that the Santaren anticline does not represent a capable tectonic structure. The sparse seismicity near this structure further supports this argument (Figure 3).

c) Provide a discussion regarding the possibility that the Santaren Anticline and the Nortecubana fault system are linked.

The Santaren anticline and the Nortecubana fault system are discussed in FSAR Subsections 2.5.1.1.1.3.2.2 and 2.5.1.1.1.3.2.4 as being spatially and temporally associated with the northern reaches of the Cuban orogeny, and, as such, it is likely they were genetically associated with similar convergent plate boundary driving forces. Additionally, the Santaren anticline appears to be on trend with the eastern portion of the

Nortecubana fault (Figure 3). The fact that there is no detailed mapping for the Nortecubana fault makes it difficult to speculate on whether or not it may have at one time been structurally linked to the Santaren anticline.

The Phase 2 earthquake catalog provides some insight into modern-day associations. As discussed in the FSAR, seismicity along the Nortecubana fault is concentrated near its intersection with the Oriente fault and substantially decreases northwestward into the site region (FSAR Subsection 2.5.1.1.1.3.2.4). Seismicity in the vicinity of the Santaren anticline, discussed in part (b) of this response, is sparse. Based on the Phase 2 earthquake catalog, there is only one earthquake that is on-trend with the Santaren anticline, and that event is located approximately 40 km to the west. There are no recorded earthquakes or mapped structures found in the literature in the approximately 30-km-wide gap between the Santaren Anticline and the Nortecubana fault system (Figure 3). Given the lack of data suggesting a structural link between these features, there is no reason to conclude that the Santaren anticline and the Nortecubana fault system are linked.

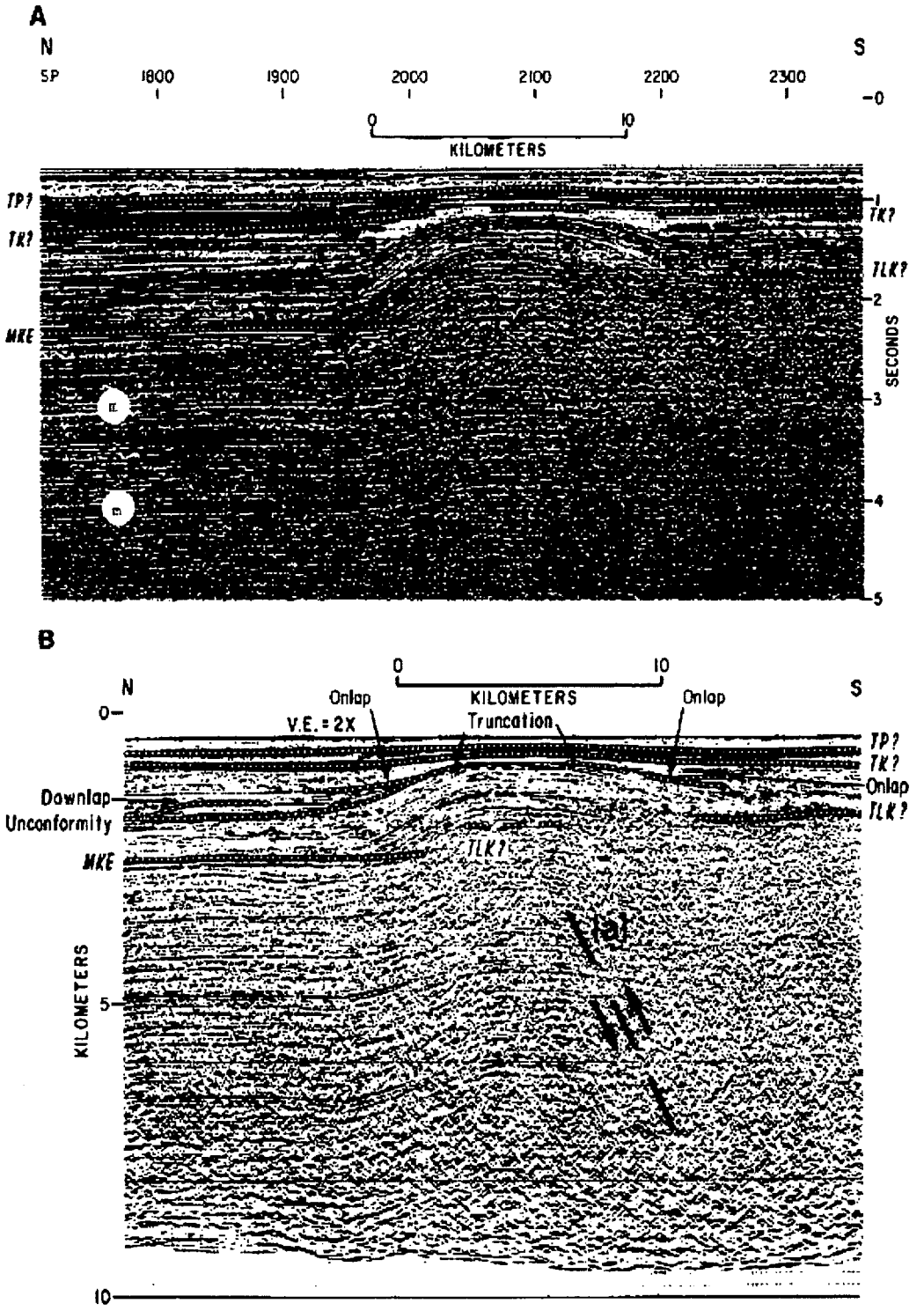

Figure 1 (A) Time section of Santaren Anticline from Ball et al. (1985) (FSAR Reference 2.5.1-501, Figure 9). (B) Migrated depth section of profile from (A) with 2x vertical exaggeration. Ball et al. (1985) (FSAR Reference 2.5.1-501) propose a fault as dashed.

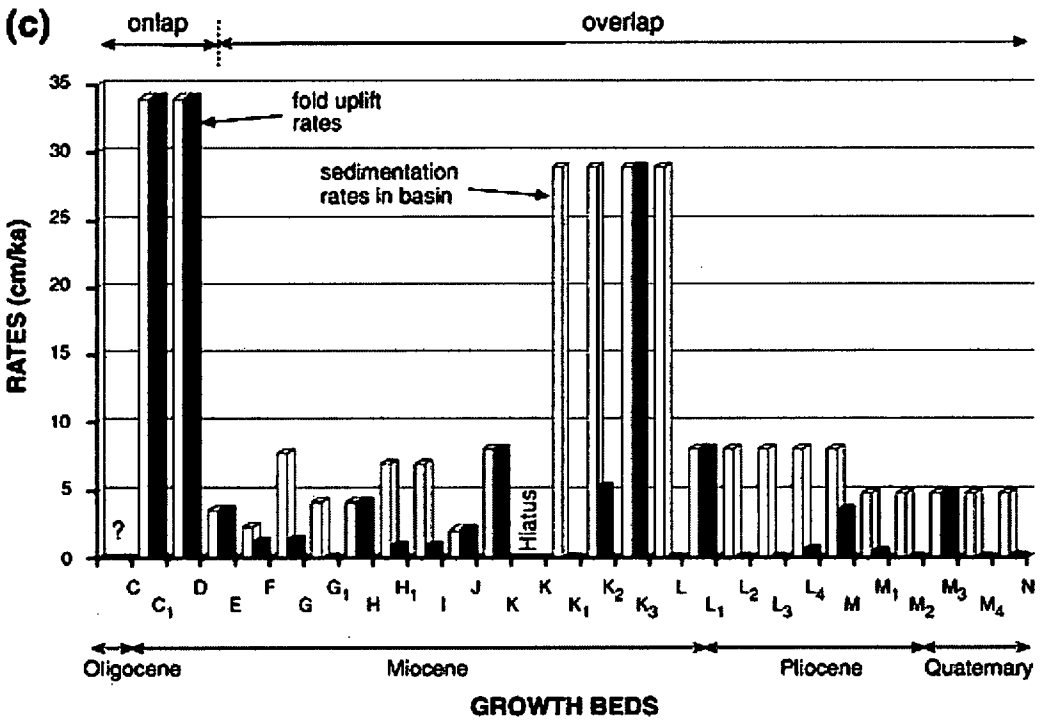

Figure 2 Calculated sedimentation and fold uplift rates for the Santaren anticline, from Masaferro et al. (2002) (FSAR Reference 2.5.1-479, Figure 4c).

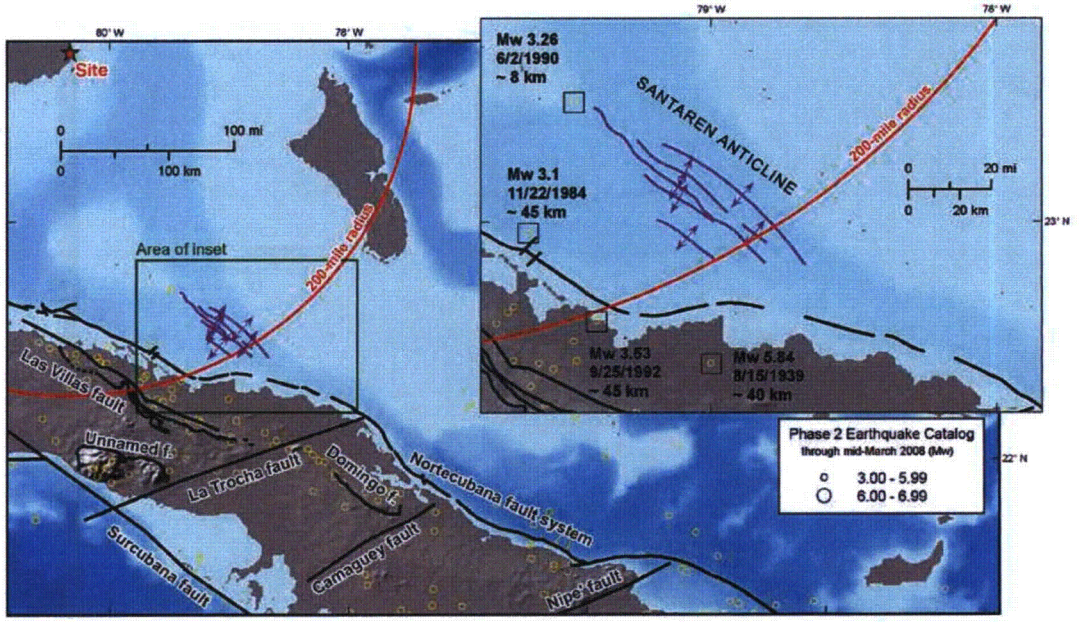

Figure 3 Regional Seismicity Plotted on a Map of the Nortecubana Fault and Santaren Anticline

Source: FSAR Section 2.5.1.3 References 2.5.1-477, 492, 443, 770, 494, 448, and 439.

This response is PLANT SPECIFIC.

References:

1. Eberli, G. P., Anselmetti, F. S., Kroon, D., Sato, T., and Wright, J. D., 2002, the chronostratigraphic significance of seismic reflections along the Bahamas Transcect, Marine Geology, v. 185, pp. 1-17.
2. Epard, J.-L., and Groshong, R.H., 1995, Kinematic model of detachment folding including limb rotation, fixed hinges and layer-parallel strain, Tectonophysics, v. 247, pp. 85-103.
3. Homza, T.X., and Wallace, W.K., 1995, Geometric and kinematic models for detachment folds with fixed and variable detachment depths, Journal of Structural Geology, v. 17, no. 4, pp. 575-588.
4. Poblet, J., and McClay, K., 1996, Geometry and kinematics of single-layer detachment folds, American Association of Petroleum Geologists Bulletin, v. 80, no. 7, pp. 1085-1109.

ASSOCIATED COLA REVISIONS:

The following changes will be made to FSAR Subsection 2.5.1.1.1.3.2.2. in a future COLA revision.

Santaren Anticline

The northwest-trending detachment fold **primarily** affects Cretaceous to Miocene strata and represents the northern limit of the Cuban fold-thrust belt (Reference 501, Figures 2.5.1-229 **and 2.5.1-350**). Initial work indicated that folding initiated in the Late Cretaceous, reached maximum expression in the early Cenozoic, and experienced differential compaction in the late Cenozoic (Reference 501), a timeline consistent with the end of Cuban orogeny in the latest Eocene.

Detailed analysis of the stratigraphy indicates that the **syntectonic** growth strata ~~may range in age from~~ **are** Eocene **and younger** ~~to Late Pliocene. The analysis~~ **and** was ~~also~~ used to infer Pliocene or potential **early** Quaternary activity on the structure (References 426 and 479, Figure 2.5.1-278). **References 426 and 479 use the geometries and inferred ages of growth strata associated with the Santaren anticline to respectively model the shortening rate and the temporal variability in sedimentation and fold-growth rates since Late Oligocene time. The authors conclude that the geometry of Santaren anticline growth strata results from the interplay between sedimentation and tectonic fold uplift and that sedimentation and fold-growth rates have been highly variable over time, though sedimentary processes, such as localized bottom-current erosion and sediment compaction (Reference 501), could be responsible for the stratigraphic variations.**

Reference 479 interprets the variation as indicating that the "evolution of the Santaren anticline consists of cycles that involved tectonically active periods separated by interruptions in which the tectonic activity fell to zero" (Reference 479). Furthermore, their analysis suggests that the preponderance of tectonic growth of the Santaren anticline occurred before 20 Ma (i.e., before bed E in Figure 2.5.1-278). Since that time, the average fold uplift rate is approximately 0.03 millimeter per year, corresponding to a shortening rate of 0.001 millimeter per year (Reference 426). Reference 479 concludes that, for the time period 6.2 Ma to present, "there were many lapses in this [time period] during which no tectonic uplift occurred" (Reference 479) and that the greatest fold uplift rate since approximately 6.2 Ma occurred during or just before deposition of beds K2 and K3, which are assigned Late Miocene age. Since deposition of beds K2 and K3, Santaren anticline fold uplift rates have been at or near zero (Figure 2.5.1-278). The youngest interval for which a non-zero uplift rate was calculated was the early Quaternary M2- M3 interval, which has a 0.05 millimeter-per-year (0.002 inch-per-year) fold uplift rate (Reference 479, Figure 2.5.1-278). However, it should be noted that the calculation of fold uplift, based on differences in crestal relief, incorporates measurements, calculations, and assumptions that are assigned an error of 10 percent (Reference 426). The calculated crestal relief between beds M2 and M3 is less than 24 meters (79 feet), and this reflects the difference between two values that each may vary by ± 130 meters (427 feet) (References 426 and 479). ~~However, this detailed stratigraphic analysis indicates that the vast majority of uplift or shortening occurred before 20 Ma, with an~~

~~average fold uplift rate of 0.03 millimeters/year characterizing the anticline after approximately 20 Ma (Reference 479).Most strata younger than 15 Ma drape across the fold crest maintaining constant bed thickness, but some beds do thin across the anti~~cline (Reference 479) (Figure 2.5.1-278). This could be the result of intermittent fold uplift (e.g., ~~Reference 479)~~ or sedimentary ~~processes, such as localized bottom current erosion and sediment compaction (e.g.,~~ Reference 501). The ~~preponderance~~ **preponderance** of data indicate that this structure ~~is Tertiary in age,~~ **was** predominantly active in the Eocene, with waning activity throughout the Miocene**, and possible, yet questionable, deformation into the early Quaternary. However, beds with ages of approximately 1 Ma and younger show no evidence of deformation (Reference 479, Figure 2.5.1-278). Horizontal shortening rates over the last 3.6 Ma are estimated to be 0.0003 millimeter/year and seismicity near this structure is sparse (Reference 426; Figure 2.5.1-350).** The fold may be rooted in Jurassic evaporites, **such as** the Punta Allegre formation (References 307 and 477), which could account for this structure's apparent longevity without clear tectonic mechanisms.

The following figure will be added as a new FSAR figure in a future COLA revision:

Figure 2.5.1-350 Regional Seismicity Plotted on a Map of the Nortecubana Fault and Santaren Anticline

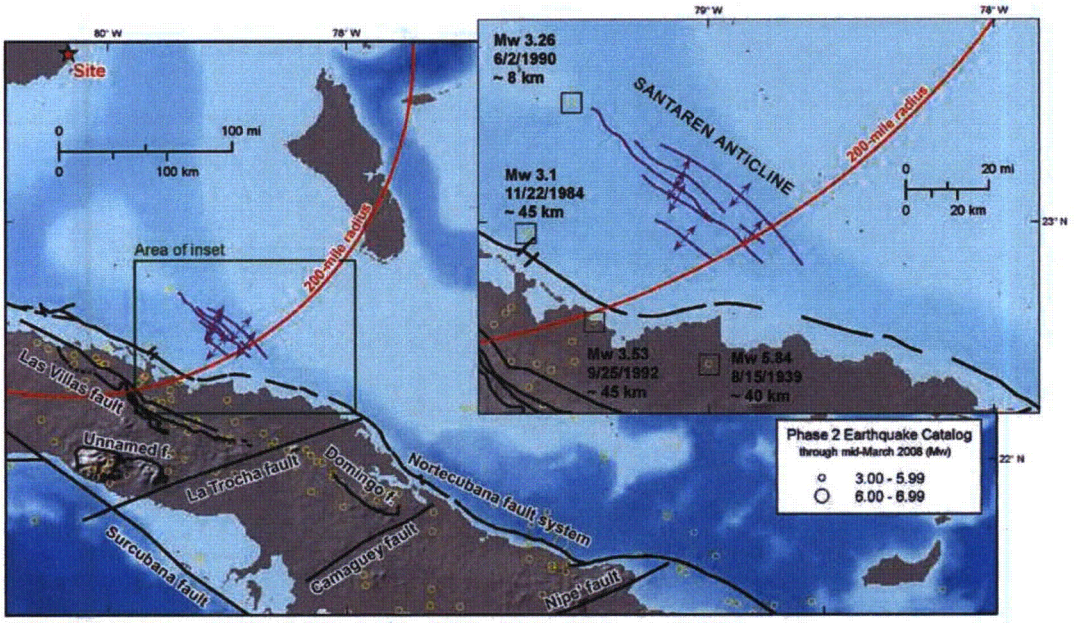

Source: References 439, 443, 448, 477, 492, 494, and 770

ASSOCIATED ENCLOSURES:

None

NRC RAI Letter No. PTN-RAI-LTR-041

SRP Section: 02.05.01 - Basic Geologic and Seismic Information

QUESTIONS from Geosciences and Geotechnical Engineering Branch 2 (RGS2)

NRC RAI Number: 02.05.01-16 (eRAI 6024)

FSAR Section 2.5.1.1.1.3.2.2 states, with respect to the Straits of Florida Normal Faults, that middle to late Eocene to early middle Miocene strata were deposited uniformly over most of the southern Straits of Florida and that similarly; continuous, unfaulted strata drape the edges of the Florida and Bahamas Platforms along the Straits of Florida. The staff needs more details with respect to the timing and location of the Straits of Florida Normal Faults.

In order for the staff to completely understand the geologic setting of the TPNPP site and in support of 10 CFR 100.23, Provide a discussion of the structural and stratigraphic evidence for the location and timing of deformation along the Mitchell, Pourtales, and Miami escarpments, the Las Villas and the Sierra de Jatibonico fault zones, and other tectonic features present in the bathymetry of subsurface of the Straits of Florida within the site region, including those located offshore northern Cuba, and in light of references such as Uchupi, 1966[a] and Malloy and Hurley, 1970[b] .

[a] Uchupi, E., 1966, Shallow structure of the Straits of Florida, Science, New Series, Vol 153, no.3735, pp.529-531, published by AAAS.

[b] Malloy and Hurley, 1970, Geomorphology and Geologic Structure: Straits of Florida, Geological Society of America Bulletin, v. 81, p. 1947-1972, 19 figs., July 1970

FPL RESPONSE:

As described in FSAR Subsection 2.5.1.1.1.3.2.2, deformation within the Straits of Florida is characterized by a series of short, steep, normal faults buried by Eocene or younger sediments (FSAR Reference 2.5.1-480) (FSAR Figure 2.5.1-229) (Figure 1). An early study by Malloy and Hurley (Reference 3) additionally hypothesized faulting along some geomorphic escarpments in the central Straits of Florida, particularly the Pourtales escarpment (the southwestern continuation of the Miami escarpment), the Mitchell escarpment, and an unnamed escarpment farther south (Figure 1). Malloy and Hurley (Reference 3) used bathymetric and other published geologic data to interpret scarps representing the Sierra de Jatibonico and Las Villas faults to the south near Cuba (Figure 1). This response presents a review of the Straits of Florida normal faults, followed by a discussion of the hypothesized faulting at the escarpments and a discussion of the Sierra de Jatibonico and Las Villas faults.

The most informative publications describing the Straits of Florida normal faults include Denny et al. (FSAR Reference 2.5.1-221) and Angstadt et al. (FSAR Reference 2.5.1-482). Denny et al. (FSAR Reference 2.5.1-221) present a detailed analysis of the seismic stratigraphy in the Straits of Florida. They identify a southward flexure in Eocene-age deposits that they interpret as the result of loading from the collision of Cuba with the Florida-Bahama Platform. Although Denny et al. (FSAR Reference 2.5.1-221) recognize the thickening of Eocene strata in the southern portion of the Straits of Florida in response to this collision, they do not interpret these strata as recording much faulting (FSAR Figures

2.5.1-272 and 2.5.1-273; Figures 2, 3, and 4). The youngest faulting observed in that study is the normal fault shown in FSAR Figure 2.5.1-273, which terminates between S5, a middle-to-late Eocene unconformity, and S6, an early-middle Miocene unconformity. Farther west, however, Angstadt et al. (FSAR Reference 2.5.1-482) present seismic reflection lines closer to Cuba that they interpret as showing normal faults that deform the Paleocene to Eocene strata (FSAR Figure 2.5.1-209). In FSAR Figure 2.5.1-209, normal faults cut the Paleocene and Eocene strata and terminate at or immediately above the base of seismic unit C, which is correlated with middle Eocene to middle Miocene strata. Similarly, FSAR Figure 2.5.1-287 shows some of the normal faults cutting the flexural basin as a result of this loading, and closer inland, thrust faults associated with the Cuban thrust belt (FSAR Reference 2.5.1-484).

Although Case and Holcombe (FSAR Reference 2.5.1-480) do not provide information about the normal faults they show north of Cuba (Figure 1), Angstadt et al. (FSAR Reference 2.5.1-482) interpret seismic reflection profiles in the same area to depict faulted Paleocene and Eocene strata, typically overlain by undeformed Miocene and younger strata (e.g., FSAR Figure 2.5.1-209). Similarly, isopach maps that show thickened Paleocene to Eocene strata adjacent to the Cuban margin and Miocene and younger strata of constant thickness indicate the faults responsible for thinning the overthickened foreland strata should have terminated at the end of the Eocene (FSAR 2.5.1 References 482 and 221).

The Straits of Florida normal faulting is interpreted as syntectonic deformation of the Cuban foreland basin during its Eocene collision with the Florida-Bahama Platform (FSAR 2.5.1 References 794 and 482). The undeformed Miocene and younger strata overlying these faults indicate that subsidence of the straits had largely ceased with a change in tectonic regime at the end of the Eocene. However, Moretti et al. (FSAR Reference 2.5.1-484) also indicate that some faults along the Cuban margin could have been reactivated in response to later Tertiary compressional stresses (e.g., FSAR Figures 2.5.1-282 and 2.5.1-287), and hence could be active into the Miocene.

Reactivation along the Cuban margin is also found farther east in the Santaren Channel. Bergman (FSAR Reference 2.5.1-906) uses multi-channel, high resolution seismic reflection survey data to interpret faults adjacent to paleo-bank margins in the Santaren Channel that extend into late Tertiary strata or younger strata and suggests faulting as young as Early Pliocene. For example, a seismic line in the northern Santaren Channel shows faulting extending to just above the 12.2 Ma reflector (Figure 5b). A seismic line south of Cay Sal records a more complicated structure (Figure 5a). Three northeast-vergent thrust faults deform a shallow-water carbonate margin, while steeper faults extend up into shallower stratigraphy. Most of these steep faults are truncated in Miocene strata, but one is drawn to the seafloor (Figure 5a). Bergman (FSAR Reference 2.5.1-906) does not comment on the fault that is drawn to the seafloor and instead states that faulting in the Santaren Channel "continued into the late Miocene and possibly Pliocene" (p. 169). Structures in the Santaren Channel are interpreted to be contractional features associated with the Cuban fold-and-thrust belt rather than the Straits of Florida normal faults (Figure 5).

The short, steep, normal faults that accommodated the formation of a foreland basin in the Straits of Florida in the Paleocene and Eocene, with possible reactivations in the late

Tertiary (FSAR 2.5.1 References 480, 221, and 484), are distinct from the geomorphic escarpments that are mapped by Malloy and Hurley (Reference 3) (Figure 1) and addressed below in this response.

Provide a discussion of the structural and stratigraphic evidence for the location and timing of deformation along the Mitchell, Pourtales, and Miami escarpments

The data presented in Uchupi (FSAR Reference 2.5.1-790) and Malloy and Hurley (Reference 3) represent the earliest speculation and coarsest views of the escarpments in the Straits of Florida. More recent seismic imaging has yielded much more detailed views of the subsurface, illuminating that these features reflect a dynamic depositional system rather than a fault-related or tectonic origin (Reference 4).

The Pourtales terrace is the southern extension of the Miami terrace (Figure 1). Both terraces are located in water depths of 650–1500 feet (200–450 meters) and represent a drowned Miocene carbonate platform (References 2 and 4). The moderate-to-steep escarpments at the eastern edge of the Miami terrace and southern edge of the Pourtales terrace are noted in early studies of the region (e.g., FSAR Reference 2.5.1-790). South of the Pourtales escarpment in the southern Straits of Florida, two smaller ledges in the bathymetry were noted by Malloy and Hurley (Reference 3). These include the Mitchell escarpment and an unnamed escarpment to the south (Figure 1).

Uchupi (FSAR Reference 2.5.1-790) presents results of a seismic survey conducted throughout the Straits of Florida (FSAR Figure 2.5.1-262) and suggests that "the steepness of the slopes flanking the Miami and Pourtales terraces along their seaward sides, and the presence of drag folds along the slope south of Pourtales Terrace, suggest that these features may be fault-line scarps. If faulting produced the slopes flanking the terraces, it probably occurred in Miocene or post-Miocene time, as the cores of both terraces consist of Lower Miocene limestones" (FSAR Reference 2.5.1-790, p. 531). However, the seismic survey did not provide any direct evidence of faulting beneath these features (FSAR Figure 2.5.1-262).

Malloy and Hurley (Reference 3) present mapping of the Straits of Florida based on bathymetry and seismic reflection data (Figure 1), but were more equivocal in their interpretation of the Pourtales and Mitchell escarpments. A seismic reflection profile of the Mitchell escarpment shows possible faulting (Figure 6), but Malloy and Hurley (Reference 3) state that whatever faulting may have occurred, it is doubtful that displacements are of regional tectonic significance. Moreover, Malloy and Hurley (Reference 3, p. 1968) state "there is evidence of features that may be normal faults on the southern side of the Southern Straits [of Florida]. It is by no means obvious that any of these faults have any regional tectonic significance. In fact, there is no need to postulate extensive faulting here."

According to Malloy and Hurley (Reference 3), seismic reflection data across the Pourtales escarpment show "the near-flat strata of the terrace possibly in fault contact with consolidated strata dipping locally 7° (apparent) to the south" (p.1966) (Figure 7). However, they also state that "the Pourtales escarpment may not represent a fault scarp, but an original sedimentary feature associated with sediments deposited against the steeper face of the old reef front. It would seem that such relationships should be expected in this region" (Reference 3, p. 1968). Indeed, Uchupi et al. (FSAR Reference 2.5.1-428) also

suggest that such escarpments are commonly formed along the Bahamas and Gulf of Mexico through carbonate accretion by Mesozoic reefs and not by tectonic deformation.

As hypothesized by Malloy and Hurley (Reference 3), the Pourtales escarpment and similar steep-sided escarpments throughout the Gulf of Mexico, Straits of Florida, and Bahamas have now been recognized as relict carbonate platform margins, sometimes steepened and modified by erosion (Figures 8, 9, and 10) (e.g., References 2 and 4, FSAR Reference 2.5.1-687). For example, Mullins and Neuman (Reference 4) conclude that there is no evidence for faulting at the eastern edge of the Miami terrace and that truncated reflectors near the surface indicate that erosion was responsible for the stratigraphic variations.

Detailed seismic mapping by Anselmetti et al. (FSAR Reference 2.5.1-228) and Eberli et al. (Reference 1) indicates that the steep west edge of the Bahama bank displays an unfaulted sedimentary transition from shallow-water carbonates to slope carbonates to drift sediments (e.g., FSAR Figure 2.5.1-245). Along the Pourtales escarpment, this margin is overlain by, and is adjacent to, large drifts of sediment that have been prograding along the Straits of Florida since the Miocene (FSAR Reference 2.5.1-221). Where these drifts rest against the paleo-reefs, discordant dips are observed that were previously interpreted as potentially fault-related (e.g., Reference 3) (compare Figures 7 and 8). Denny et al. (FSAR Reference 2.5.1-221) also describe seismic reflection lines that cross the Pourtales escarpment showing no evidence of shallow faulting (Figures 3 and 4). Two lines that obliquely cross the Mitchell escarpment (Figures 9a and 9b) (Reference 6) display similar stratigraphic characteristics near the escarpment, with drifts resting against each other in the shallow stratigraphy and erosional truncations that do not extend to depth.

In summary, the majority of the data collected in the study of the Mitchell, Pourtales, and Miami escarpments provide little basis for concluding that these features are the product of fault activity. Instead, Malloy and Hurley (Reference 3) and Uchupi et al. (FSAR Reference 2.5.1-428) suggest that these escarpments are sedimentary features common to the Bahamas and Gulf of Mexico, and later, more detailed seismic imaging has confirmed this (e.g., Reference 4, FSAR 2.5.1 References 221 and 906). Although the faults mapped along the Pourtales, Mitchell, and unnamed escarpments from Malloy and Hurley (Reference 3) are included in compilation maps such as the DNAG Map of North America (Figure 11) (Reference 7), it is unclear whether this represents the initial compilation efforts of the early 1980s, or whether newer, but unpublished, mapping supports the notion of faulting at that location. The relationships indicated on the DNAG map indicate that the faults cut surficial sediments with ages as young as Pliocene, and the faults are generally dashed in Quaternary strata (Figure 11) (Reference 7).

Provide a discussion of the structural and stratigraphic evidence for the location and timing of deformation along the Las Villas and the Sierra de Jatibonico fault zones, and other tectonic features present in the bathymetry of subsurface of the Straits of Florida within the site region, including those located offshore northern Cuba

Khudoley (FSAR Reference 2.5.1-910, p. 672) identifies the Las Villas fault as a "deep" fault of Cuba "whose length is approximately 800 kilometers, generally paralleling the island." Despite this, Khudoley's (FSAR Reference 2.5.1-910) map shows the Las Villas fault as approximately 220 miles (350 kilometers) long (Figure 12). As mapped by Khudoley (FSAR Reference 2.5.1-910), the Las Villas fault extends along the northern coast of Cuba

from approximately 80°W to 83°W, transitioning from an onshore to an offshore structure near Carahatas, Cuba (Figure 12). The total offshore length of Khudoley's (FSAR Reference 2.5.1-910) Las Villas fault is approximately 120 miles (200 kilometers). Khudoley (FSAR Reference 2.5.1-910) does not describe the data that constrain the location and extent of the offshore portions of the Las Villas fault, but this is presumably based on bathymetric data.

Khudoley (FSAR Reference 2.5.1-910, p. 672) describes the Sierra de Jatibonico fault as a "disjunctive dislocation" that is "approximately parallel with the trend of the island" and "is at least 450 kilometers long." Khudoley indicates that, according to unspecified geological and geophysical investigations, 124 miles (200 kilometers) of the fault are onshore, and 186 miles (250 kilometers) of the fault are offshore. However, in Figure 12, the Sierra de Jatibonico fault is mapped as over 620 miles (1000 kilometers) long, with a western 277 mile-long (447 kilometer-long) offshore segment transitioning to a central 302-mile-long (488 kilometer-long) onshore segment near Carahatas, Cuba. The fault then transitions offshore again near Guardalavaca, where it is mapped for an additional 126 miles (204 kilometers). As Khudoley (Reference 2.5.1-910) does not specify what data are used to define the location and extent of the offshore portion of the Sierra de Jatibonico fault, FPL presumes this mapping is based on bathymetric data.

Malloy and Hurley (Reference 3) present compiled bathymetric and seismic reflection data for the Straits of Florida. They identify escarpments in the Straits of Florida and postulate the existence of faults, including the offshore Las Villas fault and offshore Sierra de Jatibonico fault (Figure 1). Malloy and Hurley (Reference 3, p. 1962) indicate that "since traverses could not be made within 12 [nautical miles] of Cuba, no seismic reflection profiles were obtained of these steep and complex slopes." As such, they base their offshore mapping of the Las Villas fault on Khudoley's (Reference 2.5.1-910) previous mapping and on their compiled bathymetric data. Malloy and Hurley's (Reference 3) depiction of the offshore Las Villas fault extends for approximately 120 miles (200 kilometers) from roughly Matanzas Bay westward to Havana. Malloy and Hurley (Reference 3, p. 1962) state that "the Las Villas fault appears to be reflected in the bathymetry as a scarp," but they do not provide any description of scarp dimensions, including length, height, and continuity. The offshore portion of the Sierra de Jatibonico fault is mapped north of the Las Villas fault, from 81°W to 81°20'W. Malloy and Hurley (Reference 3) state that a scarp is expressed along this portion of the fault for 20 nautical miles (37 kilometers); however, specifics such as height and continuity are not discussed. Malloy and Hurley (Reference 3) note that beyond 81°35'W, nothing in the bathymetry suggests that the fault continues farther west, and they depict the fault as dashed for that segment.

More recent depictions of the Las Villas fault indicate that this structure is located mostly or entirely onshore in central Cuba (see RAI 02.05.01.21). For example, the depiction of the Las Villas fault on Figure 3 from Pardo (FSAR Reference 2.5.1-439) extends offshore near Carahatas, Cuba, and continues offshore to the northwest roughly parallel and close to the coast for only about 40 miles (65 kilometers). Pardo (FSAR Reference 2.5.1-439) does not describe bathymetric expression of this fault. Cotilla-Rodriguez et al. (FSAR Reference 2.5.1-494) show the Las Villas fault as entirely onshore and therefore not expressed in the bathymetry; however, the offshore Las Villas fault as mapped by Malloy and Hurley (Reference 3) appears to be spatially coincident with Cotilla-Rodriguez et al.'s (FSAR

Reference 2.5.1-494) Nortecubana fault. The 1:2,000,000 scale lineament map of Cuba from the *Nuevo Atlas Nacional de Cuba* (Reference 5, plate III.3.1-11) depicts and labels the Las Villas fault as an approximately 120-mile-long (190-kilometer-long), northwest-striking feature that is located entirely onshore. The 1:2,000,000 scale neotectonic map of Cuba from the same atlas (Reference 5, plate III.2.4-8) shows an unnamed fault in the vicinity of the Las Villas fault that is located entirely onshore. Based on its location, FPL assumes that this unnamed fault is the Las Villas fault. Perez-Othon and Yarmoliuk (FSAR Reference 848) show an unnamed fault on their 1:500,000 scale geologic map of Cuba. This unnamed fault is located in the vicinity of the Las Villas fault and is located entirely onshore. Pushcharovskiy's (FSAR Reference 847) 1:500,000 scale tectonic map of Cuba depicts and labels the Las Villas fault as a thrust fault located entirely onshore.

These more recent compilations do not show the offshore Sierra de Jatibonico fault as mapped by Khudoley (Reference 2.5.1-910) or Malloy and Hurley (Reference 3). It is not included in the 1:500,000 scale tectonic map of Cuba (FSAR Reference 2.5.1-847), nor is it shown in any of the 1:2,000,000 maps in the *Nuevo Atlas Nacional de Cuba* (Reference 5). Similarly, Cotilla-Rodriguez et al. (FSAR Reference 2.5.1-494) do not indicate any such fault north of Matanzas Bay. Pardo (FSAR Reference 2.5.1-439, Figure 172) does indicate a "Jatibonico fault"; however, it is entirely onshore, over 200 kilometers west of Matanzas Bay.

Bathymetry in the Straits of Florida from Malloy and Hurley (Reference 3) indicate that the Pourtales escarpment, the Mitchell escarpment, and the north slope of Cuba are the most prominent geomorphic features expressed in the region. The slope north of Cuba is somewhat steeper and more irregular than the slope south of Florida, but no particular faults or scarps are identified there in the regional study of Mann et al. (FSAR Reference 2.5.1-493). Only portions of the mapped trace of the Las Villas fault from Malloy and Hurley (Reference 3) coincide with the steepest portions of the slope, and Malloy and Hurley's (Reference 3) Sierra de Jatibonico does not appear to coincide with any scarps in the bathymetry (Figure 1). The DNAG Map of North America (Reference 7) shows the same faults as Malloy and Hurley (Reference 3) in the Straits of Florida region, with two additions (Figure 11). A fault is included south of the unnamed escarpment and northwest of the Sierra de Jatibonico that cuts Neogene sediments, and a segmented fault is included along the steep portion of the slope north of the small islands and east of the Sierra de Jatibonico fault that cuts Tertiary strata. The latter structure is coincident with representations of the Nortecubana fault in this area (e.g., FSAR Figure 2.5.1-202). The offshore area near the Nortecubana fault and south toward the Cuban coast is expected to be underlain by thrusts of the Cuban fold-and-thrust belt, which are covered by unfaulted late Tertiary and Quaternary strata (FSAR 2.5.1 References 484, 485, and 497) (FSAR Figures 2.5.1-279, 2.5.1-280, 2.5.1-282, 2.5.1-287, and 2.5.1-288).

In summary, little detail is known about the hypothesized offshore Las Villas and Sierra de Jatibonico structures drawn by Malloy and Hurley (Reference 3) on the basis of bathymetric data. More recent compilations generally do not depict offshore versions of these faults (e.g., FSAR 2.5.1 Reference 847), although the offshore Las Villas from Malloy and Hurley (Reference 3) is roughly coincident with the Nortecubana fault of Cotilla-Rodriquez et al. (FSAR 2.5.1 Reference 494) and the steepest portions of the northern Cuba slope.

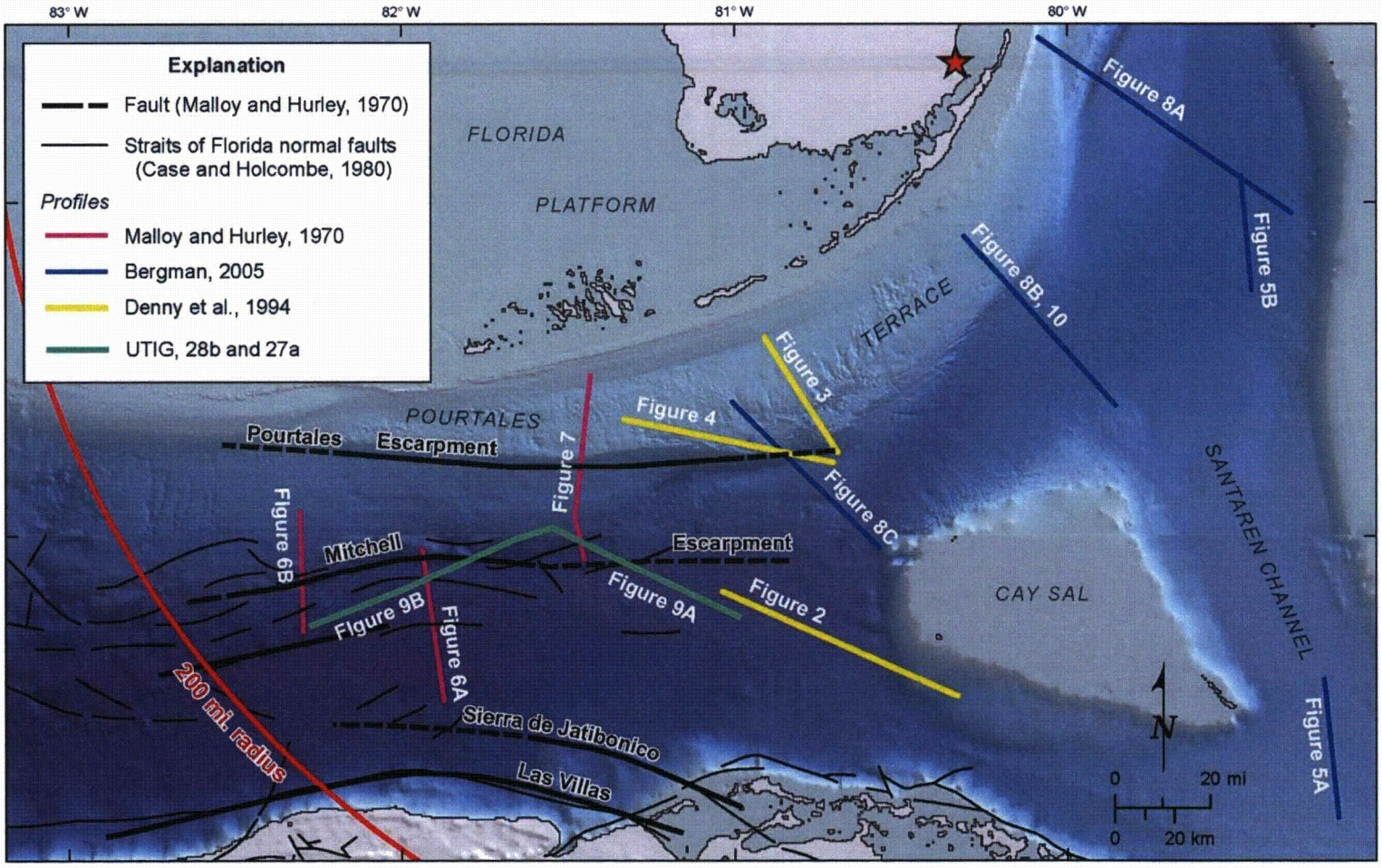

Figure 1 Location Map for Profiles Shown in Figures 2 through 10

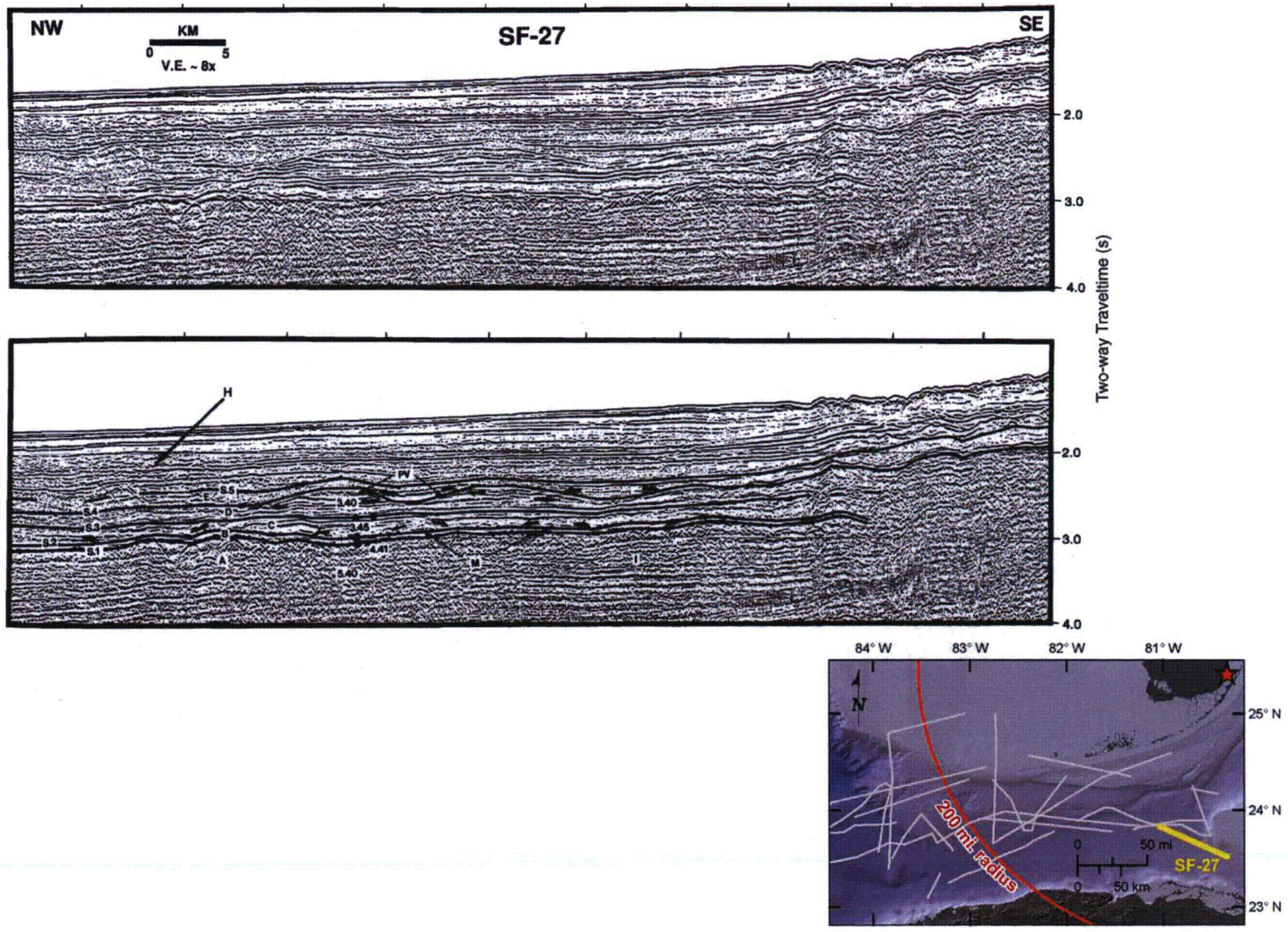

Figure 2 Seismic Line Demonstrating Unfaulted Strata in the Straits of Florida (from Denny et al., FSAR Reference 2.5.1-221)

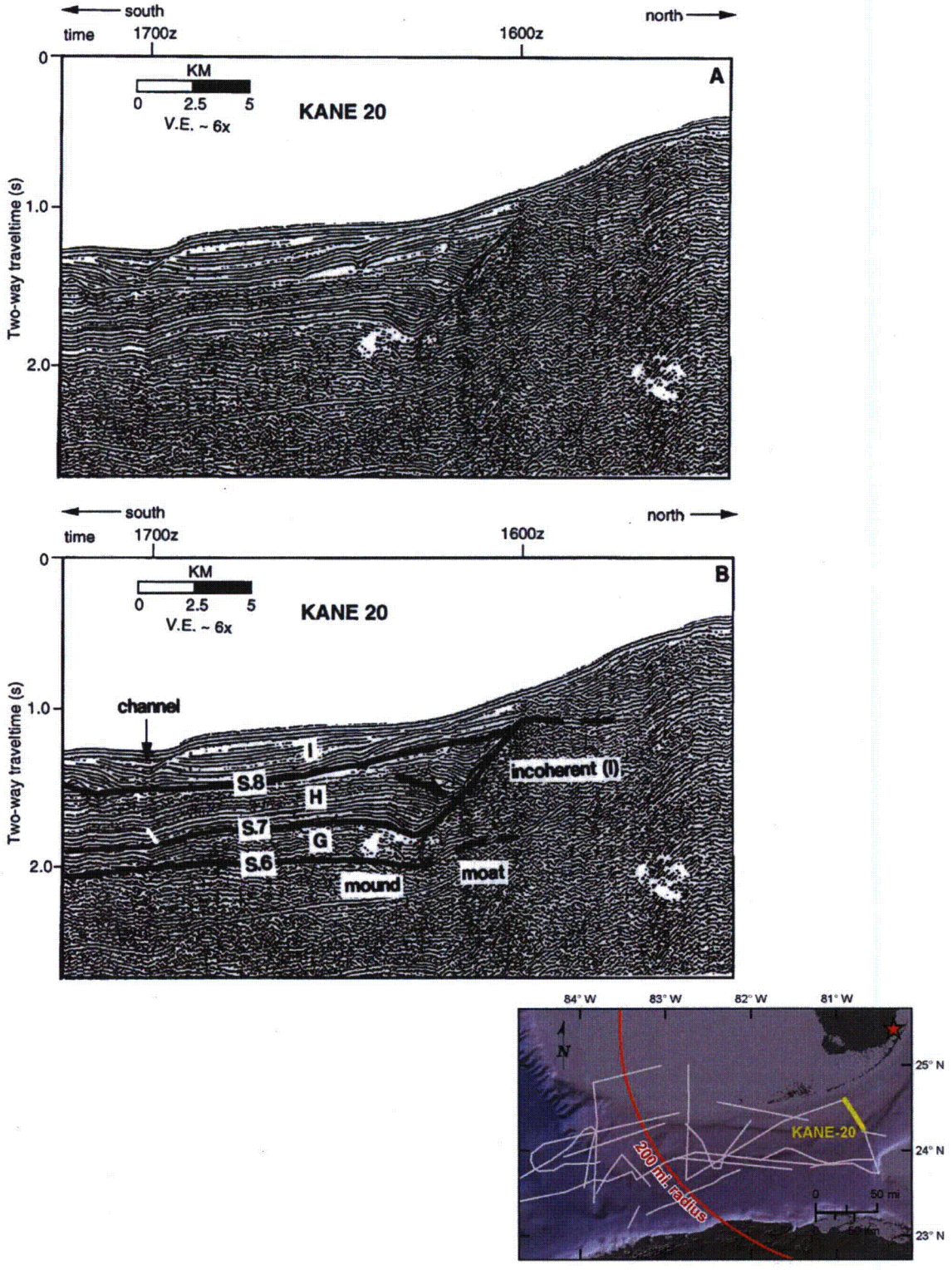

Figure 3 Seismic Line and Interpretation Crossing the Pourtales Terrace and Escarpment (from Denny et al., FSAR Reference 2.5.1-221

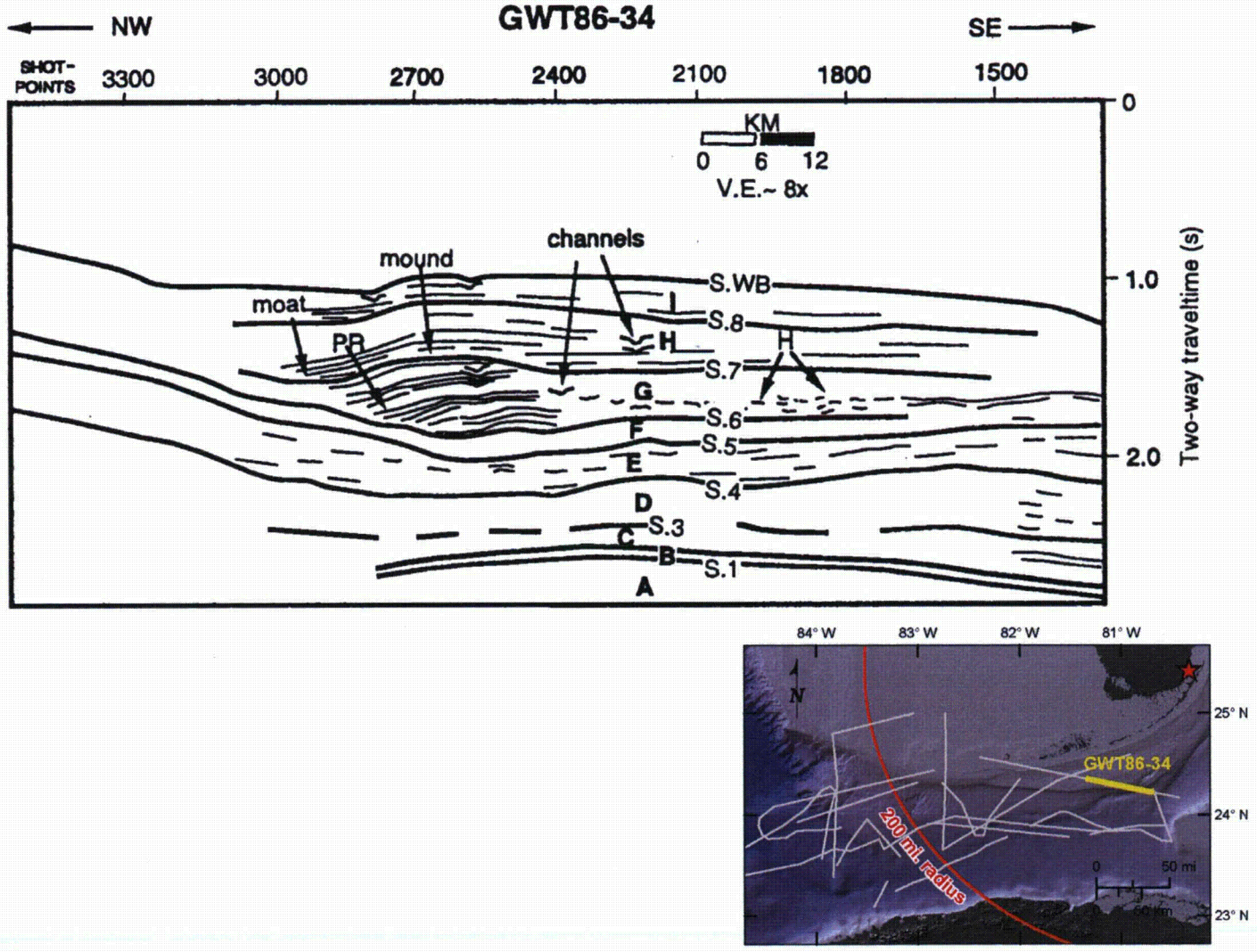

Figure 4 Interpreted Seismic Line Showing Current-Influenced Stratigraphy at the Base of the Pourtales Escarpment (from Denny et al., FSAR Reference 2.5.1-221)

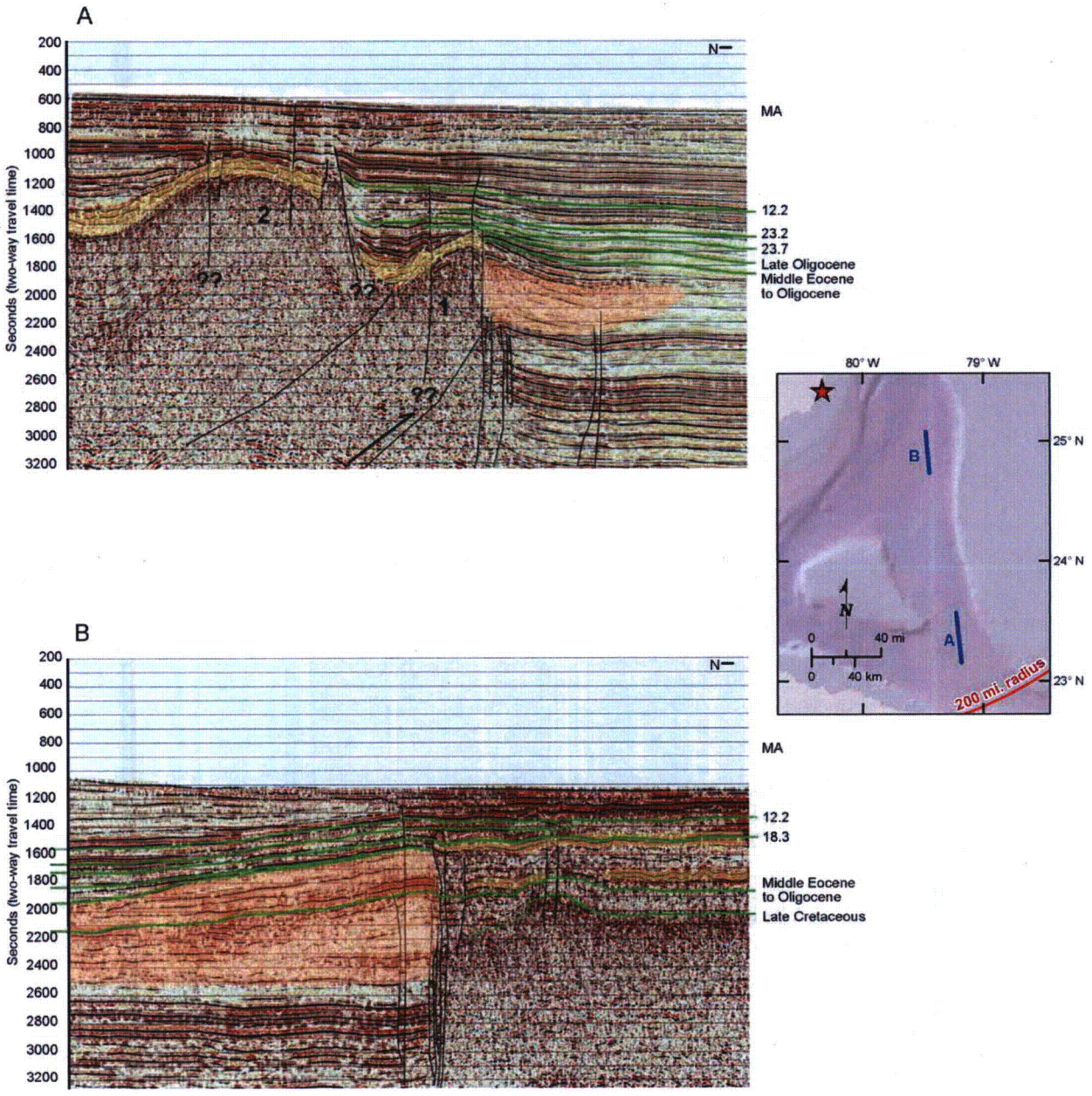

Figure 5 Santaren Channel Profiles A and B
(from Bergman, FSAR Reference 2.5.1-906)

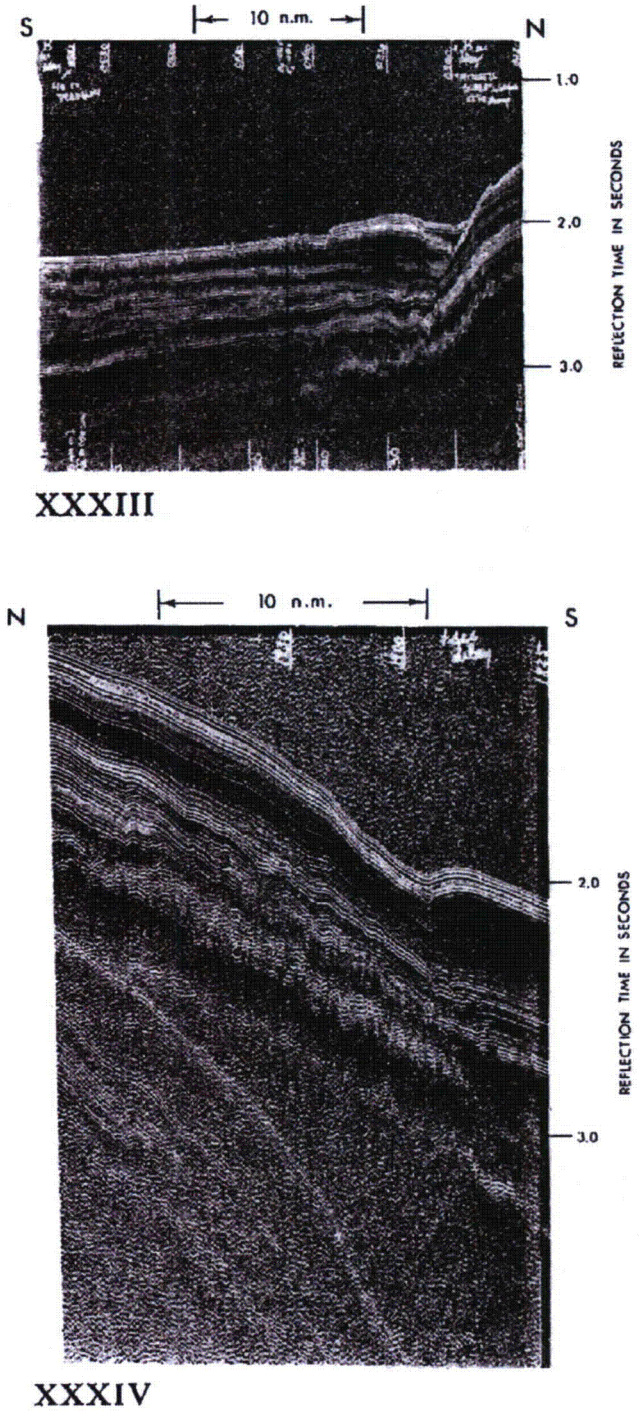

Figure 6 Portions of Seismic Lines Crossing the Mitchell Escarpment (from Malloy and Hurley, Reference 3)

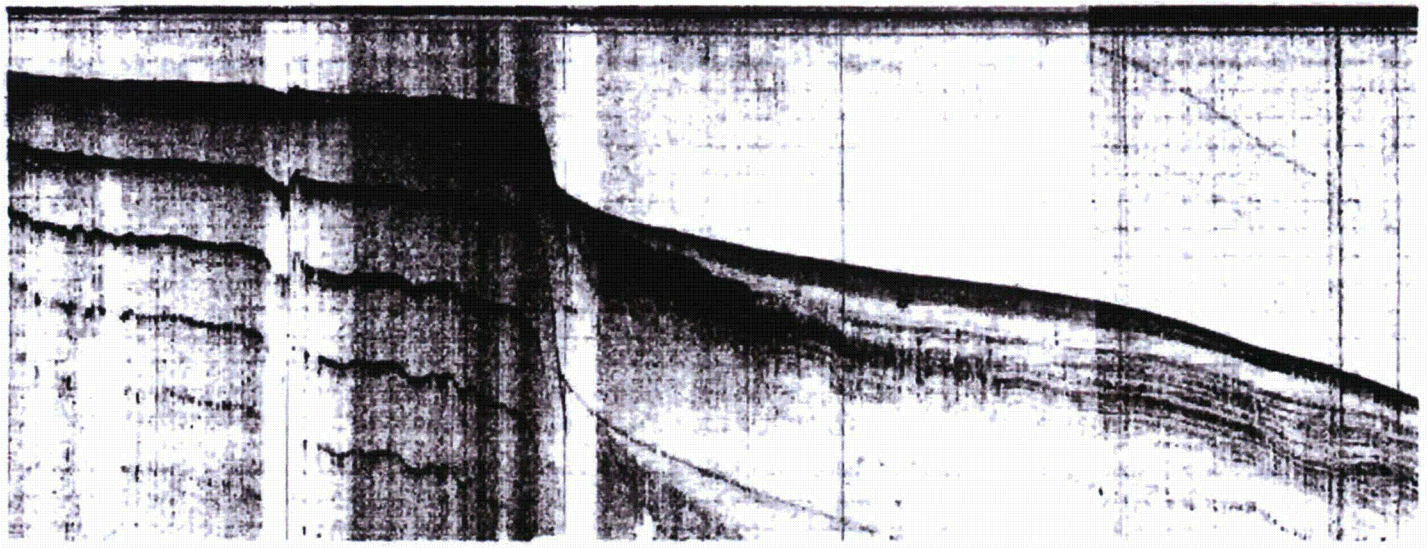

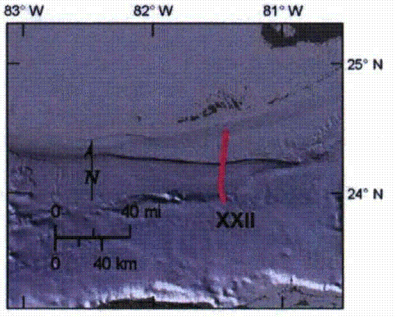

Figure 7 Portion of Seismic Line Crossing the Pourtales Escarpment (from Malloy and Hurley, Reference 3

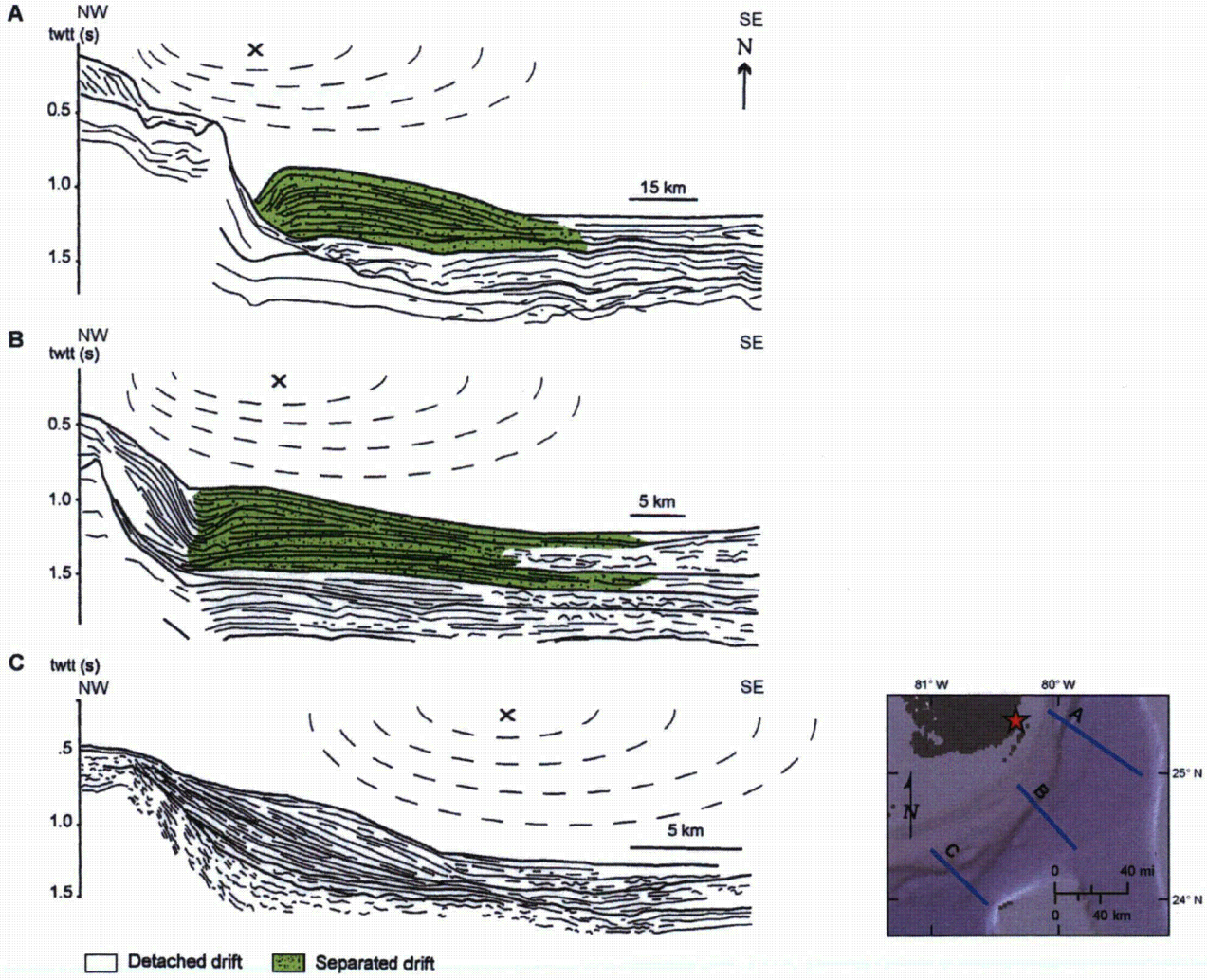

Figure 8 Profiles across the Miami/Pourtales Escarpment Illustrating the Variation in Geomorphology and Stratigraphy(from Bergman, FSAR Reference 2.5.1-906)

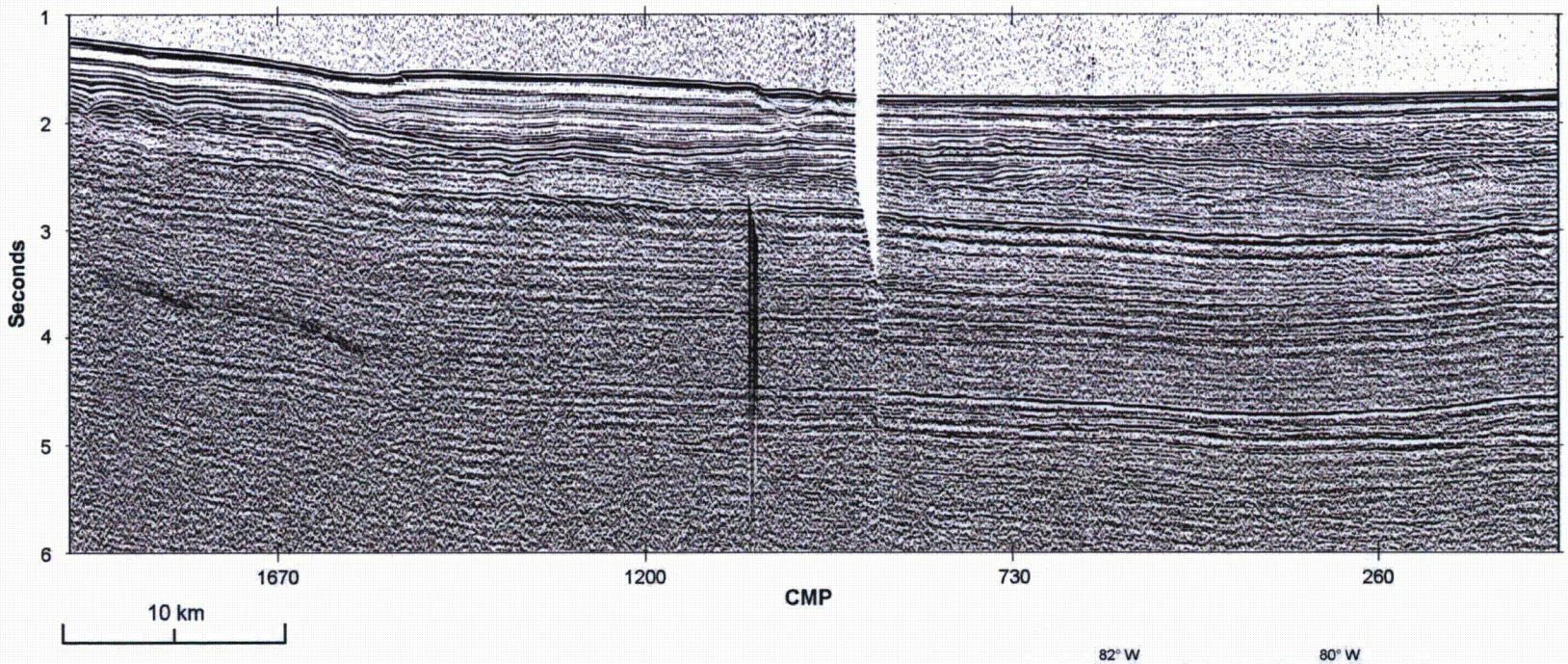

Figure 9a Uninterpreted Seismic Line 27b across the Mitchell Escarpment (from UTIG, Reference 6)

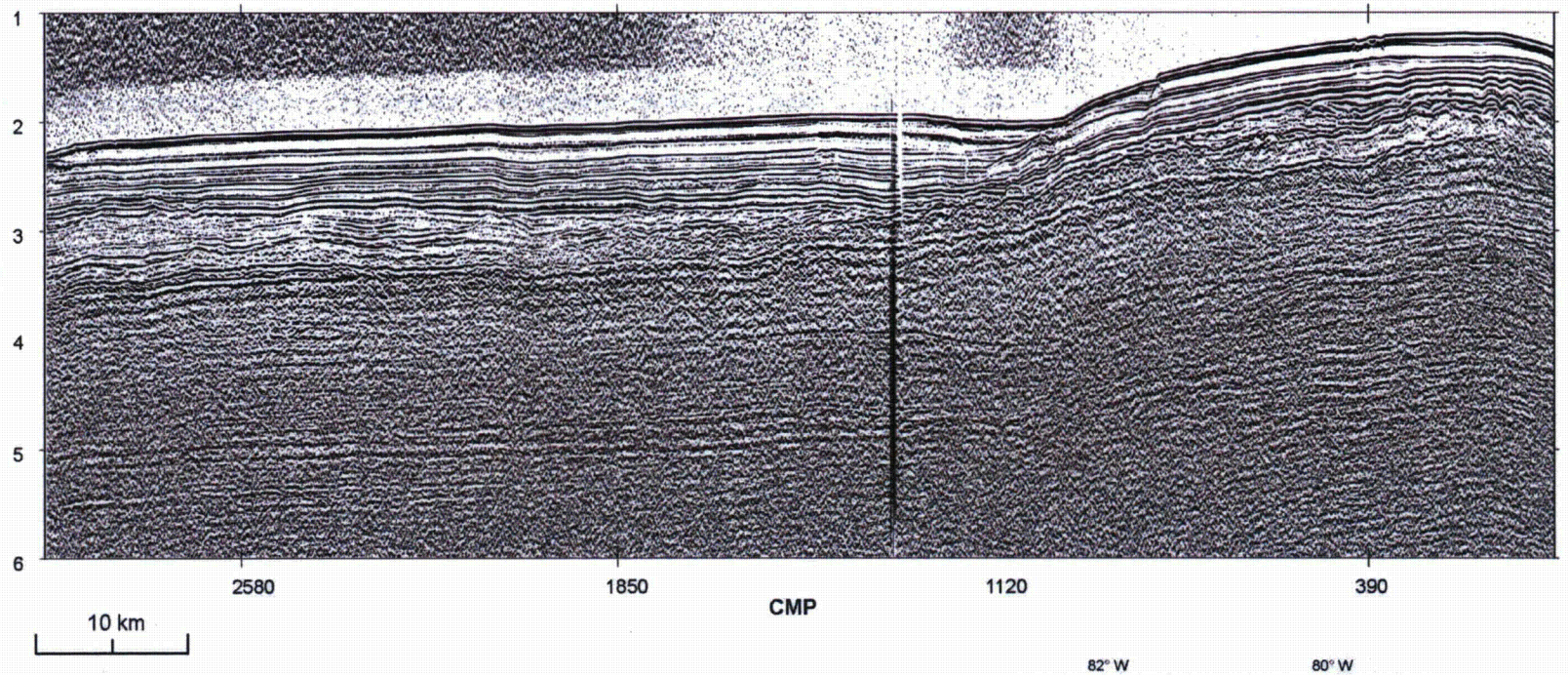

Figure 9b Uninterpreted Seismic Line 28b across the Mitchell Escarpment (from UTIG, Reference 6)

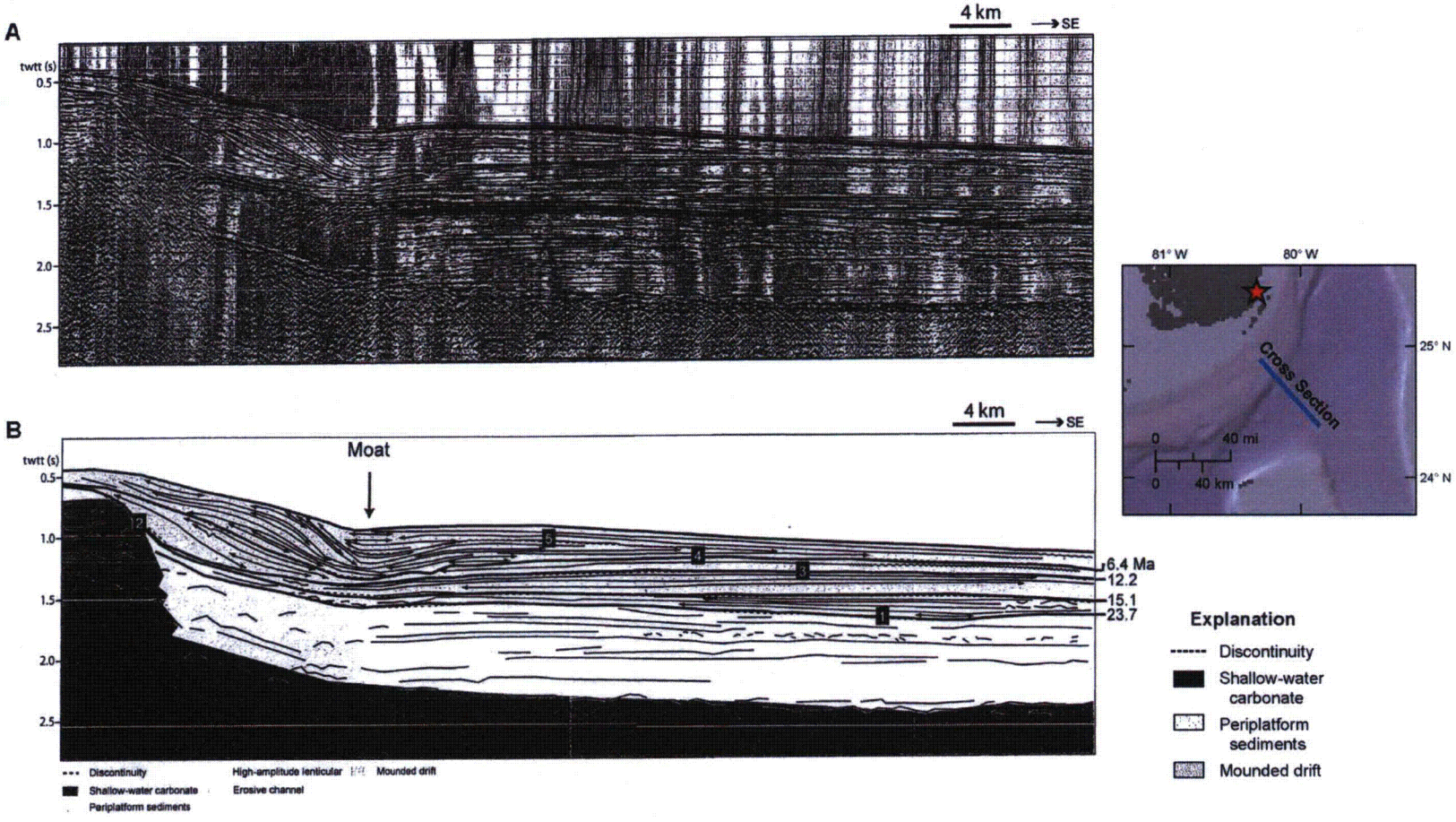

Figure 10 Seismic Line and Interpretation across the Pourtales Escarpment, Indicating Unfaulted Stratigraphy (from Bergman, FSAR Reference 2.5.1-206)

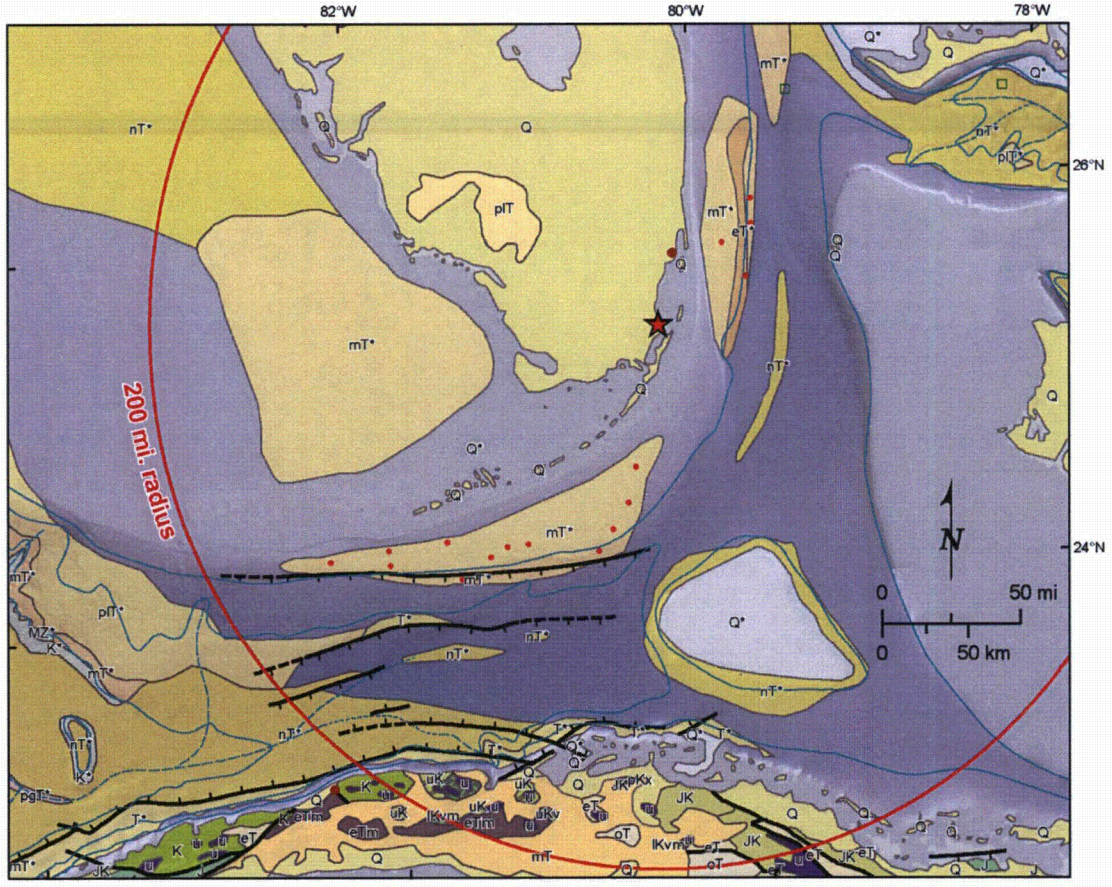

Explanation

- Phosphate nodule or pavement
- Normal fault, location accurate
- Normal fault, location approximate
- Strike-slip fault, location accurate
- Unclassified fault, location accurate
- Axis of submarine canyon, sea valley, or channel, location accurate
- Axis of submarine canyon, sea valley, or channel, ocation approximate

Geologic Units

- Q — Quaternary sedimentary rocks
- Q* — Quaternary (sea floor) sedimentary rocks
- T* — Tertiary (sea floor) sedimentary rocks
- nT* — Neogene (sea floor) sedimentary rocks
- plT — Pliocene sedimentary rock
- plT* — Paleogene (sea floor) sedimentary rocks
- mT — Miocene sedimentary rocks
- mT* — Miocene (sea floor) sedimentary rocks
- pgT* — Paleogene (sea floor) sedimentary rocks
- oT — Oligocene sedimentary rocks
- eT — Eocene sedimentary rocks
- eT* — Eocene (sea floor) sedimentary rocks
- e Im — Eocene plutonic diorite and gabbro
- MZ* — Mesozoic (sea floor) sedimentary rocks
- MZx — Mesozoic high-grade metamorphic, undivided crystalline rocks (sea floor)
- uK — Upper Cretaceous sedimentary rocks
- uKv — Upper Cretaceous volcanic rocks
- K — Cretaceous sedimentary rocks
- K* — Cretaceous (sea floor) sedimentary rocks
- pKx — Cretaceous high-grade metamorphic, undivided crystalline rocks
- lKvi — Lower Cretaceous intermediate volcanics
- lKvm — Lower Cretaceous mafic volcanics
- JK — Jurassic-Cretaceous sedimentary rocks
- J — Jurassic sedimentary rocks
- u — Ultramafic rocks of unknown age

Figure 11 DNAG Map - GMNA of Straits of Florida Region

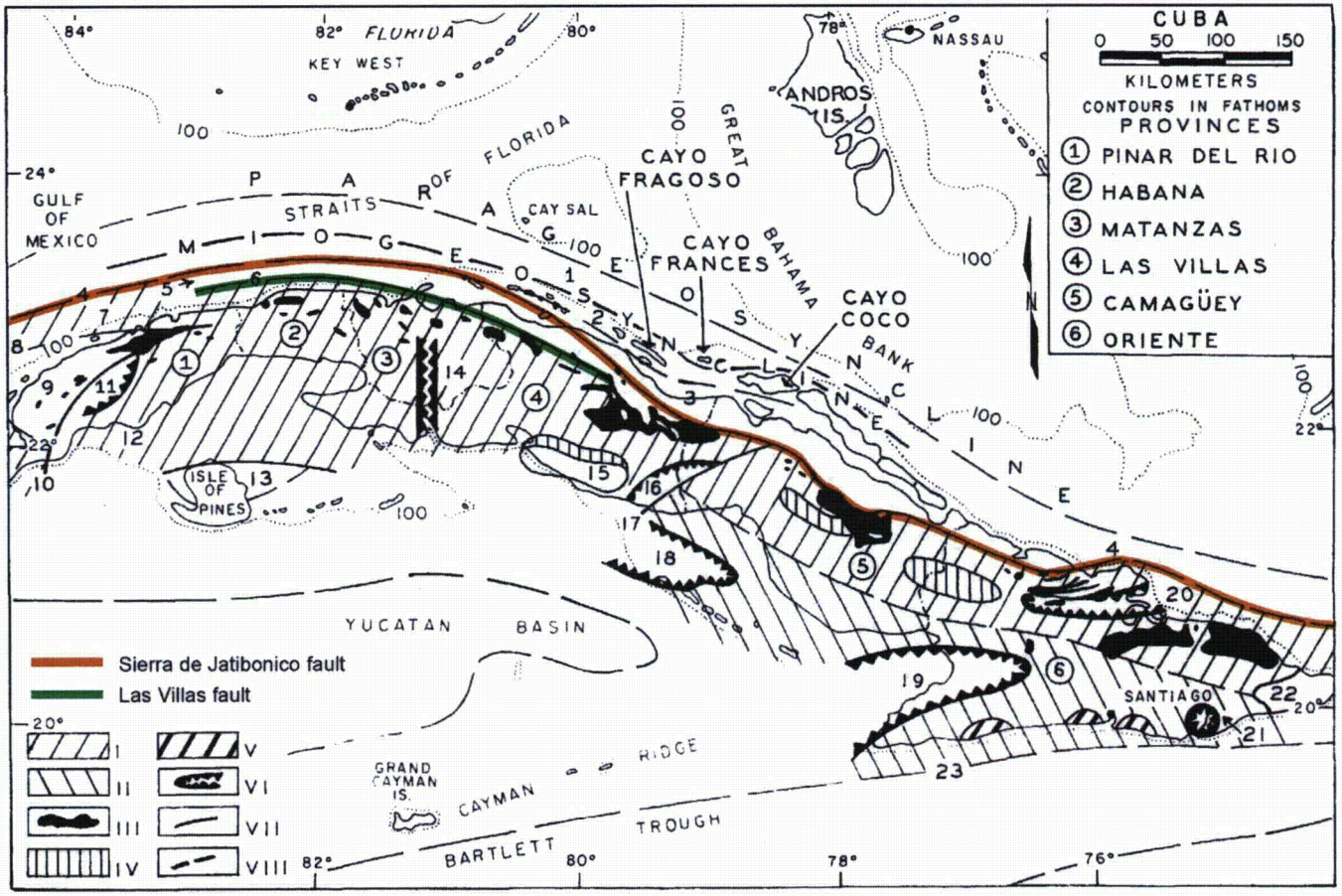

FIG. 1.—Tectonic sketch of Cuba. I–Cretaceous magmatic area (Zaza tectonic unit); II–Tertiary magmatic area (Cauto tectonic unit); III–Upper Cretaceous basic and ultrabasic intrusives; IV–Cretaceous granitoids; V–Tertiary granitoids; VI–Tertiary depressions; VII–deep fault; VIII–boundary between facies-structural zones (tectonic units).

Principal structures (north-south): *parageosyncline; miogeosyncline:* 1–Old Bahamas Channel depression; 2–Cayo Coco tectonic unit; 3–Remedios tectonic unit; 4–Sierra de Jatibonico deep fault; 5–Las Villas tectonic zone or marginal elevation; *eugeosyncline and intrageanticlines of Zaza tectonic unit:* 6–Las Villas deep fault; 7–Bahía Honda tectonic unit; 8–Consolación del Norte deep fault; 9–Pinar del Río tectonic unit; 10–Pinar del Río deep fault; 11–Palacios depression; 12–San Diego de los Baños tectonic unit; 13–Isla de Pinos tectonic unit; 14–Cochinos depression; 15–Trinidad tectonic unit; 16–Central basin depression; 17–La Trocha deep fault; 18–Ana María depression; 19–Cauto depression; 20–Nipe depression; 21–Guantánamo depression; 22–Oriente tectonic unit; 23–North Bartlett deep fault.

Figure 12 Map of the Las Villas and Sierra de Jatibonico Faults (from Khudoley, FSAR Reference 2.5.1-910)

This response is PLANT SPECIFIC.

References:

1. Eberli, G.P., Anselmetti, F.S., Kroon, D., Sato, T., and Wright, J., 2002, "The chronostratigraphic significance of seismic reflections along the Bahamas Transect," *Marine Geology*, 185, p. 1-17.
2. Land, L. A., and Paull, C. K., 2000, "Submarine karst belt rimming the continental slope in the Straits of Florida," *Geo-Marine Letters*, v. 20, p. 123-132.
3. Malloy, R.J., and Hurley, R.J., 1970, "Geomorphology and geologic structure: Straits of Florida," *Geological Society of America Bulletin*, v. 81, p. 1947-1972.
4. Mullins, H. T., and Neuman, A. C., 1979, "Geology of the Miami Terrace and its paleo-oceanographic implications," *Marine Geology*, v. 30, p. 205-232.
5. Oliva Gutierrez, G., and Sanchez Herrero, E.A. (directors), 1989. *Nuevo Atlas Nacional de Cuba*, Instituto de Geografía de la Academia de Ciencias de Cuba, the Instituto Cubano de Geodesia y Cartografía, and the Instituto Geográfico Nacional de España, 220 pp.
6. UTIG, 2012, Academic Seismic Portal at the University of Texas, Institute of Geophysics, Marine Geoscience Data System, Cruise FM0503 in 1980. Available at http://www.ig.utexas.edu/sdc/, accessed June 28, 2012.
7. Reed, J.C., Wheeler, J.O., and Tucholke, B.E., 2005, *Decade of North American Geology, Geologic Map of North America*, The Geological Society of America, Boulder, Colorado.

ASSOCIATED COLA REVISIONS:

The following text will be added to FSAR Subsection 2.5.1.1.1.3.2.2 in a future revision of the FSAR:

Straits of Florida Normal Faults

A series of short, steep normal faults exist in the western Straits of Florida southwest of Turkey Point (Reference 480) (Figure 2.5.1-229). These faults are mapped using seismic data in Paleocene and Eocene strata and are buried by undeformed Miocene and younger strata (Figures 2.5.1-209 and 2.5.1-273). This faulting represents syn-tectonic deformation of the Cuban foreland basin during its collision with the Florida-Bahama Platform (References 794 and 482). Seismic studies in central Straits of Florida indicate that Paleocene to Eocene strata dip to the south indicating the flexure of the southern margin of the Bahama Platform in response to loading from the Cuban orogeny (Reference 221). **These syntectonic Paleocene and Eocene strata are terrigenous and were shed directly from Cuba into northward tapering wedges observed in seismic data (Figure 2.5.1-209).** In contrast, the late middle Eocene to early middle Miocene strata were

deposited uniformly over most of the southern straits of Florida, with pelagic to hemipelagic sedimentation, indicating that the Straits of Florida had subsided to 'near-modern' depths with a change in tectonic regime. The development of sediment drifts in Middle Miocene and younger strata reveal increased current strength in the Straits of Florida at this time (Reference 221). **Just outside of the site region, but in a comparable tectonic environment in the southeastern Gulf of Mexico, interpretation of seismic lines indicate that generally no major displacements affect strata above an upper Eocene unconformity (Reference 482), and lines in the site region** ~~Interpreted seismic lines~~ indicate unfaulted strata above the late middle Eocene unconformity (Reference 221). **However, cases of later Tertiary reactivation of faults in the area have been documented (Reference 484).**

Also in the Straits of Florida, initial workers hypothesized faulting along the edges of the Pourtales and Miami terraces and along other seafloor escarpments, but also suggested that the escarpments could be original sedimentary features associated with sediments deposited against the steeper face of old reef fronts (Reference 967) (Figure 2.5.1-379). Higher resolution, more detailed seismic imaging has allowed the Pourtales escarpment and similar steep-sided escarpments throughout the Gulf of Mexico, Straits of Florida, and Bahamas to be recognized as relict carbonate platform margins, sometimes steepened and modified by erosion, with drifts of younger sediment resting adjacent (Figure 2.5.1-380) (References 687, 951, and 968). For example, Mullins and Neuman (Reference 968) conclude that there is no evidence for faulting at the eastern edge of the Miami terrace and that truncated reflectors near the surface indicate erosion was responsible for the observed stratigraphic variations.

South of the Straits of Florida normal faults, thrust faults are expected within a narrow apron offshore of the Cuban coastline. These thrusts, such as the Nortecubana fault, are discussed as part of the Cuban fold-and-thrust belt.

Changes to the FSAR regarding both the onshore Las Villas fault and the Nortecubana fault (possible equivalent to the offshore Las Villas of Malloy and Hurley (1970)) are incorporated as part of the response to RAI 02.05.01-21.

The following text will be inserted after the ninth paragraph of FSAR Subsection 2.5.1.1.1.3.2.4 preceding the discussion of the Pinar fault in a future revision of the FSAR:

Sierra de Jatibonico fault

The Sierra de Jatibonico fault is a 1-2 km-wide zone that parallels the trend of Cuba along its 450 km length. Both Khudoley (Reference 910) and Hatten et al. (Reference 911) describe the fault as being vertical at the surface but gradually flattening at depth, reaching a minimum dip of 55°S. Hatten et al. (Reference 911) state that there is a component of right-lateral displacement along the fault, whereas Pardo (Reference 439) only cites the throw of 1500 meters.

There are no studies that document fault activity or seismicity along the Sierra de Jatibonico fault zone. Mapping by Hatten et al. (Reference 911) shows that the fault juxtaposes the Zueleta and Remedios Units, each of which is capped by middle Eocene sediments containing high-angle faults with a component of right-lateral slip. Pardo (Reference 439) also dates the youngest units in the Jatibonico belt (approximately the same as the Remedios Unit from Hatten et al., (Reference 911)) as middle Eocene. Assuming that faulting within each unit was contemporaneous with movement on the Sierra de Jatibonico fault, that provides a minimum age of last activity.

The following references will be added to FSAR Subsection 2.5.1.3, References, in a future revision of the FSAR:

910. Khudoley, K., Principal Features of Cuban Geology, American Association of Petroleum Geologists Bulletin, Vol. 51, No. 5, pp. 668–677, 1967.

911. Hatten, C., M. Somin, G. Millan, P. Renne, R. Kistler, and J. Mattinson, Tectonostratigraphic Units of Central Cuba, Eleventh Caribbean Geological Conference Symposium Volume, Barbados, British West Indies, pp. 35:1–13, 1988.

967. Malloy, R., and R. Hurley, *Geomorphology and Geologic Structure: Straits of Florida,* Geological Society of America Bulletin, Vol. 81, pp. 1947–1972, 1970.

951. Land, L., and C. Paull, *Submarine Karst Belt Rimming the Continental slope in the Straits of Florida,* Geo-Marine Letters, Vol. 20, pp. 123–132, 2000.

968. Mullins, H., and A. Neuman, *Geology of the Miami Terrace and its Paleooceanographic Implications,* Marine Geology, Vol. 30, pp. 205–232, 1979.

The following figures will be added in a future revision of the FSAR:

Figure 2.5.1-379 Map of Selected Seismic Lines in the Straits of Florida

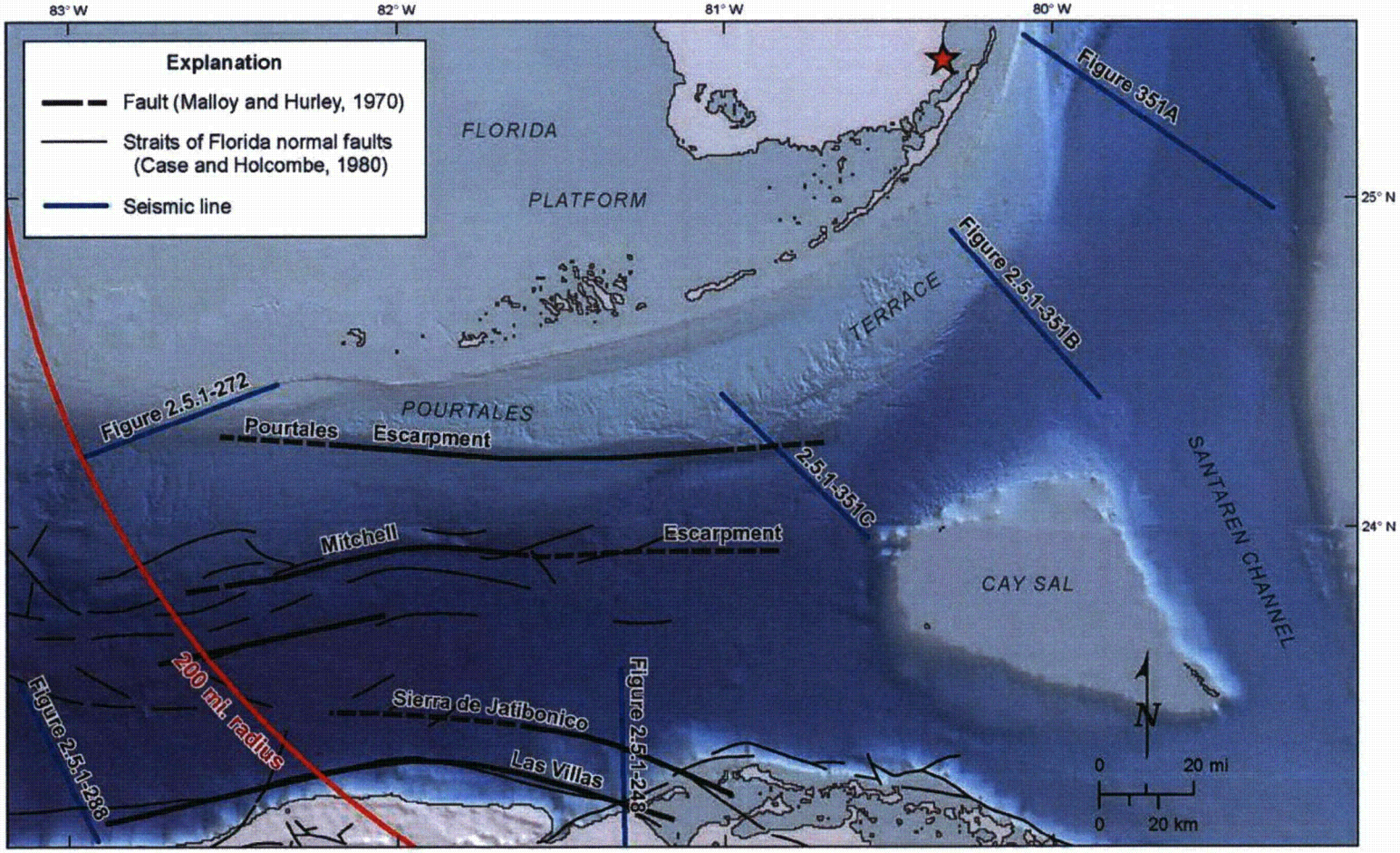

Figure 2.5.1-380 Profiles across the Miami/Pourtales Escarpment Illustrating the Variation in Geomorphology and Stratigraphy

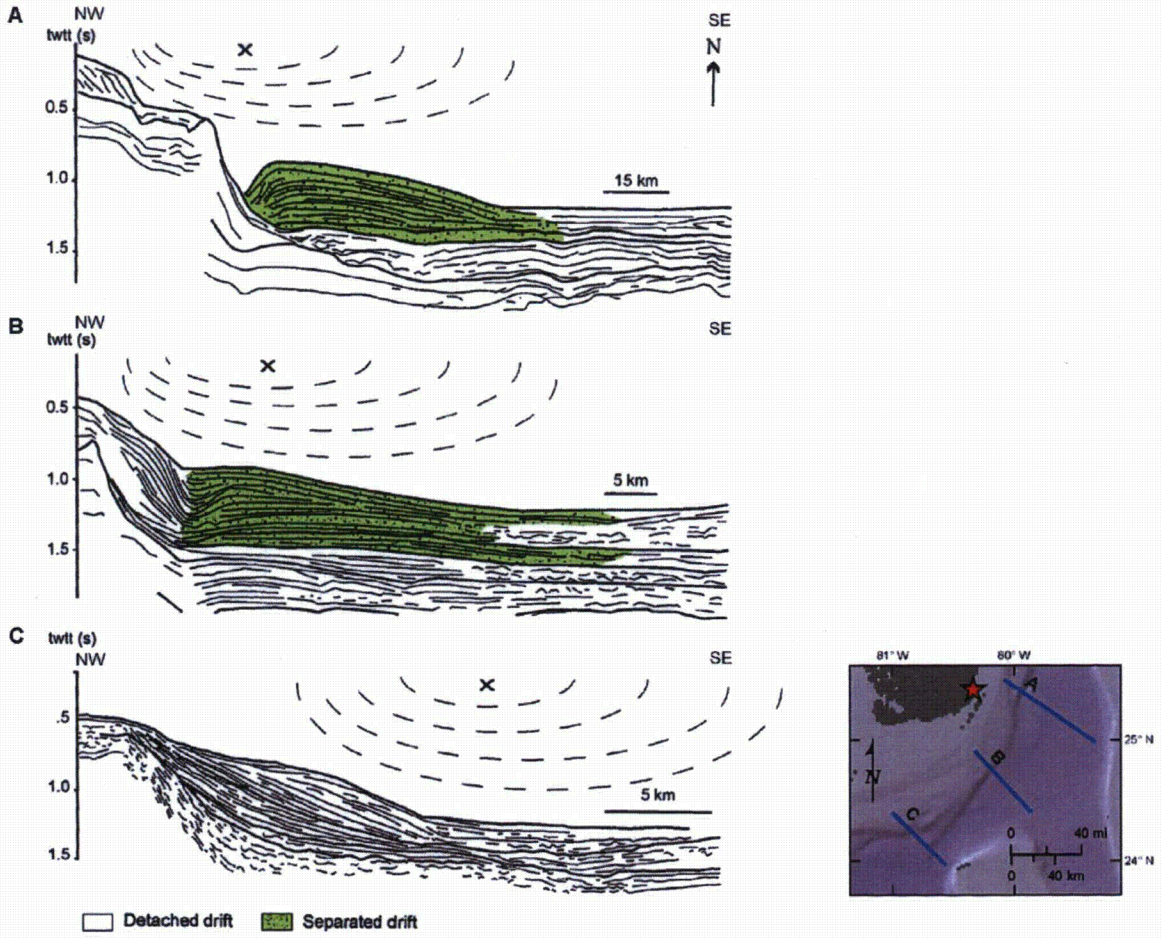

ASSOCIATED ENCLOSURES:

None